1-1-2016

Cardiolipin Is Required For Optimal Acetyl-Coa Metabolism

Vaishnavi Raja
Wayne State University,

CARDIOLIPIN IS REQUIRED FOR OPTIMAL ACETYL-COA METABOLISM

by

VAISHNAVI RAJA

DISSERTATION

Submitted to the Graduate School

of Wayne State University,

Detroit, Michigan

in partial fulfillment of the requirements

for the degree of

DOCTOR OF PHILOSOPHY

2016

MAJOR: BIOLOGICAL SCIENCES

Approved By:

_____

Advisor   Date

_____

_____

_____

_____

DEDICATION

To my beloved parents, my brother, my husband, with all my love and my dear daughter for

unconditional love and bringing me so much happiness

ACKNOWLEDGEMENTS

This dissertation would not have been possible without "ALMIGHTY GOD" and the people who embellished my life

TABLE OF CONTENTS

LIST OF TABLES

LIST OF FIGURES

LIST OF ABBREVIATIONS

CL   – cardiolipin

Fe-S   – iron-sulfur

PKC-Slt2   – Protein kinase C-Slt2 mitogen activated protein kinase

HOG   – high osmolarity glycerol

BTHS   – Barth syndrome

RCR   – respiratory control ratio

ROS   – reactive oxygen species

ALCAT1   – acyl-CoA:lysocardiolipin acyltransferase-1

ISC   – iron-sulfur cluster

CIA   – cytosolic Fe-S protein assembly

TIM   – translocase of the inner membrane

CDP-DG   – CDP-diacylglycerol

AAC   – ADP/ATP translocase

PiC   – phosphate carrier

FATP   – fatty acid transport protein

MDV   – mitochondrial derived vesicles

DMCA   – dilated cardiomyopathy with ataxia

PGP   – phosphatidylglycerolphosphate

PGPS   – phosphatidylglycerolphosphate synthase

PG   – phosphatidylglycerol

MLCL   – monolysocardiolipin

TOM   – translocase of the outer membrane

SAM   – sorting and assembly machinery

CAT   – carnitine acyltransferase

CRC   – carnitine/acylcarnitine translocase

SGA   – synthetic genetic array

PDH   – pyruvate dehydrogenase

PDH-bypass – pyruvate dehydrogenase bypass pathway

ACS   – acetyl-CoA synthetase

TCA   – tricarboxylic acid cycle

CS   – citrate synthase

ACO   – aconitase

MDH   – malate dehydrogenase

ICL   – isocitrate lyase

MLS   – malate synthase

SDH   – succinate dehydrogenase

SFC   – succinate fumarate transporter

CHAPTER 1 INTRODUCTION

Parts of this chapter have been published in the *Journal of Chem Phys Lipids* **179: 49-56, 2014** (an invited review for a special issue on cardiolipin).

1. CL BIOSYNTHESIS AND REMODELING

Cardiolipin (CL) (1,3-diphosphatidyl-sn-glycerol) is the signature phospholipid of the mitochondrial membrane. First isolated from beef heart (Pangborn, 1942), it is ubiquitous in eukaryotes and also present in prokaryotes. In yeast (*Saccharomyces cerevisiae*), CL is synthesized de novo in the inner mitochondrial membrane (Gallet et al. 1997), and it undergoes a remodeling step to replace the saturated fatty acyl chains with unsaturated fatty acyl chains (Gu et al., 2004 and Fig. 1.1). CL synthesized de novo contains predominantly saturated fatty acyl chains that are replaced with unsaturated fatty acyl groups. This remodeling is a two-step process in which a CL specific deacylase (encoded by *CLD1*) removes one fatty acyl group, forming monolysocardiolipin (MLCL), and tafazzin reacylates the MLCL to form a generally more unsaturated CL (Xu et al. 2003). Tafazzin is a CoA-independent transacylase that transfers acyl chains preferentially from phosphatidylcholine (PC) to CL (Xu et al. 2003). The accumulation of MLCL in yeast and human tafazzin-deficient cells (Gu et al., 2004; Vaz et al., 2003) is consistent with the two-step pathway of remodeling shown in Fig. 1.1. In a study comparing CL species from a wide variety of organisms, it was shown that the most abundant species of CL contained only one or two types of fatty acids, which results in a high degree of structural uniformity and molecular symmetry in CL (Schlame et al., 2005). In contrast, tafazzin-deficient cells were characterized by multiple species of CL.

Studies in yeast utilizing well-characterized deletion mutants of CL synthesis (Fig. 1.1) indicate that CL regulates many cellular functions and signaling pathways, both inside and outside of the mitochondria. The ubiquitous association of CL with energy transducing membranes is consistent with the role of this lipid in bioenergetics (reviewed by Joshi et al., 2009). In fact, CL synthesis and mitochondrial bioenergetics are inter-dependent, as CL synthesis is both required for and stimulated by oxidative phosphorylation (Gohil et al., 2004). Within the mitochondria, the effects of CL deficiency extend beyond bioenergetics to decreased mitochondrial protein import and perturbation of mitochondrial fusion (Jiang et al., 2000; Gebert et al., 2009; Joshi et al., 2012). The deleterious effects of CL deficiency outside the mitochondria include perturbation of the PKC-Slt2 cell integrity and high osmolarity glycerol (HOG) signaling pathways and decreased vacuolar function (Zhong et al., 2005; Zhong et al., 2007; Chen et al., 2008b; Zhou et al., 2009). Perturbation of CL synthesis has long been associated with aging (Paradies et al., 2010), and loss of CL was found to decrease longevity in yeast cells (Zhou et al., 2009). The significance of CL in human health is apparent from clinical findings that perturbation of CL metabolism leads to the life-threatening disorder known as Barth syndrome (BTHS) (discussed below).
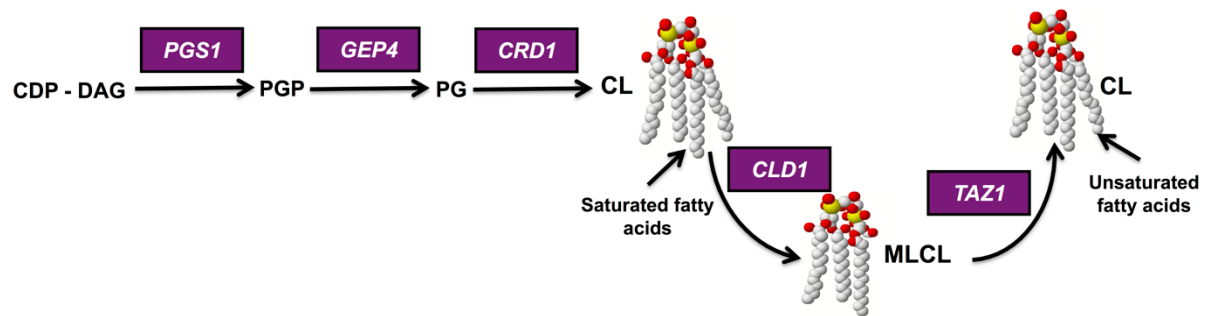
FIGURE 1.1: Synthesis and remodeling of cardiolipin (CL) in yeast. CDP-DAG is converted to phosphatidylglycerolphosphate (PGP) by phosphatidylglycerolphosphate synthase (PGPS), encoded by *PGS1* (Chang et al., 1998; Dzugasova et al., 1998). PGP phosphatase (Gep4) catalyzes the conversion of PGP to phosphatidylgylcerol (PG) (Osman et al., 2010). PG is converted to cardiolipin (CL) by CL synthase (Crd1) (Jiang et al., 1997; Chang et al., 1998; Tuller et al., 1998). CL is remodeled in a two-step process in which the CL specific deacylase encoded by *CLD1* removes a fatty acyl group, forming monolysocardiolipin (MLCL) (Beranek et al., 2009), and tafazzin (Taz1) reacylates MLCL to form a generally more unsaturated CL (Xu et al., 2003). In mammalian cells, CL is deacylated by more than one enzyme (Kiebish et al., 2013). Tafazzin is the enzyme that is mutated in Barth syndrome.

In addition to the cellular functions listed above, recent studies indicate that CL is intricately involved in cellular metabolism (Fig. 1.2). These studies are the focus of this dissertation. CL interacts with components of the electron transport chain and is required for stabilization of electron transport chain supercomplexes and for optimal respiratory control (Bazan et al., 2013; Pfeiffer et al., 2003; Zhang et al., 2002; Zhang et al., 2005). Perturbation of iron-sulfur (Fe-S) biogenesis has been reported in CL deficient yeast cells, suggesting that iron homeostasis as well as enzymatic activities requiring Fe-S cofactors are dependent on CL biosynthesis (Patil et al., 2013). CL is also required for activities of carrier proteins that transport metabolites for energy metabolism (Kadenbach et al., 1982; Fiermonte et al., 1998; Sedlak et al., 1999; Lange et al., 2001; Hoffmann et al., 1994; Jiang et al., 2000; Bisaccia and Palmieri, 1984), as well as for enzymes in the carnitine shuttle (Pande et al., 1986; Noel and Pande, 1986). In addition, CL might also be required for cellular metabolism outside mitochondria. CL is present in the membrane of peroxisomes (Zinser et al., 1991) and may affect β-oxidation and other metabolic activities of this organelle. The role of CL in mitochondrial protein import is discussed as a potential mechanism underlying the metabolic defects associated with CL deficiency. We speculate that defects in these functions may be physiological modifiers that account for the wide disparity of clinical phenotypes observed in BTHS, and conclude with a discussion of important unanswered questions that are exciting directions for future research.
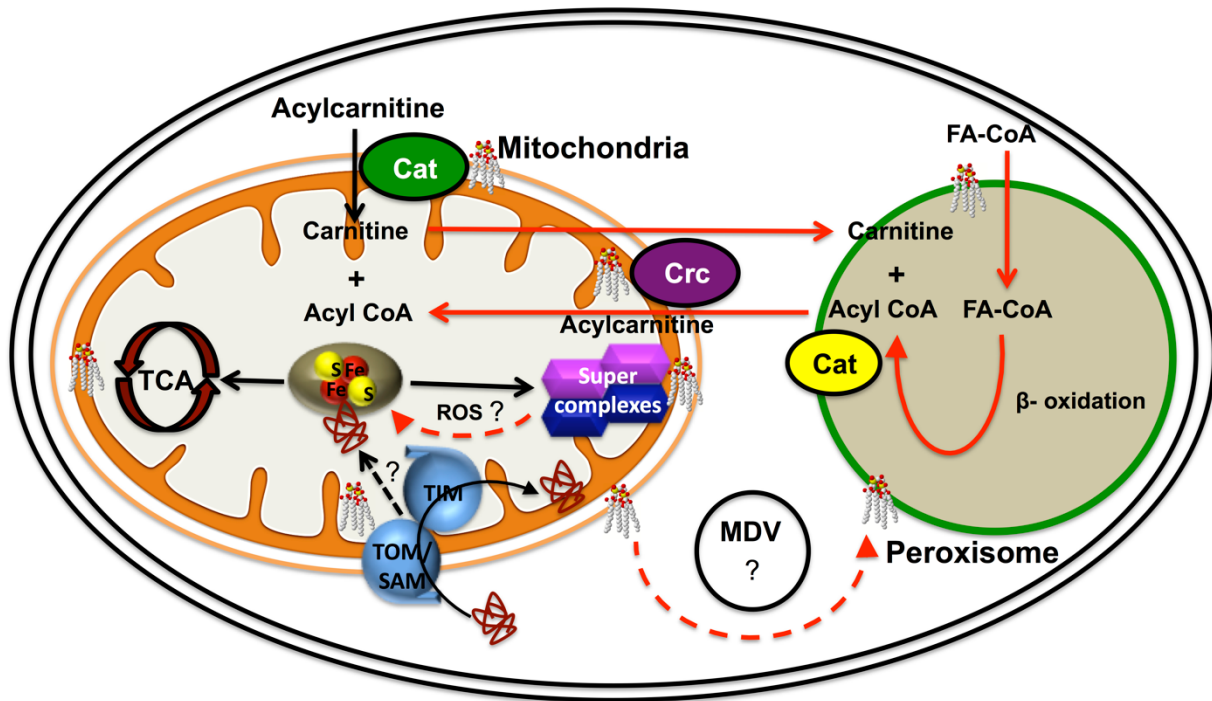
FIGURE 1.2: Functions of cardiolipin (CL) in metabolic pathways. CL is most abundant in the inner membrane and is also present in the outer membrane of mitochondria. It is required for activities of transporters and electron transport chain enzymes and for stabilization of electron transport supercomplexes. Loss of CL leads to perturbation of Fe-S biogenesis, resulting in decreased activity of Fe-S enzymes in the TCA cycle, electron transport, and other pathways. The mechanism linking CL and Fe-S biogenesis is unknown. Because CL is required for the import of proteins through mitochondrial import complexes (TOM, SAM and TIM), it is possible that import of specific proteins required for Fe-S synthesis is defective in CL deficient cells. Alternatively, increased ROS generated by inefficient electron transport in CL deficient cells may damage Fe-S proteins. CL is also present in the membrane of the peroxisome, an organelle that carries out β-oxidation of fatty acids, ether lipid synthesis, and reactions of the glyoxylate cycle. The route whereby CL is transported from mitochondria to peroxisomes is unclear, but may involve mitochondria derived vesicles (MDVs). Acyl CoA produced by β-oxidation of long chain fatty acids in peroxisomes is transported to the mitochondria via the carnitine shuttle. The acyl CoA is transferred to carnitine in the peroxisome by carnitine acyltransferase (Cat). Acylcarnitine from the peroxisome crosses the mitochondrial membrane, facilitated by the carnitine/acylcarnitine translocase (Crc). CL is required for efficient activity of both mitochondrial carnitine enzymes in mammalian cells.

2. CL AND MITOCHONDRIAL BIOENERGETICS

CL is enriched in the membranes of bacteria, mitochondria, and hydrogenosomes, which play a role in ATP synthesis through the generation of a transmembrane electrochemical gradient (Daum et al., 1985; Dowhan et al., 1997; de Andrade Rosa et al., 2006). The association of CL with energy transducing membranes is consistent with the crucial role of this lipid in cellular bioenergetics (reviewed by Schlame et al., 2000; Hoch, 1992). The physical interaction between CL and mitochondrial respiratory chain complexes and other components of membranes also helps in the formation of a lipid scaffold, which functions to stabilize, tether, and increase the enzyme activity of interacting proteins (Beyer et al., 1985; Beyer et al., 1996; Sedlak et al., 1999). In this light, it is not surprising that perturbation of CL synthesis affects the structure and function of mitochondrial respiratory chain complexes and transporters.

2.1 CL and respiration

Analyses of CL function in yeast have been facilitated by the availability of yeast mutants of each step in CL synthesis (Fig. 1.1). In particular, the CL synthase null mutant *crd1Δ*, which lacks CL (Jiang et al., 1997; Tuller et al., 1998; Chang et al., 1998), has been the focus of numerous studies. Although *crd1Δ* cells can grow in non-fermentable carbon sources, indicating that CL is not essential for respiration, the ADP/O and respiratory control ratios (RCR) of *crd1Δ* mitochondria are reduced in these conditions (Koshkin et al., 2002). CL is required for optimal RCR and ADP/O ratios and for maintenance of the mitochondrial membrane potential (Jiang et al., 2000; Claypool et al., 2008), especially during unfavorable conditions such as increased temperature and

osmolarity (Koshkin et al., 2002; Koshkin et al., 2000). The role of CL in respiration has been recently reviewed (Joshi et al., 2009; Patil and Greenberg, 2013).

2.2 CL is required for stabilization of supercomplexes

The electron transport chain complexes are organized into supramolecular structures referred to as supercomplexes (Schagger and Pfeiffer, 2000). *S. cerevisiae* lacks complex I (NADH complex) but contains NADH dehydrogenase composed of a single subunit (Ndi1). Yeast supercomplexes are formed by the association of two units of complex III with units of complex IV. Supercomplexes in mammalian cells are formed by the association of complex I with two units of complex III and multiple units of complex IV (Schagger, 2002). The proposed role of supercomplexes is that of efficient substrate channeling between the individual complexes. The *crd1Δ* mutant exhibits destabilization of the supercomplexes (Pfeiffer et al., 2003; Zhang et al., 2002; Zhang et al., 2005). Bazan and co-workers reported the in vitro reconstitution of supercomplexes and showed that supercomplex III_2IV_2 reconstitution is dependent on CL (Bazan et al., 2013). The loss of CL decreases activity of ADP/ATP carrier protein activity and its association with the supercomplexes (Claypool et al., 2008; Jiang et al., 2000). Destabilization of supercomplexes was also reported in tafazzin-deficient human fibroblasts (McKenzie et al., 2006) and, more recently, in tafazzin-deficient induced pluripotent stem cells (Dudek et al., 2013).

2.3 Loss of CL leads to increased generation of reactive oxygen species (ROS)

Destabilization of supercomplexes is expected to result in increased electron leakage and ROS production (Maranzana et al., 2013). Not surprisingly, the absence of CL in yeast cells leads to increased protein carbonylation, a hallmark of increased ROS

(Chen et al., 2008a). The primary sites of ROS generation are complexes I and III (Turrens et al., 1985; Barja, 1999; Kushnareva et al., 2002; Grivennikova and Vinogradov, 2006). The CL acyl chains, which are in close proximity to these ROS generating sites, are susceptible to peroxidation (Li et al., 2010; Li et al., 2012; Liu et al., 2012). The superoxides generated by respiratory complex III were shown to cause peroxidation of CL and to reduce the activity of cytochrome c oxidase (Paradies et al., 1998; Paradies et al., 2000; Paradies et al., 2001). The exogenous supplementation of CL, but not peroxidized CL or other phospholipids, rescued both reduced activity of cytochrome c oxidase and increased generation of ROS in reperfused heart (Paradies et al., 2001; Petrosillo et al., 2007). As CL is extensively remodeled by the transacylase tafazzin (Malhotra et al., 2009), we speculate that this may be a mechanism whereby damaged fatty acyl chains are replaced. Under oxidative stress conditions, acyl-CoA:lysocardiolipin acyltransferase-1 (ALCAT1) may also be involved in remodeling of CL. Increased expression of ALCAT1 leads to aberrant remodeling of CL with long polyunsaturated fatty acyl chains, which are sensitive to ROS (Watkins et al., 1998; Hong et al., 2002; Li et al., 2010). Increased expression of ALCAT1 is linked to diabetes and diet-induced obesity in humans and to hyperthyroid cardiomyopathy in mice (Cao et al., 2009; Li et al., 2010; Li et al., 2012; Liu et al., 2012). In summary, CL deficiency is linked to increased generation of ROS, which in turn damage CL by peroxidation of CL acyl chains.

3. PERTURBATION OF IRON HOMEOSTASIS IN CL DEFICIENT CELLS

A recent report indicates that CL is required for Fe-S biogenesis and iron homeostasis (Patil et al., 2013). Fe-S clusters are present in all kingdoms of life (Lill and Muhlenhoff, 2008; Johnson et al., 2005). They are cofactors for many biochemical

reactions, including those required for electron transport and for the TCA cycle (Hausmann et al., 2008; Gerber et al., 2004; Li et al., 1999; Lill and Muhlenhoff. 2008). In eukaryotes, three Fe-S cluster biogenesis systems have been characterized, including the iron-sulfur cluster (ISC) import system in mitochondria (required for the generation of all cellular Fe-S proteins), the cytosolic Fe-S protein assembly (CIA) machinery, and the ISC export apparatus in mitochondria. The latter two processes are also involved in maturation of Fe-S proteins in the cytosol and nucleus (Balk et al., 2004; Ye et al., 2006; Kessler et al., 2005; Balk et al., 2005).

A role for CL in iron homeostasis was first suggested by a microarray analysis of genes exhibiting altered expression in the *crd1Δ* mutant (Patil et al., 2013). Most notably, the genes for iron uptake were greatly upregulated in *crd1Δ* cells, which exhibited increased mitochondrial iron as well as increased sensitivity to iron and to oxidative stress. Perturbation of iron homeostasis is a demonstrated outcome of defective Fe-S biogenesis (Rutherford et al., 2005; Hausmann et al., 2008). Consistent with an Fe-S defect, the *crd1Δ* mutant exhibits decreased activities of both mitochondrial and cytosolic enzymes that require Fe-S co-factors, including mitochondrial enzymes succinate dehydrogenase, aconitase, and ubiquinol cytochrome c oxidoreductase, and cytosolic enzymes sulfite reductase and isopropylmalate isomerase (Patil et al., 2013). The CL deficient mutant also exhibited synthetic interaction with the Fe-S scaffold mutant *isu1.*

The mechanism linking CL to Fe-S biogenesis is not currently understood. We speculate that defective import of proteins required for Fe-S biogenesis may underlie the defect, as several studies have shown that mitochondrial protein import as well as assembly of outer membrane complexes are decreased in yeast CL mutants and in

lymphoblasts derived from BTHS patients (Jiang et al., 2000; Gebert et al., 2009). Additional evidence for the role of CL in mitochondrial protein import comes from functional studies of the translocator assembly and maintenance protein Tam41, which is required for the assembly and maintenance of the TIM mitochondrial import complex (Gallas et al., 2006; Tamura et al., 2006). Interestingly, the phenotypes of the *tam41Δ* mutant were found to be similar to those of the CL mutant *crd1Δ*. These include defective protein translocases and respiratory chain supercomplexes, decreased assembly of the ADP/ATP carrier (AAC), and decreased CL levels (Tamura et al., 2006; Gallas et al., 2006; Kutik et al., 2008). These findings suggested that protein import defects in the *tam41Δ* mutant were due to the loss of CL. Consistent with this possibility, Tamura and co-workers demonstrated that Tam41 is the mitochondrial CDP-DG synthase that catalyzes the synthesis of CDP-DG, which is required for CL synthesis (Tamura et al., 2013). An alternative mechanism is that Fe-S proteins may be damaged by the increase in ROS in CL deficient cells, as the inactivation of Fe-S enzymes by superoxide has been demonstrated (Flint et al., 1993; Gardner, 1997). Increasing antioxidants by overexpression of the *YAP1* gene did not rescue the iron sensitivity phenotypes of the CL mutant (Patil et al., 2013), a finding that might argue against Fe-S damage due to increased ROS. However, it is quite possible that free radicals that are not scavenged by Yap1-induced antioxidants may cause Fe-S damage in CL deficient cells. In light of the role of Fe-S clusters in a wide variety of cellular functions (Rouault et al., 2012), perturbation of Fe-S biogenesis in CL deficient cells has far-reaching implications.

4. CL AND MITOCHONDRIAL TRANSPORTERS

Soluble molecules and substrates are transferred across organelle membranes via carrier proteins. Transporters that play major roles in energy transfer include the ADP/ATP translocase (AAC), phosphate carrier (PiC), pyruvate carrier, fatty acid transport protein (FATP), tricarboxylate transporter, and 2-oxoglutarate/malate carrier protein, among others (Nury et al., 2006; Klingenberg, 1990; Walker, 1992; Kuan et al., 1993; Nelson et al., 1993; Palmieri, 1994). The reader is referred to an excellent review of the role of CL in the stabilization of mitochondrial carrier proteins (Claypool, 2009). Membrane lipids play an important role in the assembly of carrier proteins (Hunte, 2005). Both the AAC and PiC, which are required for oxidative phosphorylation, interact with CL (Kadenbach et al., 1982; Fiermonte et al., 1998; Sedlak et al., 1999; Lange et al., 2001). Of the three isoforms of AAC that have been identified in yeast and humans, activity of the major isoform, AAC2, requires CL (Hoffmann et al., 1994). Furthermore, activity of AAC purified from the yeast *crd1Δ* mutant is decreased (Jiang et al., 2000). A recent report indicates that AAC also interacts with the TIM mitochondrial protein import complex, and this interaction is dependent on CL (Gebert et al., 2011).

In addition to oxidative phosphorylation, transporters play a role in two other sources of energy production, the oxidation of pyruvate and β-oxidation of fatty acids. Pyruvate is transported into the mitochondria of yeast, Drosophila, and humans by the pyruvate carrier proteins MPC1 & MPC2 (Bricker et al., 2012). The purification of pyruvate carrier proteins requires phospholipids, especially CL (Bisaccia and Palmieri, 1984). In the absence of CL, transport activity of the pyruvate carrier protein was not observed (Nalecz et al., 1986). Fatty acids are taken up by fatty acid transport proteins (FATP1 –

FATP 6) in the plasma membrane (Van der Vusse et al., 2000; Gimeno, 2007; Jia et al., 2007). While a role for CL in FATP activation has not been reported, Mitchell et al. (2009) demonstrated that knockdown of FATPs in HEK 293 cells inhibits de novo CL synthesis, suggesting that fatty acid transport and CL synthesis may be interdependent. In summary, CL is required for the transport of metabolites utilized in the major cellular energy producing metabolic pathways.

5.   INTER-RELATIONSHIP BETWEEN CL AND CARNITINE

Activated fatty acids (fatty acyl-CoAs) are metabolized to acetyl-CoA by the enzymes of β-oxidation. As membranes are impermeable to activated acyl-CoAs, their transport into mitochondria is facilitated by the quaternary ammonium compound L-carnitine (3-hydroxy-4-N-trimethylaminobutanoate) (Reuter and Evans, 2012). The transfer of acyl residues from CoA to carnitine is catalyzed by carnitine acyltransferase (van der Leij et al., 2000; Jogl and Tong, 2003; Franken et al., 2008). Carnitine/acylcarnitine translocase catalyzes the transport of acylcarnitine across the mitochondrial membrane (Murthy and Pande, 1984; Van Roermund et al., 1995). The carnitine shuttle is conserved throughout the eukaryotic kingdom (Bremer, 1983). A role for CL in the carnitine shuttle is suggested by reports that CL is required for the activities of the carnitine shuttle enzymes. Carnitine acyltransferase (carnitine palmitoyltransferase) purified from rat liver cells was shown to contain CL (Fiol et al., 1984), and enzymatic activity of the enzyme was stimulated by CL (Pande et al., 1986). Carnitine/acylcarnitine translocase activity was also shown to require CL (Noel and Pande, 1986). Furthermore, the stimulating effect of carnitine on state 2 respiration in rat liver mitochondria was abolished by doxorubicin, which binds CL, and activity was

restored by adding CL (Battelli et al., 1992).

In addition to its function in the transport of acyl groups, carnitine also plays a role in oxidative stress and aging. In *S. cerevisiae*, carnitine was shown to improve growth in the presence of oxidative stress (Franken et al., 2010). Several features of aging in rats are reversed by supplementation with carnitine, including both decreased CL and mitochondrial dysfunction. Decreased levels and pathological remodeling of CL with polyunsaturated fatty acids (arachidonic and docosahexaenoic acids) have been described in old rats (Lee et al., 2006; Sparagna et al., 2009; Maftah et al., 1994; Lewin et al., 1984; Paradies et al., 1993; Paradies et al., 1997; Lenaz et al., 1997; Paradies et al., 1990). Mitochondrial dysfunction in old animals is also associated with defects in ATP synthesis and oxidative phosphorylation (Maftah et al., 1994; Hoch, 1992; Hagen et al., 1998; Sen et al., 2006; Sen et al., 2007). Dietary supplementation of old rats with acylcarnitine significantly improved cellular respiration and mitochondrial membrane potential and, interestingly, also increased CL levels (Hagen et al., 1998). These studies suggest an inter-relationship between CL and carnitine in regulating mitochondrial functions. CL is required for optimal activity of the carnitine acetylcarnitine transloacse, with implications for the generation of energy from β-oxidation and mitochondrial functions associated with aging. In addition, CL levels may be affected by carnitine supplementation.

6. CL, PEROXISOMES, AND β - OXIDATION

The peroxisome is a unique, versatile, single membrane bound organelle found in all eukaryotes. The number, size, and function of peroxisomes vary among cell types and in response to physiological conditions (Van den Bosch et al., 1992; Veenhuis et al.,

1988). Studies of peroxisomal biogenesis have been hampered by the fragility and low abundance of the organelle (Platta et al., 2007). Peroxisomal enzymes carry out β-oxidation of fatty acids, ether lipid synthesis, and reactions of the glyoxylate cycle (Van den Bosch et al., 1992). In eukaryotes, fatty acids are degraded by α-, β-, and ω-oxidation (Wanders et al., 2003). The major pathway, β-oxidation, is conserved from yeast to higher eukaryotes (Houten et al., 2010; Wanders et al., 2010), although localization of the pathways differs. In yeast, peroxisomes are the sole site of β-oxidation. In mammals, β-oxidation takes place in both mitochondria and peroxisomes (Barlett and Eaton, 2004; Van der Klei and Veenhuis, 1997). β-oxidation of fatty acids plays a key role in energy homeostasis in liver, heart, and skeletal muscle (Houten et al., 2010). The depletion of glucose during fasting is compensated by β-oxidation of fatty acids in many tissues (but not brain) to generate energy (Houten et al., 2010). Fatty acids are also converted to ketone bodies, an additional source of energy that can be utilized by all tissues, including the brain (Houten et al., 2010). The reader is referred to excellent recent reviews of β-oxidation in peroxisomes and mitochondria (Houten et al., 2010; Wanders et al., 2010).

Zinser et al. (1991) reported that the peroxisomal membrane of *S. cerevisiae* grown in rich media (yeast extract-peptone-dextrose) contains considerable levels of CL (7% of total phospholipid). This amount of CL is slightly more than half the level observed in mitochondria (13% of total phospholipid). The CL content of peroxisomal membranes of *Pichia pastoris* cells grown under conditions that induce peroxisomes (methanol or oleic acid as the sole source of carbon) was reported to be about a third of the level observed in mitochondria (Wriessnegger et al., 2007). It is unclear how CL, which is synthesized in mitochondria, is transported to peroxisomes. Neuspiel et al. (2008)

showed that, in mammalian cells, mitochondria derived vesicles (MDV) fuse to a fraction of pre-existing peroxisomes. The MDVs formed are of two types, single-membrane MDVs (mitochondrial outer membrane derived vesicles) and double-membrane MDVs (mitochondrial inner and outer membrane derived vesicles). Both types of MDVs fuse to form single membrane enclosed peroxisomes (Neuspiel et al., 2008). MDVs are thought to be involved in vesicular trafficking of membrane lipids (possibly including CL) and proteins from the intermembrane space of mitochondria to peroxisomes (Schumann et al., 2008; Braschi et al., 2010; Sugiura et al., 2014).

In summary, while there is currently no direct evidence for a role of CL in peroxisomal metabolism, CL is clearly present at significant levels in the peroxisomal membrane. As discussed above, it is now well established that CL affects numerous mitochondrial functions by interacting with proteins and complexes in the mitochondrial membrane. We speculate that this structurally unique lipid also affects peroxisomal function as a consequence of interacting with peroxisomal membrane enzymes and transporters.

7. BARTH SYNDROME (BTHS)

BTHS is a severe X-linked disorder characterized by cardiomyopathy, skeletal myopathy, neutropenia, 3- methylglutaconic aciduria and growth retardation due to abnormal mitochondria and defective oxidative phosphorylation (Barth et al., 1981). Other metabolic abnormalities found in BTHS patients include elevated urinary excretion of 3-methylglutaconic acid (Cardonick et al., 1997) and hypercholesterolemia (Mazzocco et al., 2007). About ten years after the first description of BTHS, the locus was mapped to Xq28 (Bolhuis et al., 2007), and mutations were identified in G4.5, now referred to as

tafazzin (TAZ1) (Bione et al., 1996). Mutations in BTHS result in the complete loss of Taz1p or the expression of severely truncated Taz1p; a biochemical explanation for the phenotypes associated with any identified BTHS point mutation is not known (Bione et al., 1996). Cardiomyopathy is a characteristic feature and primary cause of death in BTHS patients. Cardiomyopathy is a structural disease in which the heart muscle is marked by rigidity and loss of flexibility of the heart walls, leading to weakness and fatigue (Barth et al., 1983). Skeletal myopathy and cardiomyopathy lead to delayed motor development in some BTHS patients and to changes in cardiac mitochondrial appearance (Xu et al., 2006). Skeletal myopathy and cardiomyopathy are due to muscle weakness, which can be related to deficient oxidative phosphorylation (Barth et al., 1999). The molecular basis underlying the pathologies observed in BTHS patients is not understood. Interestingly, tafazzin mutations do not correlate with the extent of clinical abnormalities in BTHS, and substantial phenotypic variation occurs even for a single tafazzin mutation (Johnston et al., 1997). Thus, the clinical symptoms of BTHS vary from those who have severe incapacitating disease to those who are nearly asymptomatic, even among patients with the identical mutation. The high degree of variation in the symptoms of BTHS patients with the same TAZ1 mutation suggests that physiological factors influence the outcome of defective tafazzin.

8.   IMPLICATIONS FOR BARTH SYNDROME

BTHS is characterized by a decrease in total CL, an accumulation of MLCL, and the absence of the predominant unsaturated CL species due to the loss of the CL remodeling enzyme tafazzin (Schlame and Ren, 2006). The molecular basis underlying the pathology observed in BTHS patients is not understood. Interestingly, tafazzin

mutations do not correlate with the extent of clinical abnormalities in BTHS, and substantial phenotypic variation occurs even for a single tafazzin mutation. The high degree of variation in the symptoms of BTHS patients with the same tafazzin mutation suggests that physiological factors influence the outcome of defective tafazzin (Johnston et al., 1997). We suggest that the functions of CL discussed above may be potential physiological modifiers of the BTHS phenotype.

8.1   Fatty acid metabolism, peroxisome biogenesis and the carnitine shuttle

In a landmark study, Spencer et al. (2011) observed that impaired oxygen utilization directly contributes to exercise intolerance in BTHS patients. It is well-established that mild or moderate exercise is driven by a significant increase in fat oxidation. This suggests the possibility that BTHS patients exhibit exercise intolerance due to the inability to adequately metabolize fat. The clinical outcomes observed in many human disorders of β-oxidation are similar to those seen in BTHS. Perturbation of β-oxidation of fatty acids in mitochondria was shown to cause cardiomyopathy and arrhythmia (Bonnet et al., 1999; Saudubray et al., 1999). The role of CL in the carnitine shuttle suggests that the loss of CL may lead to defects in β-oxidation and or carnitine mediated transport of acyl-CoA. Consistent with this possibility, carnitine mutations lead to clinical outcomes similar to those seen in BTHS (Wanders et al., 2010). Exercise intolerance has been demonstrated in carnitine palmitoyltransferase deficiency (Ørngreen et al., 2003). Carnitine-acylcarnitine translocase deficiency results in cardiomyopathy with arrhythmia (Longo et al., 2006). Cardiomyopathy and skeletal myopathy are observed in deficiencies of the *OCTN2*-encoded carnitine transporter and very long chain acyl-CoA dehydrogenase (Rinaldo et al., 2002). In summary, numerous

disorders of fatty acid metabolism lead to clinical phenotypes similar to those found in BTHS, including cardiomyopathy, skeletal myopathy, arrhythmia, and exercise intolerance. Elucidating the role of CL in β-oxidation and carnitine-mediated transport of fatty acids may identify potential avenues for treatment of BTHS.

8.2   Bioenergetics and Fe-S biogenesis

Three human genetic disorders of Fe-S biogenesis have been described (Rouault and Tong, 2008). These include defects in the iron chaperone frataxin, the iron sulfur cluster assembly protein ISCU, and glutaredoxin. Mutations in frataxin in the disorder Friedreich ataxia lead to hypertrophic cardiomyopathy, heart failure, and deficiencies in enzymes requiring Fe-S cofactors, including aconitase and complex I-III enzymes. Interestingly, mitochondrial deficiencies similar to those seen in CL deficient cells can be rescued by overexpression of frataxin, including decreased mitochondrial membrane potential and ATP levels, sensitivity to oxidative stress, and reduced life span (Ristow et al., 2000; Runko et al., 2008). Cardiomyopathy and cardiac failure in mice were also shown to be relieved by overexpression of frataxin (Schulz et al., 2010). A mutation in the Fe-S scaffold protein ISCU has been described in an inherited skeletal muscle disorder characterized by muscle weakness, exercise-induced lactic acidosis, deficiencies in aconitase and succinate dehydrogenase, and iron overload (Mochel at al., 2008; Kollberg et al., 2009). This finding was consistent with earlier reports of aconitase and succinate dehydrogenase deficiencies in muscle disorders (Haller et al., 1991; Hall et al., 1993). In light of the role of CL in Fe-S biogenesis, we speculate that the clinical presentation in BTHS may be exacerbated by additional deficiencies in Fe-S metabolism.

8.3   Mitochondrial protein import

The clinical presentation of a disorder known as dilated cardiomyopathy with ataxia (DCMA) syndrome is very similar to BTHS despite normal CL metabolism in DCMA. Symptoms include cardiomyopathy, elevated 3-methylglutaconic acid, and neutropenia. DCMA syndrome is due to a mutation in a gene thought to function in protein import, TIM14 (which shares homology with yeast Tim14p) (Davey et al., 2006). The similarity in the clinical outcomes of DCMA and BTHS suggests that BTHS may be caused or exacerbated by defective mitochondrial import of specific proteins, the identities of which may shed light on the pathology of the disorders. We speculate that proteins required for Fe-S biogenesis may be likely candidates.

9.   YEAST AS A MODEL FOR STUDYING BTHS

Yeast (*Saccharomyces cerevisiae*) is an excellent model organism for the study of BTHS. Yeast is nonpathogenic, can be easily used for genetic analyses, and has a rapid growth rate, which renders it one of the most favorable eukaryotic model systems. The tafazzin gene, which is defective in BTHS, is conserved from yeast to humans (Vaz et al., 2003; Gu et al., 2004; Ma et al., 2004). The CL biosynthetic pathway is well characterized, and knockout mutants of all steps are available in *S. cerevisiae* (Schlame and Greenberg, 1997; Schlame and Hostetler, 1997; Schlame et al., 2000; Osman et al., 2010; Xu et al., 2003; Beranek et al., 2009). This has enabled us to study the effects of a defective CL pathway in yeast cells. The availability of the yeast deletion mutant collection of all non-essential genes facilitates the construction of double mutants for studies of synthetic lethality. Synthetic lethality analysis is a technique in which double mutants of two nonessential genes show a lethal/sick phenotype when they interact with each other,

directly or indirectly (Hartman et al. 2001). Synthetic lethality studies can contribute to understanding the functions of the interacting genes. The genetic screen to identify synthetic interactions with CL mutants (discussed in chapter 2 and 4) among all 4,800 yeast deletion mutants is not currently possible in any other model for BTHS. We used synthetic lethality to screen 4,800 non-essential genes for synthetic interaction with CL mutant cells and identified pathways relevant to the clinical presentation of BTHS. The role of CL in there pathway is the subject of my dissertation.

10.   PROJECT OUTLINE

The goal of my doctoral research described in this dissertation was to elucidate the role of CL in cellular processes that may identify mechanisms responsible for the variations in BTHS symptoms, especially cardiomyopathy. Using the "awesome power of yeast genetics," I have conducted the following studies.

As discussed above, the loss of CL causes a wide variety of phenotypes, suggesting that the identification of different physiological modifiers will elucidate the various biochemical pathways defective due to CL-deficiency. A genome-wide Synthetic Genetic Array (SGA) screen of all the non-essential yeast genes was performed to identify mutants that synthetically interact with CL mutants. I grouped these genes based on biological function and validated interactions by tetrad analysis. The interacting genes could identify cellular functions that require CL. Preliminary experiments indicated that CL mutants interact with the pyruvate dehydrogenase complex (PDH). Because the role of PDH is to convert pyruvate to acetyl-CoA by a process called pyruvate decarboxylation, I hypothesized that the loss of CL leads to decreased acetyl-CoA synthesis. The studies in Chapter 2 show that cells lacking CL exhibit decreased acetyl-CoA levels and acetate

utilization, suggesting that CL is required for acetyl-CoA synthesis. Thus, Chapter 2 identifies acetyl-CoA synthesis as a metabolic pathway that may affect the clinical presentation in BTHS.

Previous studies have reported that perturbation of Fe-S biogenesis leads to defects in the TCA cycle. The studies in Chapter 2, demonstrating that the loss of CL decreases acetyl-CoA synthesis, identifies another route whereby the TCA cycle may be perturbed, i.e., the intracellular transport of acetyl-CoA. Because acetyl-CoA synthesized in different compartments is transported into mitochondria by specific shuttle systems, I hypothesized that perturbation of the acetyl-CoA shuttle system may contribute to the TCA cycle deficiency. The studies in Chapter 3 show that decreased growth of the CL mutant at elevated temperature was rescued by carnitine and acetylcarnitine. Consistent with this, the loss of CL leads to decreased carnitine-acetylcarnitine translocase activity. I also provide evidence that the decreased transport of acetyl-CoA into the mitochondria increases the need for transfer of TCA cycle intermediates by the glyoxylate cycle. These findings suggest that in addition to decreased activity of Fe-S enzymes in the TCA cycle, another mechanism that is expected to contribute to TCA cycle deficiency is defective transport of acetyl-CoA, which contributes to the depletion of precursors for the TCA cycle.

Chapter 4 identifies cellular functions that are perturbed in the absence of tafazzin. An SGA screen was carried out with the *taz1Δ* mutant to identify potential synthetic interactions, which are likely to identify genes that share essential functions with tafazzin. The screen identified 70 potential synthetic lethal mutants and 102 potential synthetic sick mutants, which were then grouped based on biological function. Exciting interactions

were observed with genes coding for phospholipase B, argininosuccinate shunt enzyme, mitochondrial iron homeostasis, and vacuolar protein sorting. These findings suggest that tafazzin may be involved in remodeling of phospholipids other than CL, and that CL and tafazzin deficiency may result in a defective TCA cycle and perturbation of vacuole function.

Although the studies described in this thesis identify interesting cellular functions of CL, many questions related to the mechanism underlying the role of CL in these processes remain unclear. I anticipate that understanding the role of CL in essential cellular processes could help to elucidate the phenotypic disparities in BTHS and will have a significant positive impact on the disorder, because it may identify new metabolic targets for treatment. Future studies and unanswered questions are summarized in Chapter 5.

CHAPTER 2 LOSS OF CARDIOLIPIN LEADS TO PERTURBATION OF ACETYL-COA SYNTHESIS

INTRODUCTION

Cardiolipin (CL) is a unique phospholipid with dimeric structure that constitutes about 15% of total phospholipid in mitochondria (Pangborn, 1947; Schlame and Ren, 2009; Schlame et al., 2000; Jakovcic et al., 1971). CL is synthesized *de novo* in the inner mitochondrial membrane (Gallet et al. 1997), and it undergoes remodeling to replace the saturated fatty acyl chains with unsaturated fatty acyl chains (Beranek et al., 2009; Xu et al., 2003). CL plays an important role in maintaining mitochondrial structure, interaction with mitochondrial membrane proteins, stability of respiratory chain supercomplexes (Cruciat et al., 2000; Zhang et al., 2002b; Pfeiffer et al., 2003), and other mitochondrial functions such as membrane potential, protein import, and respiration (Schlame and Ren, 2006; Jiang et al., 2000; Gebert et al., 2009). Loss of CL perturbs mitochondrial bioenergetics and decreases ATP synthesis (Koshkin and Greenberg, 2000; Jiang et al., 2000; Koshkin and Greenberg, 2002; Claypool et al., 2008). Aberrant CL remodeling leads to the severe genetic disorder Barth syndrome (BTHS) (Schlame et al., 2005). Mutation of tafazzin, the transacylase that remodels CL, leads to decreased total CL, increased MLCL, and aberrant CL species (Schlame et al., 2002; Valianpour et al., 2005; Schlame et al., 2003). The clinical presentation of BTHS includes cardio- and skeletal myopathy, neutropenia, 3 - methylglutaconic aciduria, growth retardation, abnormal mitochondria, and defective oxidative phosphorylation (Barth et al., 1981). Interestingly, disparities in clinical manifestation are identified in BTHS (Johnston et al., 1997; Bleyl et al., 1997; Barth et al., 1999b), indicating that physiological modifiers affect the phenotype associated with CL deficiency.

To identify modifiers that exacerbate CL deficiency, I carried out a Synthetic Genetic Analysis (SGA) with the yeast CL synthase mutant *crd1Δ*, which lacks CL. Interestingly, genetic interaction of *crd1Δ* was observed with pyruvate dehydrogenase (PDH), which converts pyruvate to acetyl-CoA (Pronk et al., 1996). PDH null mutants are viable because acetyl-CoA can be synthesized by the cytosolic PDH-bypass pathway, the last step of which is the acetyl-CoA synthetase catalyzed conversion of acetate to acetyl-CoA, which is shuttled into the mitochondria. Other routes to acetyl-CoA synthesis include oxidative degradation of amino acids (Vorapreeda et al., 2012), decarboxylation of pyruvate (Guest et al., 1989), and oxidation of fatty acids (Trotter, 2001). I hypothesized that synthetic lethality with PDH mutants may be explained by a requirement for CL in one or more alternate routes of acetyl-CoA synthesis. In this study, I demonstrate that *crd1Δ* cells have reduced acetyl-CoA levels and diminished ability to utilize acetate, suggesting that the PDH-bypass pathway is perturbed in cells lacking CL. These results show for the first time that CL is required for acetyl-CoA synthesis to maintain energy metabolism.

MATERIALS AND METHODS

Yeast strains, plasmids, and growth media

The yeast *S. cerevisiae* strains used in this study are listed in Table 2.1. Single deletion mutants were obtained from the yeast knockout deletion collection (Invitrogen). Double mutants were obtained by tetrad dissection. Synthetic complete (YNB) medium contained adenine (20.25 mg/liter), arginine (20 mg/liter), histidine (20 mg/liter), leucine (60 mg/liter), lysine (200 mg/liter), methionine (20 mg/liter), threonine (300 mg/liter),

tryptophan (20 mg/liter), uracil (20 mg/liter), yeast nitrogen base without amino acids (Difco), and glucose (2%) (YNBD) or sodium acetate (2%) (YNBA). Synthetic dropout medium contained all ingredients mentioned above but lacked specific compounds required for selection. Sporulation medium contained potassium acetate (1%), glucose (0.05%), and the essential amino acids. Complex medium contained yeast extract (1%), peptone (2%), and glucose (2%) (YPD). Solid medium was prepared by adding 2% agar.

To construct the *crd1Δcan1Δ* starting strain, a 1.8 kb *CAN1* deletion cassette was amplified from Y5563 (kindly provided by Dr. Charles Boone) by sense primer (5'-TAGGGCGAACTTGAAGAATAACC-3') and antisense primer (5'-ACGAAAAATGAGTAAAAATTATCTT-3') and inserted into the genome of BY4741 *(MATa)* with the disruption confirmed by PCR. The *can1Δ* mutant was then crossed to BY4742 *(MATα)* to obtain an *MATα can1Δ* strain by tetrad analysis. The *CRD1* gene in the *can1Δ* mutant *(MATα)* was disrupted by a 1.8 kb *URA3* fragment released from the PUC19 plasmid digested using PvuII. The disruption of *CRD1* was confirmed by PCR, Southern blot, and phospholipid analysis.

Synthetic Genetic Array (SGA)

The *MATα can1Δcrd1Δ* mutant was crossed to the array of deletion mutants in the *MATa* background, in which the deletions are linked to the dominant selectable marker for geneticin resistance, *KanMX4*. Diploids were selected and sporulation was induced. Haploid spore progeny were transferred to synthetic medium lacking histidine, which allowed for selective germination of *MATa* cells. Following two rounds of selection in His-synthetic medium, double mutant *MATa* progeny were selected in Ura- medium supplemented with geneticin. Independent confirmation of synthetic lethality was carried

out by tetrad analysis to rule out false positives and false negatives (Tong et al., 2001). Synthetic interaction between CL and deletion mutants was determined by examining growth of the double mutant compared to single mutants and wild-type on YPD.

Acetyl-CoA determination

Cells were grown to the logarithmic growth phase and a sample (3 ml) of the culture was centrifuged at 1700 g. Pellets were resuspended in 1 ml ddH$_2$O and centrifuged for 1 min at 9300 g. The resulting cell pellet was subjected to cell lysis and the lysed samples were rapidly quenched with 130 µl of 45:45:10 acetonitrile / methanol / H2O + 0.1% glacial acetic acid and spiked with 10 µmol l^{-1} glutaryl-CoA as an internal standard. The resuspended extract was incubated on ice with intermittent vortexing for 15 min. An equal molar volume of ammonium hydroxide was added post incubation to neutralize the acetic acid, and each extract was centrifuged for 3 min at 15,700 g, transferred to a new 1.5 ml microfuge tube and centrifuged for 5 min at 15,700 g. The clarified extract (10 µl) was injected for HPLC-MS/MS analysis (Bennett et al., 2009; Armando et al., 2011).

Quantitative PCR (qPCR)

Cultures (10 ml) were grown to the logarithmic growth phase, cells were harvested, and total RNA was isolated using the RNeasy Plus mini kit from Qiagen. Complementary DNA (cDNA) was synthesized using a Transcriptor First Strand cDNA Synthesis Kit (Roche Applied Science) according to the manufacturer's manuals. qPCRs were performed in a 25µl volume using Brilliant III Ultra-Faster SYBR Green qPCR Master Mix (Agilent Technologies, Santa Clara, CA). The primers for qPCR are listed in Table 2.2. PCRs were initiated at 95°C for 10 min for denaturation followed by 40 cycles consisting of 30 s at 95°C and 60 s at 55°C. RNA levels were normalized to *ACT1*. Relative values

of mRNA transcripts are shown as fold change relative to indicated controls. Primer sets were validated according to the Methods and Applications Guide from Agilent Technologies. Optimal primer concentrations were determined, and primer specificity of a single product was monitored by a melt curve following the amplification reaction. All primers were validated by measurement of PCR efficiency and have calculated reaction efficiencies between 95 and 105%.

Gene tagging, SDS-PAGE, and Western blot analysis

The C-terminal HA-tagged Pda1, Pdb1, Lat1, Lpd1, and Pdx1 strains were derived from the BY4742 wild-type and *crd1Δ* strains by transforming with a PCR product amplified from pFA6-3HA-TRP1 (TRP marker). The primers used for tagging are listed in Table 2.3. Proteins were extracted from cells grown to an A_{550} of 0.5, separated by 8% SDS-PAGE, transferred to a PVDF membrane, and analyzed using primary antibodies to the HA tag (1:1000) and to α-tubulin (1:1000) (Santa Cruz Biotechnology). Proteins were visualized using appropriate secondary antibody conjugated to horseradish peroxidase (1:3000) and detected using the ECL chemiluminescence system (GE Healthcare).

PDH activity

Mitochondria were isolated from cell lysates prepared as described previously (Diekert et al., 2001). Briefly, spheroplasts created by lyticase were ruptured by dounce homogenization, and mitochondria were isolated by differential centrifugation. Total protein concentration was determined with a Bradford assay kit (Pierce) with BSA as the standard. The activity of PDH in isolated mitochondria was measured spectrophotometrically by determining the reduction of NAD^+ to NADH, coupled to the reduction of a reporter dye to yield a colored reaction product with an increase in

absorbance at 450 nm in kinetic mode for 10-60 min. at 37°C (BioVision PDH activity colorimetric assay kit; Catalog # K679-100).

RESULTS

Genome-wide synthetic lethal SGA screen with *crd1Δ*

Genome-wide synthetic lethality screen was performed using SGA methodology by mating the query strain (*BY4742 MATα can1Δcrd1Δ*) to the yeast deletion set and selecting double mutants (Tong et al., 2001) at two different temperatures (30°C and 37°C). In the query strain, the *crd1Δ* mutation was linked to the dominant selectable marker *URA3* and the *can1Δ* mutation was linked to the reporter construct *MFA1pr-HIS3*, which is expressed only in *MATa* cells. This strain (*MATα*) was separately crossed with the array of all 4,800 deletion mutants in the *MATa* background, in which the deletion is linked to the dominant selectable marker for geneticin resistance, *KanMX*. The *MATα* strain was lys⁻ met⁺, and the *MATa* strain was met⁻ lys⁺. Diploids were selected on plates lacking both lysine and methionine, and sporulation was induced. Haploid spore progeny were transferred to synthetic medium lacking histidine, which allows for selective germination of *MATa* cells. Following two rounds of selection, the *MATa* cells were transferred to medium lacking uracil and containing geneticin. Synthetic interaction was indicated by decreased growth of the haploid progeny. As expected, the SGA screen identified a large number of synthetic interactions that include 105 potential synthetic lethal interactions at 30°C and 65 potential lethal interactions at 37°C. These were grouped based on biological function (Fig. 2.1A, Tables 2.4 and 2.5).

The screen identified mutants previously shown to be synthetically lethal with *crd1Δ*, including *psd1Δ* (Gohil et al., 2005), *tom5Δ* (Gebert et al., 2009), and *get3Δ* (Joshi

et al., 2016). Synthetic lethal mutants were also identified in two cellular functions previously shown to require CL, including cell wall biogenesis and Fe-S biogenesis. Synthetic lethality with PDH identified a new role of CL in energy metabolism.

a. Cell wall biogenesis: The SGA screen identified genes involved in cell wall biogenesis, a process that was previously shown to require a functional CL pathway (Fig. 2.1B). CL mutants exhibit temperature-sensitive growth that is associated with defects in the cell wall and vacuole (Zhong et al., 2005; Zhong et al., 2007; Chen et al., 2008b). Zhong et al. (2007) showed that the PKC-Slt2 cell integrity pathway and glucan synthase activity require the synthesis of mitochondrial phospholipids PG and/or CL. *pgs1Δ* cells, which are blocked in the first step of CL synthesis, have reduced glucan synthase activity and a decreased glucan synthase catalytic subunit. In addition, activation of Slt2, the downstream effector of the PKC-activated cell integrity pathway was defective. In this light, it was interesting that the SGA screen identified *KRE6*, which encodes an integral membrane protein required for β-1,6 glucan biosynthesis (Roemer and Bussey, 1991). Disruption of *KRE6* results in perturbation of cell wall biogenesis and decreased growth on fermentable carbon source. Mutants of other genes involved in the cell integrity pathway were identified in the screen, including *MSG5*, *PIR3*, *RHO2*, *ROM2*, and *UTR2*.

b. Mitochondrial processes: The synthetic lethality screen identified mutants in mitochondrial processes that have been shown to required CL (Fig. 2.1B). These include *ISA1*, *ISA2* and *SSQ1* in Fe-S biogenesis, and *SOD2* and *GRX5* required for oxidoreductase activity. Previous studies indicated that the loss of CL leads to perturbation of mitochondrial and cellular iron homeostasis (Patil et al., 2013). *ISA1* and *ISA2* encode a protein required for maturation of mitochondrial Fe-S proteins. *GRX5* and

SSQ1 encode a protein required for assembly of Fe-S clusters. These findings support a role for CL in Fe-S cluster formation and/or transfer of Fe-S clusters to apoprotein. *crd1Δ* was also synthetically lethal with a mutant in *SOD2*, which codes for mitochondrial manganese superoxide dismutase, an enzyme that protects cells against oxygen toxicity (Saffi et al., 2006; van Loon AP et al., 1986). Disruption of *SOD2* leads to lethality due to the accumulation of free radicals. It is likely that the *crd1Δ* mutant accumulates free radicals due to defects in mitochondrial respiration (Chen et al., 2008a). Therefore, *SOD2* may play a pivotal role in scavenging free radicals in *crd1Δ*.

Loss of CL leads to decreased acetyl-CoA synthesis

The SGA screen revealed that *crd1Δ* is synthetically lethal with *pdb1Δ* (the E1β subunit of PDH), as shown in Fig. 2.2A. This finding was especially interesting as it suggested for the first time that CL may play a role in the synthesis of acetyl-CoA. I screened all mutants of the PDH complex for synthetic lethality with *crd1Δ*. In *S. cerevisiae*, PDH is an ~8 MDa multi enzyme complex (Uhlinger et al., 1986) consisting of multiple copies of three enzymes: pyruvate dehydrogenase (E1) (Pda1p, and Pdb1p) (Steensma et al., 1990; Miran et al., 1993), dihydrolipoamide acetyltransferase (E2) (Lat1p) (Niu et al., 1988), and dihydrolipoamide dehydrogenase (E3) (Lpd1p) (Dickinson et al., 1986). A fourth component, protein X (Pdx1p), does not appear to have a catalytic function but is probably involved in assembly of the complex (Lawson et al., 1991). The double mutants were checked for growth at elevated temperatures. The *crd1Δ* mutant in this genetic background (BY4741) can grow at 37°C but not at 39°C. With the exception of E3, all PDH mutants were synthetically lethal with *crd1Δ*, including mutants of E1 & E2 subunits and protein X of the PDH complex (Fig. 2.2B). Because acetyl-CoA levels

depend primarily on pyruvate utilization by PDH in the mitochondria and PDH-bypass in the cytosol, decreased growth of the double mutants suggested that *crd1Δ* cells exhibit defective synthesis of acetyl-CoA.

Acetyl-CoA levels were measured in wild-type and *crd1Δ* cells at optimal (30°C) and elevated (35°C, 37°C, and 39°C) temperatures. The acetyl-CoA levels in *crd1Δ* were decreased at elevated temperature relative to those in wild-type cells. At 39°C, an 80% reduction was observed in *crd1Δ* cells (Fig. 2.3). Previous studies reported that the PDH-bypass pathway predominates over the PDH pathway during fermentative growth (Boubekeur et al.,1999; Ciriacy, 1975; Paquin and Williamson, 1986; Briquet, 1977; Nalecz et al., 1991; Johnston, 1999), suggesting that decreased acetyl-CoA levels in *crd1Δ* cells is likely due to perturbation of this pathway.

PDH-bypass deficiencies in *crd1Δ*

The PDH-bypass pathway, which converts pyruvate to acetyl-CoA during fermentative growth, occurs predominantly in the cytosol. Pyruvate decarboxylase decarboxylates pyruvate to acetaldehyde, which is converted to acetate by acetaldehyde dehydrogenase. The conversion of acetate to acetyl-CoA is catalyzed by acetyl-CoA synthetase (Pronk et al., 1996; Dickinson, 1996; Van den Berg et al., 1995; Meaden et al., 1997; Van den Berg et al., 1996). I explored the possibility that decreased acetyl-CoA levels in the *crd1Δ* mutant resulted from perturbation of the PDH-bypass. Defects in this pathway cause decreased growth on medium containing acetate as a sole carbon source, because the last step of the PDH-bypass is the conversion of acetate to acetyl-CoA (De Virgilio et al., 1992; Remize et al., 2000; Boubekeur et al., 1999; Kozak et al., 2014). On acetate medium, *crd1Δ* cells exhibited decreased growth (Fig. 2.4A) and an increased

doubling time (Fig. 2.4B). Decreased growth on acetate suggested that acetyl-CoA levels might be decreased. In agreement with this, *crd1Δ* cells exhibited ~50% decrease in acetyl-CoA levels in these growth condition (Fig. 2.5).

PDH and PDH-bypass null mutants are viable, which suggests that either pathway is sufficient to synthesize acetyl-CoA in CL-deficient cells. If CL is required for synthesis of acetyl-CoA in the cytosol by the PDH-bypass, further perturbation of PDH-bypass is not expected to exacerbate growth of *crd1Δ* cells. To test this prediction, I examined genetic interaction between *crd1Δ* and mutants in acetyl-CoA synthetase (*ACS1* and *ACS2*). In agreement with the prediction, *acs1Δ* and *acs2Δ* did not interact genetically with *crd1Δ* (Fig. 2.6).

Published studies have shown that cells compensate for a defective PDH-bypass by up-regulating PDH gene expression and increasing protein levels (Boubekeur et al., 1999; Kozak et al., 2014; Wei et al., 2009; Avidan and Pick, 2015). The *crd1Δ* mutant exhibited more than 2-fold increased PDH gene mRNA levels, including *PDA1*, *PDB1*, *LAT1*, *LPD1*, and *PDX1* (Fig. 2.7A). Protein levels of *PDB1, LAT1, LPD1,* and *PDX1* were also elevated in *crd1Δ* cells, although levels of *PDA1* were not (Fig. 2.7B). However, in spite of increased mRNA and protein levels, the specific activity of PDH was not increased in the *crd1Δ* mutant (Fig. 2.8). As CL is required for mitochondrial protein import (Jiang et al., 2000; Gebert et al., 2009) and association of mitochondrial matrix proteins with mitochondrial membrane (Campuzano et al., 1997), it is possible that CL deficiency may account for decreased specific activity of PDH. Taken together, these experiments indicate that CL-deficient cells have a decreased ability to convert acetate to acetyl-CoA via the PDH-bypass, and possibly decreased enzymatic activity of PDH.
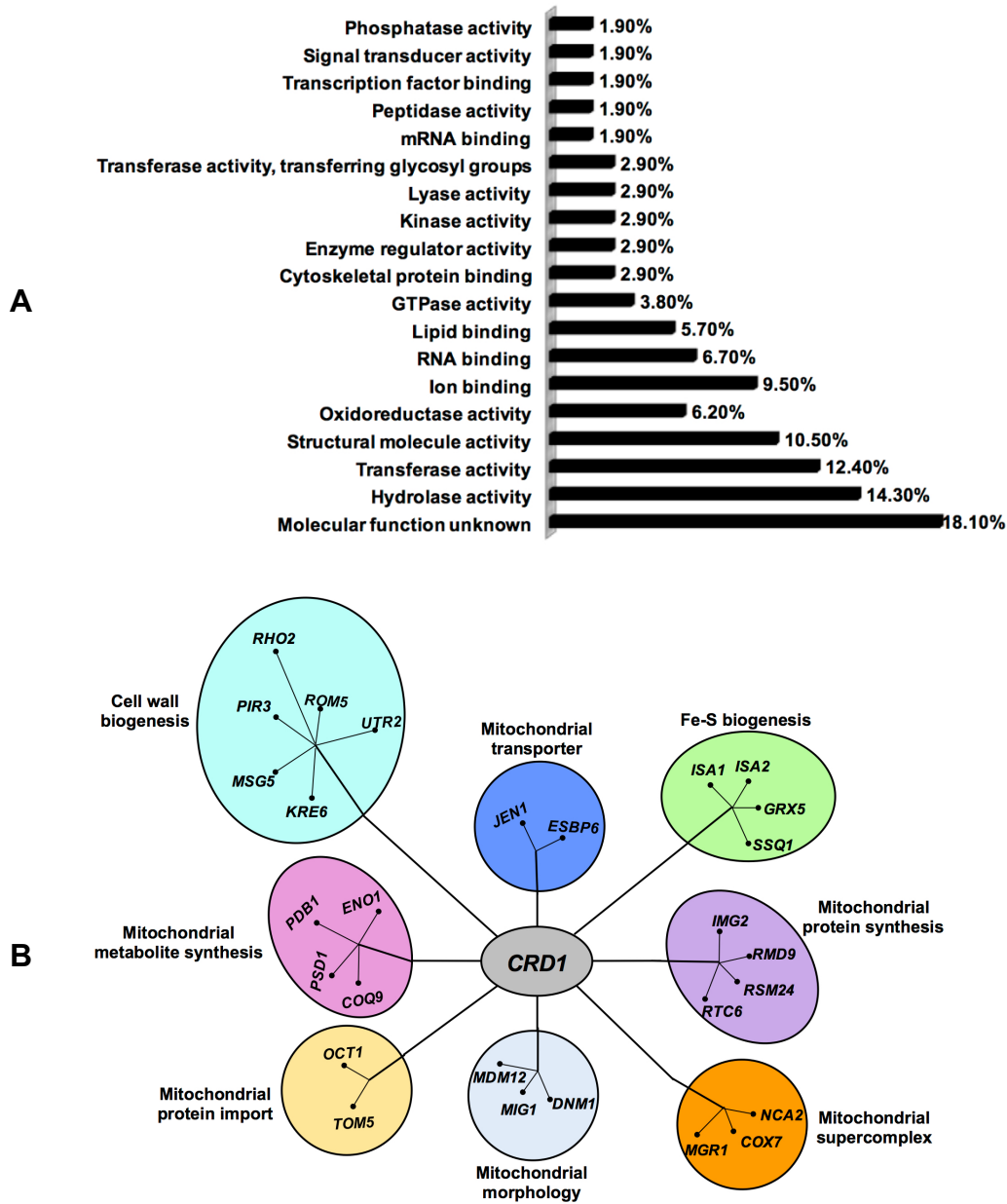
FIGURE 2.1. **Functional classification of genes exhibiting synthetic lethality with** *crd1Δ*. (A) Synthetic lethal interactions identified by the SGA were classified by biological process, based on gene ontology. (B) Synthetic lethal partners of *crd1Δ* identified eight biological processes. Genes that are functionally related radiate from a central point.

FIGURE 2.2. Genetic interaction of PDH mutants with *crd1Δ*. (A) Cells were pre-cultured in YPD overnight, serially diluted, plated on YNBD, and incubated at 30°C and 37°C for 3-5 days. (B) Synthetic interaction between *CRD1* and PDH mutants was determined by examining growth of the double mutant compared to isogenic parental strains and wild type.
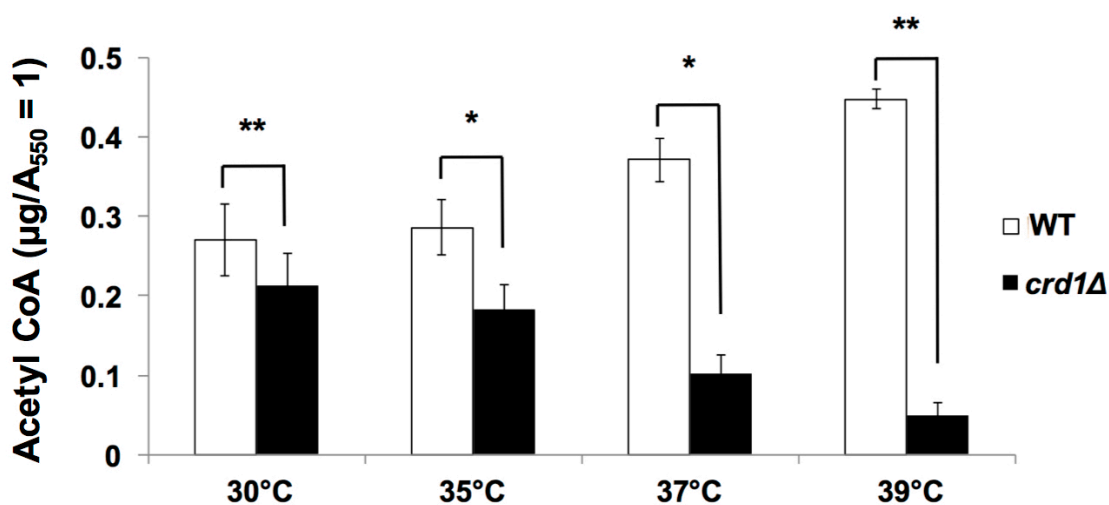
FIGURE 2.3. Decreased acetyl-CoA levels in *crd1Δ* cells. Wild-type and *crd1Δ* cells were grown at the indicated temperatures in YPD until cells reach an A_{550} of 1. Cells were pelleted and acetyl-CoA was extracted using glutaryl-CoA as an internal standard. The clarified extract (10 µl) was analyzed by HPLC-MS/MS. Data shown are mean ± S.E. (n = 6) (*p<0.05, **p<0.01). (Mass spectrometry was carried out by Krishna Rao Maddipati, Director, WSU Lipidomics Core).
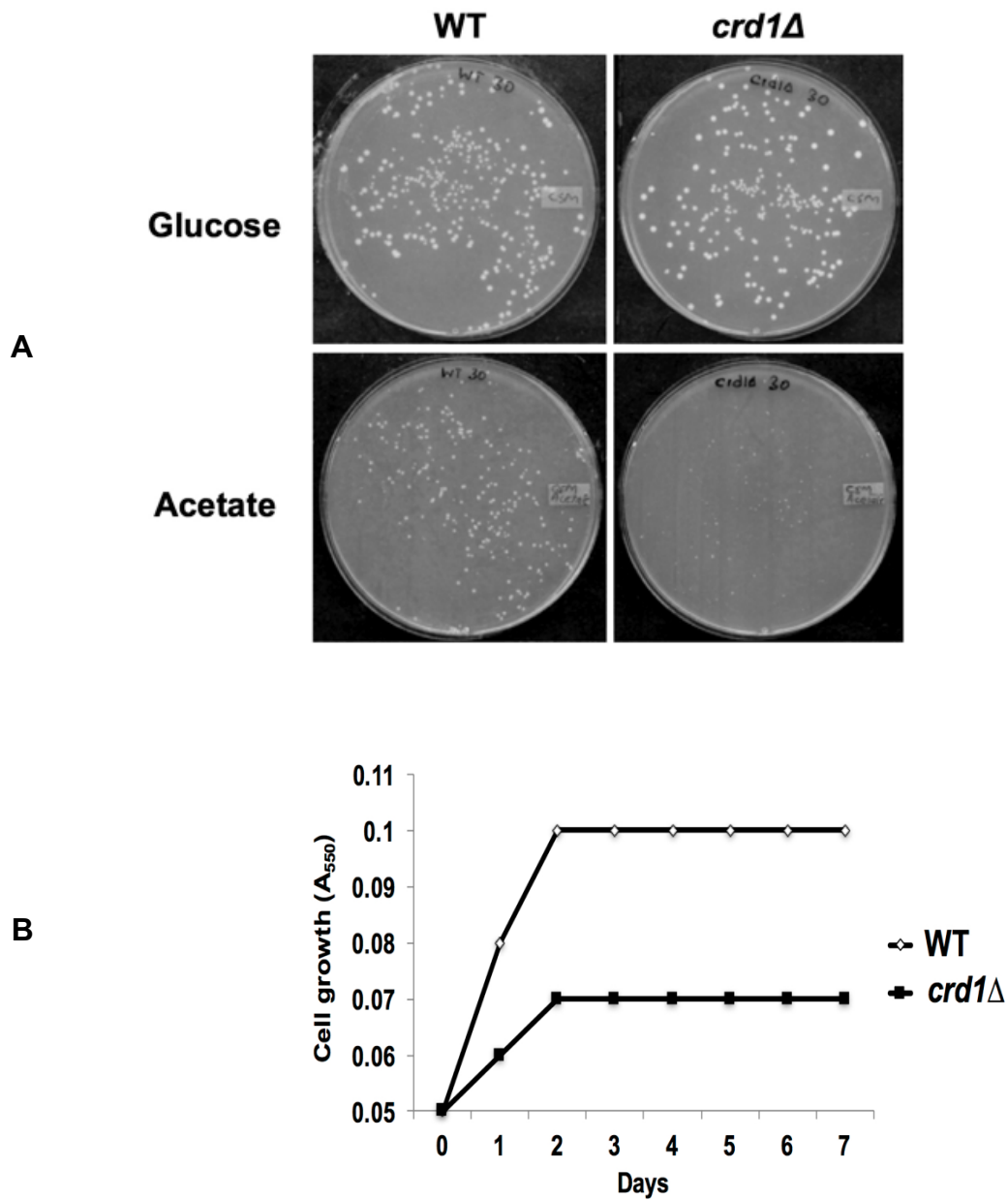
FIGURE 2.4. Decreased growth of *crd1Δ* cells on acetate. (A) Cells were pre-cultured overnight in YNBD and serially diluted, plated on YNBD and YNBA, and incubated at 30°C for 3-5 days. (B) Growth in liquid YNBA was determined by measuring A_{550}. The growth curves are representative of three experiments.
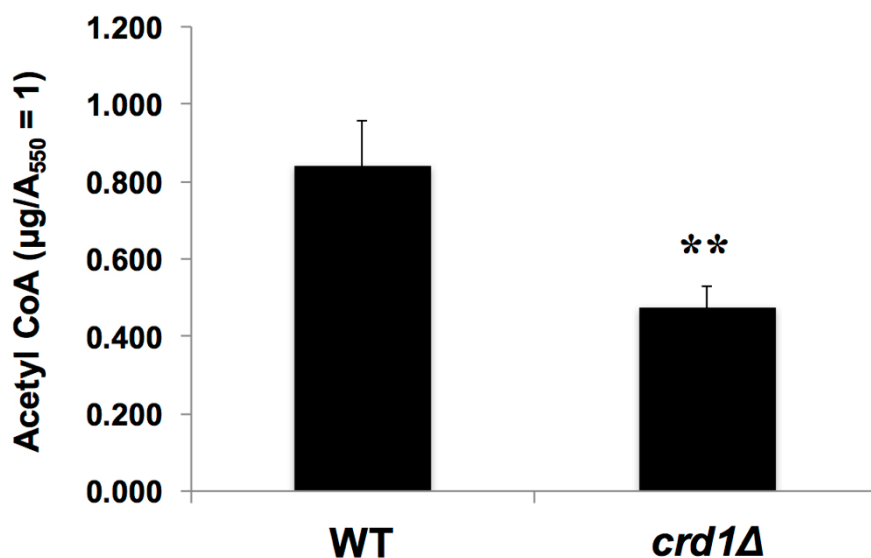
FIGURE 2.5. Decreased acetyl-CoA levels in *crd1Δ* cells grown on acetate. Acetyl-CoA levels in wild-type and *crd1Δ* cells grown in YNBA was determined as described in "Methods and Materials". Data shown are mean ± S.E. (n = 6) (**p<0.01). Data shown are mean ± S.E. (n = 3). (Mass spectrometry was carried out by Krishna Rao Maddipati, Director, WSU Lipidomics Core).
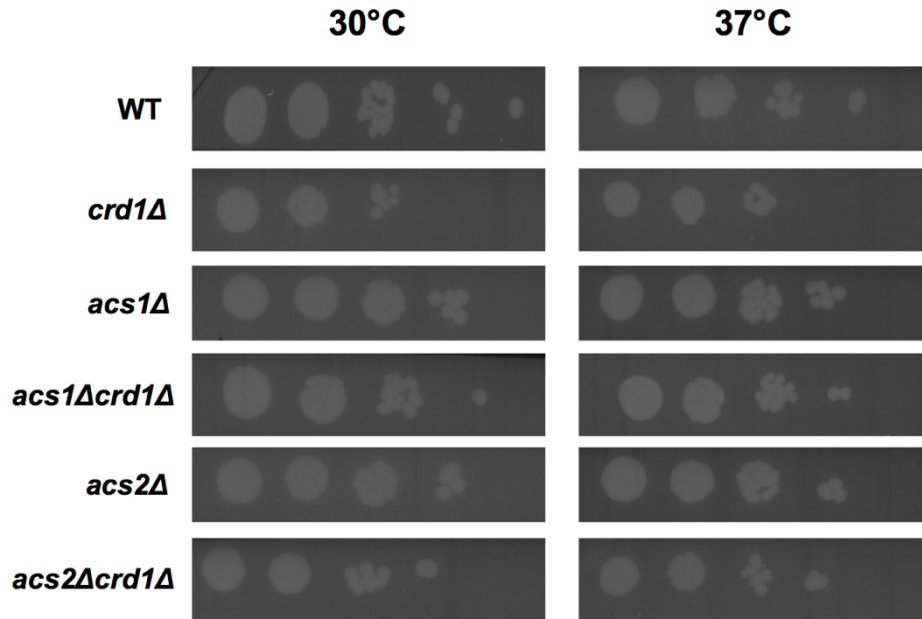
FIGURE 2.6. *crd1Δ* and acetyl-CoA synthetase mutants do not exhibit genetic interaction. Cells were pre-cultured in YPD overnight, serially diluted, plated on YNBD, and incubated at 30°C or 37°C for 3-5 days.
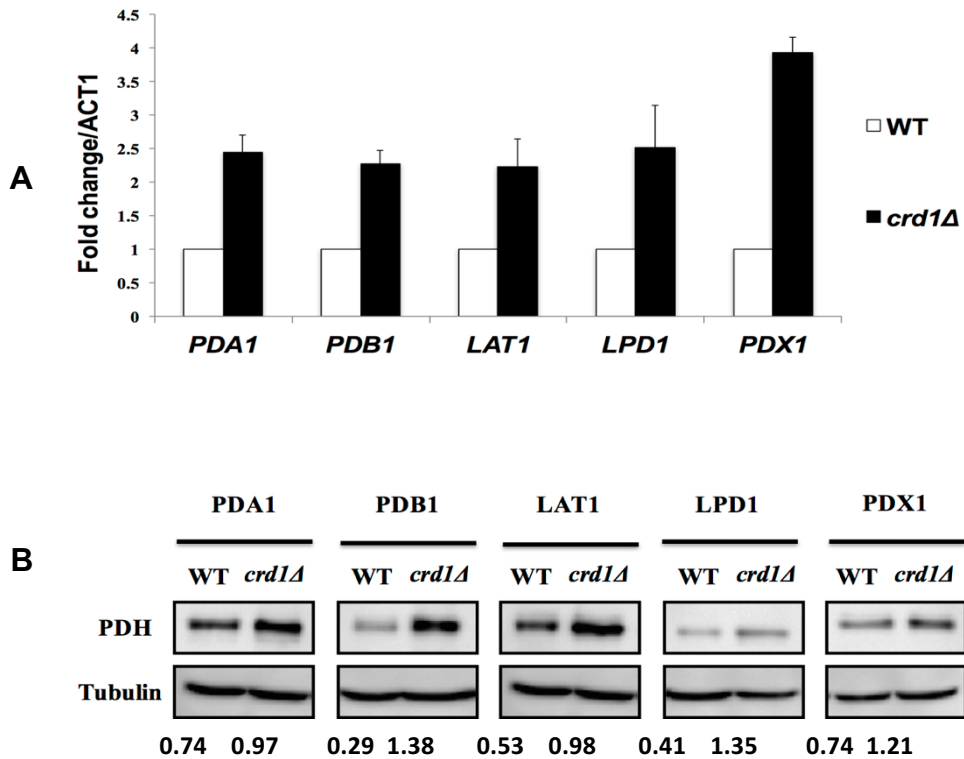
FIGURE 2.7. Increased expression and protein levels of PDH subunits in *crd1Δ*. (A) The mRNA levels of PDH genes from cells grown in YPD at 30°C to the logarithmic phase were quantified by qPCR. Values are reported as fold change in expression over wild-type. Expression was normalized to the mRNA levels of the internal control *ACT1*. Data shown are mean ± SE (n=6). (B) Wild-type and *crd1Δ* cells expressing the indicated HA-tagged genes were cultured in YPD to the mid-logarithmic phase (A_{550} of 0.5) at 30°C and cell lysates were prepared. Anti-HA antibody was used to detect HA-tagged proteins using Western blot analysis. 50 µg of total protein was loaded for each sample, and α-tubulin was used as an internal control. The levels of PDH protein were quantified using ImageJ software. The figure shown is representative of three experiments.
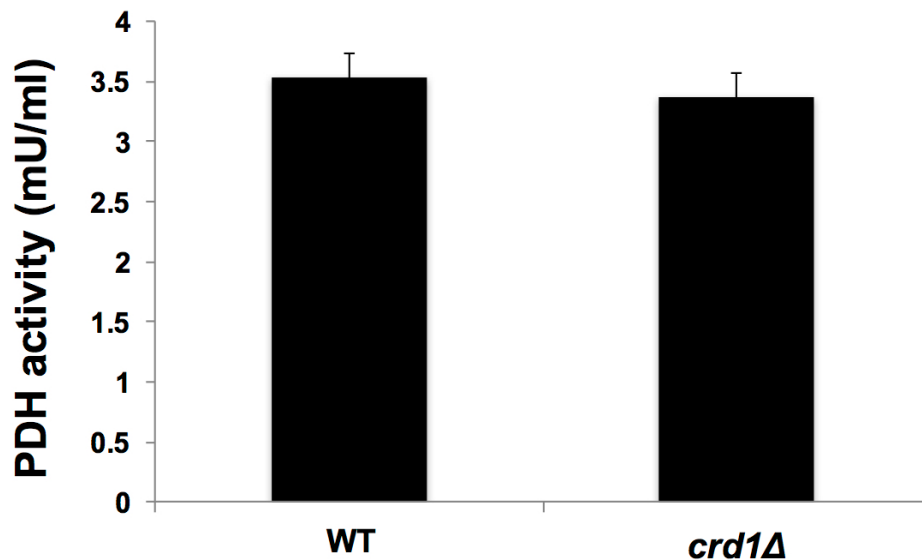
FIGURE 2.8. PDH activity is not altered in *crd1Δ* cells. Wild-type and *crd1Δ* cells were grown in YPD at 30°C to the logarithmic phase and activity was calculated in mitochondria prepared from wild-type and *crd1Δ* cells (10 µg). PDH activity (mU/mg) or (nmol/min/ml) were assayed as described in the "Materials and Methods". One unit of PDH is the amount of enzyme that generates 1.0 µmol of NADH per min. at pH 7.5 at 37°C. Data shown are mean ± SE (n=6).

DISCUSSION

In this study, I carried out a genome-wide genetic screen to identify cellular processes that require CL. The most striking finding was synthetic lethality between *crd1Δ* and PDH mutants. Subsequent experiments revealed that acetyl-CoA synthesis was perturbed in CL-deficient cells. The mechanism underlying this defect is perturbation of the PDH-bypass, as *crd1Δ* cells exhibit decreased acetyl-CoA levels and decreased growth on acetate as sole carbon source. The screen also identified synthetic lethal interactions that support a role for CL in cell wall biogenesis and mitochondrial processes previously shown to require CL.

How does CL deficiency cause perturbation of the PDH-bypass pathway? The PDH-bypass pathway converts acetate to acetyl-CoA in the cytosol during fermentative growth. Indeed, I found that, compared to WT, *crd1Δ* cells grew poorly on medium containing acetate as a sole carbon source and exhibited decreased acetyl-CoA levels. The most likely defect is in acetyl-CoA synthetase (*ACS1* and *ACS2*), as deletion of acetyl-CoA synthetase does not exacerbate growth of *crd1Δ*. Several possibilities may account for the hypothesized decreased acetyl-CoA synthetase activity in the CL mutant. Acetyl-CoA synthetase may require CL for activation or stability, as the enzyme is localized in the outer mitochondrial membrane and may this interact with CL (Fujino et al., 2001). It is also possible that import of the protein into mitochondria may be decreased, as cells lacking CL exhibit decreased mitochondrial protein import (Jiang et al., 2000; Gebert et al., 2009). Another possibility is that mRNA and protein levels of acetyl-CoA synthetase may be decreased.

Based on these results, I propose the following model to account for decreased acetyl-CoA synthesis in *crd1Δ* (Fig. 2.9). The two common routes for acetyl-CoA synthesis are through direct conversion of pyruvate, either by the PDH-bypass under fermentative conditions (Shiba et al., 2007) or PDH under respiratory conditions (Guest et al., 1989). These routes complement each other when either pathway is defective. Under fermentative conditions, CL-deficient cells cannot convert acetate to acetyl-CoA, resulting in decreased acetyl-CoA levels. The cellular response to decreased acetyl-CoA in *crd1Δ* is increased PDH gene expression and protein synthesis. However, in *crd1Δ* cells PDH enzyme activity is not increased, and acetyl-CoA levels are decreased.

The SGA screen also provided additional support for the role of CL in Fe-S biogenesis and cell wall synthesis. Patil et al. (2013) showed that *crd1Δ* cells exhibit defective Fe-S biogenesis resulting in perturbation of iron homeostasis. Defective Fe-S biogenesis leads to decreased activity of Fe-S enzymes, including TCA cycle enzymes aconitase and succinate dehydrogenase, which in turn perturbs the TCA cycle. This study identified genes that are involved in assembly of the Fe-S cluster and maturation of mitochondrial Fe-S proteins. These findings further support a role of CL in Fe-S biogenesis. The CL pathway was also shown to be required for cell wall synthesis (Zhong et al., 2007). The cell wall integrity mitogen-activated protein kinases Slt2 is not phosphorylated in the *pgs1Δ* mutant. Perturbation of the PKC pathway in *pgs1Δ* leads to the breakdown of glucan and chitin in the cell wall. The current study identified the cell wall biogenesis gene *KRE6* as synthetically lethal with *crd1Δ*, further supporting the role of CL in maintaining cell integrity.
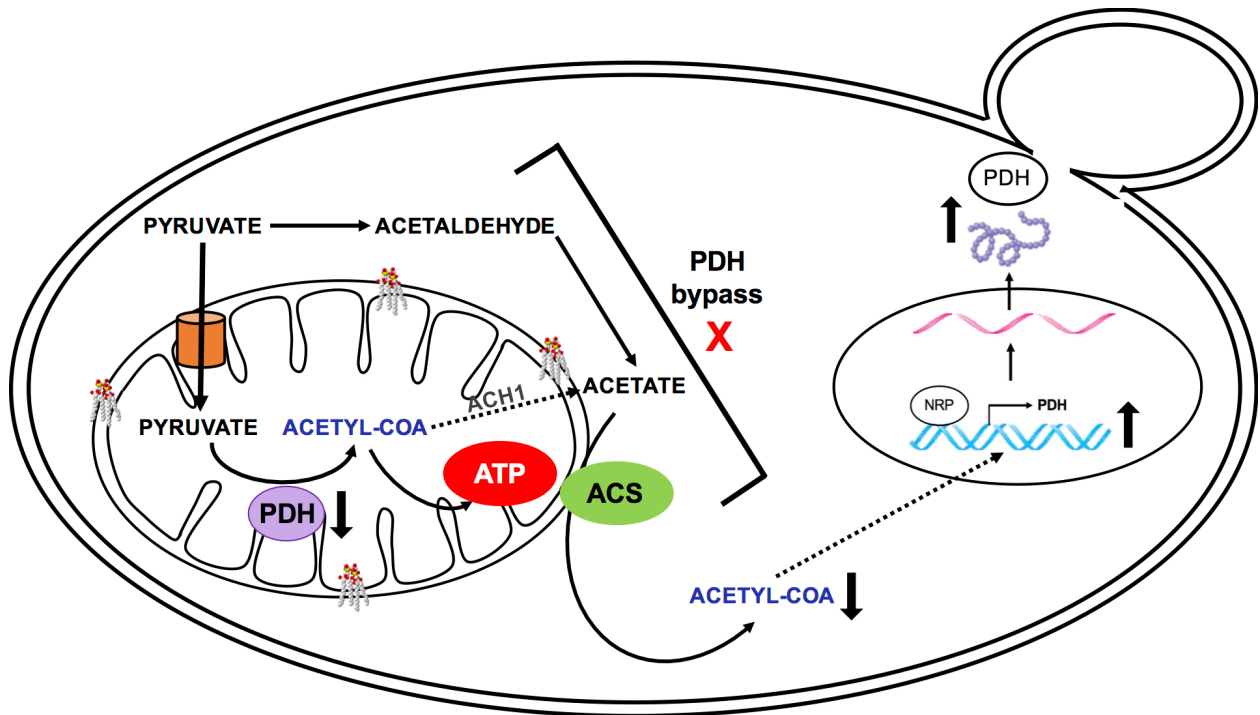
FIGURE 2.9. Model: Perturbation of acetyl-CoA synthesis in *crd1Δ* cells. In the proposed model, loss of CL leads to decreased conversion of acetate to acetyl-CoA by acetyl-CoA synthetase. To compensate for this, PDH gene expression is up-regulated and protein synthesis of PDH is increased. However, PDH activity is not increased in CL-deficient cells.

How is the role of CL in acetyl-CoA synthesis relevant to BTHS and other cardiac disorders? Acetyl-CoA interconnects metabolic pathways that are crucial for cardiac energy metabolism (Abo Alrob and Lopaschuk, 2014). Mutations in the human E1-α subunit of the PDH complex, which is homologous to yeast *PDA1*, leads to Leigh's syndrome, which is characterized by hypertrophic cardiomyopathy among other phenotypes (Stacpoole et al., 1997; Fyer et al., 2008). Mutations in mitochondrial acetyl-CoA synthetase (AceCS1 and AceCS2) impair acetyl-CoA synthesis and induce cardiac hypertrophy (Ellis et al., 2011; Fujino et al., 2001). Cardiomyopathy and heart failure are generally caused by depletion of cardiomyocyte ATP and impaired energy homeostasis (Ingwall, 2009; Neubauer, 2007). Elucidating the role of CL in acetyl-CoA synthesis may shed light on the wide disparities in clinical phenotypes observed in patients with BTHS and other cardiac disorders.

TABLE 2.1. Yeast strains used in this study.

Strains	Genotype	Source or Ref.
Y5563	*MATα, his3Δ1, leu2Δ0, ura3Δ0, met15Δ0, LYS2$^+$, lyp1Δ, can1Δ::MFA1pr-HIS3*	Tong et al., 2001
BY4741	*MATα, his3Δ1, leu2Δ0, ura3Δ0, met15Δ0*	Invitrogen
BY4742	*MATα, his3Δ1, leu2Δ0, ura3Δ0, lys2Δ0*	Invitrogen
crd1Δcan1Δ	*MATα, his3Δ1, leu2Δ0, lys2Δ0, crd1Δ::URA3, can1Δ::MFA1pr-HIS3*	This study
VGY1	*MATα, his3Δ1, leu2Δ0, lys2Δ0, ura3Δ0, crd1Δ::URA3*	Gohil et al., 2005
CG922-a	*MATa, lys2-801, ade2-101, trp1Δ1, his3Δ200, leu2Δ1, crd1Δ::URA3*	Invitrogen
CG923-α	*MATα, lys2-801, ade2-101, trp1Δ1, his3Δ200, leu2Δ1, crd1Δ::URA3*	Invitrogen
pda1Δ	*MATa, his3Δ1, leu2Δ0, met15Δ0, ura3Δ0, pda1Δ::KanMX4*	Invitrogen
pdb1Δ	*MATa, his3Δ1, leu2Δ0, met15Δ0, ura3Δ0, pdb1Δ::KanMX4*	Invitrogen
lat1Δ	*MATa, his3Δ1, leu2Δ0, met15Δ0, ura3Δ0, lat1Δ::KanMX4*	Invitrogen
lpd1Δ	*MATa, his3Δ1, leu2Δ0, met15Δ0, ura3Δ0, lpd1Δ::KanMX4*	Invitrogen

pdx1Δ	*MATa, his3Δ1, leu2Δ0, met15Δ0, ura3Δ0, pdx1Δ::KanMX4*	Invitrogen
acs1Δ	*MATa, his3Δ1, leu2Δ0, met15Δ0, ura3Δ0, acs1Δ::KanMX4*	Invitrogen
acs2Δ	*MATa, his3Δ1, leu2Δ0, met15Δ0, ura3Δ0, acs2Δ::KanMX4*	Invitrogen
pda1Δcrd1Δ	*MATa, his3Δ1, leu2Δ0, met15Δ0, ura3Δ0, pda1Δ::KanMX4, crd1Δ::KanMX4*	This study
pdb1Δcrd1Δ	*MATa, his3Δ1, leu2Δ0, met15Δ0, ura3Δ0, pdb1Δ::KanMX4, crd1Δ::KanMX4*	This study
lat1Δcrd1Δ	*MATa, his3Δ1, leu2Δ0, met15Δ0, ura3Δ0, lat1Δ::KanMX4, crd1Δ::KanMX4*	This study
lpd1Δcrd1Δ	*MATa, his3Δ1, leu2Δ0, met15Δ0, ura3Δ0, lpd1Δ::KanMX4, crd1Δ::KanMX4*	This study
pdx1Δcrd1Δ	*MATa, his3Δ1, leu2Δ0, met15Δ0, ura3Δ0, pdx1Δ::KanMX4, crd1Δ::KanMX4*	This study
acs1Δcrd1Δ	*MATa, his3Δ1, leu2Δ0, met15Δ0, ura3Δ0, acs1Δ::KanMX4, crd1Δ::KanMX4*	This study
acs2Δcrd1Δ	*MATa, his3Δ1, leu2Δ0, met15Δ0, ura3Δ0, acs2Δ::KanMX4, crd1Δ::KanMX4*	This study

TABLE 2.2. Primers used for qPCR analyses.

Gene		Primer sequence
ACT1	Forward	ACGTTCCAGCCTTCTACGTTTCCA
	Reverse	CGTGAGTAACACCATCACCGGAA
PDA1	Forward	ATTGATGGGTAGAAGAGCCGGTGT
	Reverse	AGGCGTCCTCGTTCTTGTATTGGT
PDB1	Forward	TCCCATCATTTGGTGTTGGTGCTG
	Reverse	TGGAACATCGGCACCAGTAACTCT
LAT1	Forward	AGGAACTAGTCAAGCGTGCCAGAA
	Reverse	TCCACAGCGACCCTTTCAACAGTA
LPD1	Forward	AGAGCCAAGACCAACCAAGACACT
	Reverse	CATTTCACCGGCATTTGGACCGAT
PDX1	Forward	GCAGCCAAGCCAATCTTGAACAGA
	Reverse	TTGGAACCAGATGGCGCAATTTCC

TABLE 2.3. **Primers used for C-terminal tagging of proteins.**

5` F2-pda1-HA-tag	TCCCTGAAGATACTTGGGACTTCAAAAAGCAAGGTT TTGCCTCTAGGGAT CGGATCCCCGGGTTAATTAA
3` R1- pda1 -HA-tag	GAATATCATGCGATCACAGCACTATTATTTTATTTTTC CTTACGATTTAA GAATTCGAGCTCGTTTAAAC
5` F2-pdb1-HA-tag	CTGATACTCCAACCATCGTTAAAGCTGTCAAAGAAGT CTTGTCAATTGAA CGGATCCCCGGGTTAATTAA
3` F2-pdb1-HA-tag	AAAGTTCCCTATCTCCTTCTTTCTCTCCTTCCTATTG GATTGAAGTTTAT GAATTCGAGCTCGTTTAAAC
5` F2-lat1-HA-tag	TCATGAAGGAATTGAAAACTGTTATTGAAAATCCTTT GGAAATGCTATTGCGGATCCCCGGGTTAATTAA
3` F2-lat1-HA-tag	ATTTTCTCCAAGATACGCATTTACTGGCGAATTTTAT TTTCATTCTAACCGAATTCGAGCTCGTTTAAAC
5` F2-lpd1-HA-tag	AAGCATTTAAGGAAGCTAACATGGCTGCCTATGATA AAGCTATTCATTGT CGGATCCCCGGGTTAATTAA
3` F2-lpd1-HA-tag	AAGCGGTTCTTCATAAATATATATACTATACTGTTTAT TATTTCCTGTTT GAATTCGAGCTCGTTTAAAC
5` F2-pdx1-HA-tag	AGGCCAAGGCAAAAGATTCCTTGATTACGTAAGGG AGTTAGAATCATTT CGGATCCCCGGGTTAATTAA
3` F2-pdx1-HA-tag	ATGGCAGTATTGATAATGATAAACTCGAACTGAAAAA GCGTGTTTTTTAT GAATTCGAGCTCGTTTAAAC
5' Forward HA tag	CGGATCCCCGGGTTAATTAA
3` Reverse HA tag	GAATTCGAGCTCGTTTAAAC
3'HA-KMX-D-general	GGTAGAGGTGTGGTCAATAAGAGC
3'HA-tag-Diag	GGGACGTCATACGGATAGCC

TABLE 2.4. Synthetic interaction with *crd1Δ* at 30°C. Summary of the list of genes identified as synthetically lethal with the *crd1Δ* mutant at 30°C. The identified genes are grouped based on biological function.

GO term	Frequency	Gene(s)
Molecular function unknown	19 out of 105 genes, 18.1%	ERP2, ERP1, VBA4, NBP2, MIT1, RMD6, HMF1, CGR1, SOH1, MDS3, EMC5, HOS4, RAX2, SPH1, NKP2, ESC8, APM4, SGO1, TCO89
Hydrolase activity	15 out of 105 genes, 14.3%	RRT12, DYN2, BNA7, PTC2, RSR1, VMA16, MYO3, OCT1, DBR1, DNM1, ELP6, MSG5, RHO2, ARL3, KRE6
Transferase activity	13 out of 105 genes, 12.4%	SAS4, BUD16, UTR2, GUP1, NMA2, KTR7, TPK3, RTT109, RCK2, KTR5, MET2, MUM3
Structural molecule activity	11 out of 105 genes, 10.5%	RPL21A, IMG2, STE5, RSM24, RPL22B, CHC1, CLC1, RPL27A, PIR3, RPS12, RTC6
Ion binding	10 out of 105 genes, 9.5%	SHS1, BMH2, STE5, GIC2, RTF1, ATG27, ISA1, ROM2, ISA2
Structural constituent of ribosome	7 out of 105 genes, 6.7%	RPL21A, IMG2, RSM24, RPL22B, RPL27A, RPS12, RTC6

Transmembrane transporter activity	7 out of 105 genes, 6.7%	FCY22, VPS73, VMA16, JEN1, COX7, YVC1, TOM5
RNA binding	7 out of 105 genes, 6.7%	SRO9, RMD9, RTF1, RIM4, ELP6, THP1, CBC2
Oxidoreductase activity	6 out of 105 genes, 5.7%	SDH4, ERG4, SOD2, COX7, GRX5
DNA binding	6 out of 105 genes, 5.7%	RRN10, BMH2, ECM22, THP1, TYE7, DIG1
Lipid binding	6 out of 105 genes, 5.7%	RVS161, STE5, GIC2, ATG27, ROM2, TCB1
GTPase activity	4 out of 105 genes, 3.8%	RSR1, DNM1, RHO2, ARL3
mRNA binding, peptidase activity	4 out of 105 genes, 3.8%	SRO9, RMD9, RRT12, OCT1
ATPase activity, signal transducer activity	4 out of 105 genes, 3.8%	VMA16, ELP6, RSR1, ROM2
Cytoskeletal protein binding	3 out of 105 genes, 2.9%	RVS161, BUD6, TPM1
Enzyme regulator activity	3 out of 105 genes, 2.9%	GIC2, BUD6, IRA2
Small conjugating protein binding	3 out of 105 genes, 2.9%	SLA1, STP22, VPS36

Kinase activity	3 out of 105 genes, 2.9%	BUD16, TPK3, RCK2
Protein binding transcription factor activity	3 out of 105 genes, 2.9%	SSN2, RTF1, STB1
Nucleic acid binding transcription factor activity	3 out of 105 genes, 2.9%	RRN10, ECM22, TYE7
Lyase activity	3 out of 105 genes, 2.9%	ARO10, ENO1, PSD1
Transferase activity, transferring glycosyl groups	3 out of 105 genes, 2.9%	UTR2, KTR7, KTR5
Transcription factor binding	2 out of 105 genes, 1.9%	STB1, DIG1
Phosphatase activity	2 out of 105 genes, 1.9%	PTC2, MSG5
Nuclease activity, Ligase activity	2 out of 105 genes, 1.9%	DBR1, ARG1
Enzyme binding, Chromatin binding	2 out of 105 genes, 1.9%	GIC2, TOS4
Hydrolase activity, acting on glycosyl bonds	1 out of 105 genes, 1%	KRE6
Protein transporter activity	1 out of 105 genes, 1%	TOM5

Protein binding, bridging	1 out of 105 genes, 1%	SLA1
Nucleotidyl transferase activity	1 out of 105 genes, 1%	NMA2
Unfolded protein binding	1 out of 105 genes, 1%	SSQ1
Guanyl-nucleotide exchange factor activity	1 out of 105 genes, 1%	ROM2

TABLE 2.5. Synthetic interaction with *crd1Δ* at 37°C. Summary of the list of genes identified as synthetically lethal with the *crd1Δ* mutant at 37°C. The identified genes are grouped based on biological function.

GO term	Frequency	Gene(s)
Molecular function unknown	24 out of 65 genes, 36.9%	DEP1, PRM9, FIG2, HBT1, RTN1, PMP3, RAD34, EAF1, ITC1, EMP24, OST5, TED1, MAD2, ABM1, BUD28, COQ9, REC102, PAU4, AIM34, MDM12, MAM3, TMA16, PRM3, NCA2
Transferase activity	14 out of 65 genes, 21.5%	DPB3, GRX1, SAT4, PAA1, DBF2, MET14, ELM1, TGL4, ERG6, GTO3, PSK2, PSH1, TUM1, NAT5
Kinase activity	5 out of 65 genes, 7.7%	SAT4, DBF2, MET14, ELM1, PSK2
Oxidoreductase activity	4 out of 65 genes, 6.2%	PDB1, GRX1, TSA1, GCY1
Hydrolase activity	4 out of 65 genes, 6.2%	GET3, TIF2, CPS1, TGL4
RNA binding	4 out of 65 genes, 6.2%	EFT2, TIF2, GCY1, LEO1

Structural constituent of ribosome	3 out of 65 genes, 4.6%	RPL27A, RPS24B, RPS4A
DNA binding	3 out of 65 genes, 4.6%	DPB3, BDF2, MIG2
Lipid binding	3 out of 65 genes, 4.6%	SWH1, TCB2, YPR097W
Transcription factor binding	3 out of 65 genes, 4.6%	BDF2, GAL80, SIN4
Structural molecule activity	3 out of 65 genes, 4.6%	RPL27A, RPS24B, RPS4A
Ion binding	3 out of 65 genes, 4.6%	SWH1, LEO1, YPR097W
Translation factor activity, nucleic acid binding	2 out of 65 genes, 3.1%	EFT2, TIF2
Enzyme regulator activity	2 out of 65 genes, 3.1%	GAL80, CLN2
ATPase activity	2 out of 65 genes, 3.1%	GET3, TIF2
Transmembrane transporter activity	2 out of 65 genes, 3.1%	FLC2, HUT1
mRNA binding, peptidase activity	2 out of 65 genes, 3.1%	GCY1, CPS1

Protein transporter activity, protein binding transcription	2 out of 65 genes, 3.1%	KAP114, LEO1
Nucleic acid binding transcription factor activity, nucleotidyl transferase activity	2 out of 65 genes, 3.1%	MIG2, DPB3
Lyase activity / Ligase activity	2 out of 65 genes, 3.1%	DSD1, ADE6
Methyltransferase activity, histone binding	2 out of 65 genes, 3.1%	ERG6, BDF2
Helicase activity	1 out of 65 genes, 1.5%	TIF2
Small conjugating protein binding	1 out of 65 genes, 1.5%	GGA1
Protein binding transcription factor activity	1 out of 65 genes, 1.5%	LEO1
Protein binding, bridging	1 out of 65 genes, 1.5%	INP1
Unfolded protein binding	1 out of 65 genes, 1.5%	TSA1
Guanyl-nucleotide exchange factor activity	1 out of 65 genes, 1.5%	GET3

TABLE 2.6. Genes identified by SGA as synthetically lethal with *crd1Δ* at 30°C.
(Ref: Gene description from Saccharomyces genome database)

Genes	SGD Gene description
APM4	Mu2-like subunit of the clathrin associated protein complex (AP-2)
ARG1	Arginosuccinate synthetase
ARL3	GTPase of the Ras superfamily required recruiting Arl1p
ARO10	Phenylpyruvate decarboxylase
ATG27	Type I membrane protein involved in autophagy
BMH2	14-3-3 protein, minor isoform
BNA7	Formylkynurenine formamidase
BUD1	Protein kinase that forms a complex with Mad1p and Bub3p
BUD16	Putative pyridoxal kinase
BUD20	Protein involved in bud-site selection
BUD6	Actin- and formin-interacting protein
CBC2	Small subunit of the heterodimeric cap binding complex
CGR1	Protein involved in nucleolar integrity and processing
CHC1	Clathrin heavy chain
CLC1	Clathrin light chain
COX7	Subunit VII of cytochrome c oxidase
DBR1	RNA lariat debranching enzyme
DIG1	Regulatory protein of unknown function
DNM1	Dynamin-related GTPase required for mitochondrial fission
DYN2	Cytoplasmic light chain dynein, microtubule motor protein

ECM22	Sterol regulatory element binding protein
ELP6	Subunit of Elongator complex
ENO1	Enolase I, a phosphopyruvate hydratase
ERG4	C-24 (28) sterol reductase
ERP1	Involved in ER to Golgi transport and localized to COPII vesicles
ERP2	Involved in ER to Golgi transport and localized to COPII vesicles
ESBP6	Protein with similarity to monocarboxylate permeases
ESC8	Protein involved in telomeric and mating-type locus silencing
FCY22	Putative purine-cytosine permease
GIC2	Redundant rho-like GTPase Cdc42p effector
GRX5	Hydroperoxide and superoxide-radical
GUP1	Plasma membrane protein involved in remodeling GPI anchors
HMF1	Member of the p14.5 protein family with similarity to Mmf1p
HOS4	Subunit of the Set3 complex
IMG2	Mitochondrial ribosomal protein of the large subunit
IRA2	GTPase-activating protein that negatively regulates RAS
ISA1	Mitochondrial matrix protein involved in biogenesis iron-sulfur
ISA2	Protein required for maturation of mitochondrial and cytosolic
JEN1	Lactate transporter
KRE27	Required for efficient folding of proteins in the ER
KRE6	Protein required for beta-1,6 glucan biosynthesis
KTR5	Putative mannosyltransferase involved in protein glycosylation
KTR7	Putative mannosyltransferase involved in protein glycosylation

MDS3	Putative component of the TOR regulatory pathway
MET2	L-homoserine-O-acetyltransferase
MGR1	Subunit of the mitochondrial (mt) i-AAA protease supercomplex
MIT1	Putative protein with sequence similarity to gluconate transporter
MSG5	Dual-specificity protein phosphatase
MUM3	Similarity to the tafazzins superfamily of acyltransferases
MYO3	One of two type I myosins; localizes to actin cortical patches
NBP2	Protein involved in the HOG (high osmolarity glycerol) pathway
NKP2	Non-essential kinetochore protein
NMA2	Nicotinic acid mononucleotide adenylyltransferase
OCT1	Mitochondrial intermediate peptidase
PIR3	O-glycosylated covalently-bound cell wall protein
PSD1	Phosphatidylserine decarboxylase
PTC2	Type 2C protein phosphatase
RAX2	N-glycosylated protein involved in the maintenance of bud site
RCK2	Protein kinase involved in the response to oxidative and osmotic
RHO2	Non-essential small GTPase of the Rho/Rac subfamily of Ras-like
RIM4	Putative RNA-binding protein
RMD6	Protein required for sporulation
RMD9	Mitochondrial protein required for respiratory growth
ROM2	GDP/GTP exchange protein (GEP) for Rho1p and Rho2p
RPL21A	Protein component of the large (60S) ribosomal subunit
RPL22B	Protein component of the large (60S) ribosomal subunit

RPL27A	Protein component of the large (60S) ribosomal subunit
RPS12	Protein component of the small (40S) ribosomal subunit
RRN10	Protein involved in promoting high level transcription of rDNA
RRT12	Probable subtilisin-family protease
RSM24	Mitochondrial ribosomal protein of the small subunit
RTC6	Homolog of the prokaryotic ribosomal protein L36
RTF1	Subunit of the RNA polymerase II-associated Paf1 complex
RTT109	Histone acetyltransferase
RVS161	Amphiphysin-like lipid raft protein
SAS4	Subunit of the SAS complex (Sas2p, Sas4p, Sas5p
SDH4	Membrane anchor subunit of succinate dehydrogenase
SGO1	Component of the spindle checkpoint
SHS1	One of five related septins
SLA1	Cytoskeletal protein binding protein
SOD2	Mitochondrial superoxide dismutase
SOH1	Subunit of the RNA polymerase II mediator complex
SPH1	Protein involved in shmoo formation and bipolar bud site selection
SRO9	Cytoplasmic RNA-binding protein
SSN2	Subunit of the RNA polymerase II mediator complex
SSQ1	Mitochondrial hsp70-type molecular chaperone
STB1	Protein with a role in regulation of MBF-specific transcription
STE5	Pheromone-response scaffold protein
STP22	Component of the ESCRT-I complex

TCB1	Lipid-binding protein
TCO89	Subunit of TORC1
THP1	Nuclear pore-associated protein
TOM5	Component of the TOM (translocase of outer membrane) complex
TOS4	Forkhead Associated domain
TPK3	cAMP-dependent protein kinase catalytic subunit
TPM1	Major isoform of tropomyosin
TYE7	Serine-rich protein that contains a basic-helix-loop-helix (bHLH)
UTR2	Chitin transglycosylase
VBA4	Protein of unknown function suggests a role in autophagy
VMA16	Subunit c'' of the vacuolar ATPase
VPS36	Component of the ESCRT-II complex
VPS73	Mitochondrial protein; mutation affects vacuolar protein sorting
YVC1	Vacuolar cation channel

TABLE 2.7. Genes identified by SGA as synthetically lethal with *crd1Δ* at 37°C.
(Ref: Gene description from Saccharomyces genome database)

Genes	SGD gene description
ABM1	Protein of unknown function, required for microtubule organization
ADE6	Formylglycinamidine-ribonucleotide (FGAM)-synthetase
BDF2	Protein involved in transcription initiation at promoters
BFA2	Component of the GTPase-activating Bfa1p-Bub2p complex
BUD28	ubious open reading frame
CLN2	G1 cyclin involved in regulation of the cell cycle
COQ9	Protein required for ubiquinone biosynthesis and respiratory growth
CPS1	Vacuolar carboxypeptidase yscS
DBF2	Ser/Thr kinase involved in transcription and stress response
DEP1	Transcriptional modulator involved in regulation phospholipid
DPB3	Third-largest subunit of DNA polymerase II
DSD1	D-serine dehydratase (aka D-serine ammonia-lyase
EAF1	Component of the NuA4 histone acetyltransferase complex
EFT2	Elongation factor 2 (EF-2), also encoded by EFT1
ELM1	Serine/threonine protein kinase
EMP24	Integral membrane component of ER-derived COPII vesicles
ERG6	Delta (24)-sterol C-methyltransferase
FIG2	Involved in maintenance of cell wall integrity during mating
FLC2	Putative FAD transporter; required for uptake of FAD into ER
GAL80	Transcriptional regulator involved in the repression of GAL genes

GCY1	Putative NADP (+) coupled glycerol dehydrogenase
GET3	Involved in Golgi to ER trafficking and insertion of proteins into ER
GGA1	Golgi-localized protein with homology to gamma-adaptin
GRX1	Glutathione-dependent disulfide oxidoreductase
GTO3	Omega class glutathione transferase; putative cytosolic localization
HBT1	Substrate of the Hub1p ubiquitin-like protein
HUT1	Protein with a role in UDP-galactose transport to the Golgi lumen
INP1	Peripheral membrane protein of peroxisomes
ITC1	Component of the ATP-dependent Isw2p-Itc1p
KAP114	Karyopherin, responsible for nuclear import of Spt15p
LEO1	Component of the Paf1 complex
MAD2	Component of the spindle-assembly checkpoint complex
MAM3	Protein required for normal mitochondrial morphology
MCH1	Protein with similarity to mammalian monocarboxylate permeases
MDM12	Mitochondrial outer membrane protein
MET14	Adenylylsulfate kinase
MIG2	Protein containing zinc fingers, involved in repression
NAT5	Subunit of the N-terminal acetyltransferase NatA
NCA2	Protein involved in regulation of mitochondrial expression of Atp6p
NOL4	Endoplasmic reticulum and nuclear membrane protein
OST5	Zeta subunit of the oligosaccharyltransferase complex
PAA1	Polyamine acetyltransferase
PAU4	Member of the seripauperin multigene family

PDB1	E1 beta subunit of the pyruvate dehydrogenase (PDH) complex
PMP3	Small plasma membrane protein
PRM3	Pheromone-regulated protein required for nuclear envelope fusion
PSH1	Nuclear protein, putative RNA polymerase II elongation factor
PSK2	One of two (see also PSK1) PAS domain
RAD34	Protein involved in nucleotide excision repair (NER)
REC102	Protein involved in early stages of meiotic recombination
RPS24B	Protein component of the small (40S) ribosomal subunit
RPS4A	Protein component of the small (40S) ribosomal subunit
RTN1	ER membrane protein that interacts with Sey1p
SAT4	Ser/Thr protein kinase involved in salt tolerance
SIN4	Subunit of the RNA polymerase II mediator complex
SWH1	Protein similar to mammalian oxysterol-binding protein
TCB2	Bud-specific protein with a potential role in membrane trafficking
TED1	Conserved phosphoesterase domain-containing protein
TGL4	Multifunctional triacylglycerol lipase and steryl ester hydrolase
TIF2	Translation initiation factor eIF4A
TMA16	Protein of unknown function that associates with ribosomes
TSA1	Thioredoxin peroxidase
TUM1	Mitochondrial protein that is similar to mammalian thiosulfate
YHR010W	Protein component of the large (60S) ribosomal subunit
YPR097W	Protein that contains a Phox homology (PX) domain

CHAPTER 3 THE GLYOXYLATE CYCLE IS ESSENTIAL IN CARDIOLIPIN DEFICIENT CELLS

INTRODUCTION

In the studies discussed in the previous chapter, I demonstrated that acetyl-CoA levels were decreased and acetate utilization was perturbed in the *crd1Δ* mutant. Previous studies reported that CL mutants exhibit decreased activity of Fe-S enzymes in the TCA cycle, and up-regulation of genes involved in the transport of acetyl-CoA and TCA cycle intermediates into the mitochondria (Patil et al., 2013). These studies suggest that CL-deficiency leads to perturbation of the TCA cycle. The mechanisms linking CL deficiency and defects in the TCA cycle are not fully understood. Acetyl-CoA is synthesized and compartmentalized in four cellular compartments, cytosol, nucleus, peroxisome, and mitochondria (Krivoruchko et al., 2014; Nielsen et al., 2014, Chen et al., 2012). Acetyl units are transported into the mitochondria as acetylcarnitine through the carnitine shuttle or converted into intermediates of the TCA cycle through the glyoxylate cycle and transported into the mitochondria (Chen et al., 2015). Therefore, to maintain basic cellular functions that depend on a functional TCA cycle, I predicted that CL-deficient cells require these pathways to synthesize TCA cycle intermediates.

In *Saccharomyces cerevisiae*, precursors for the carnitine shuttle and glyoxylate cycle are synthesized by β-oxidation of fatty acids in the peroxisomes. Fatty acids oxidized to acetyl-CoA inside the peroxisomes are exported to the mitochondria through a carnitine-dependent pathway or utilized by the glyoxylate cycle to synthesize intermediates of the TCA cycle (Van der Klei and Veenhuis 1997; Kunau et al., 1995; Hettema and Tabak 2000; van Roermund et al., 1995). In one route, acetyl-CoA enters the glyoxylate cycle, which is also described as a "modified TCA cycle" (Kunze et al.,

2006). The glyoxylate cycle consists of five enzymes, including citrate synthase (CS), aconitase (ACO), malate dehydrogenase (MDH), isocitrate lyase (ICL), and malate synthase (MLS) (Fig. 3.1). The first three enzymes are shared with the TCA cycle, while the last two enzymes are unique to the glyoxylate cycle. Most of the glyoxylate cycle mutants, including *icl1Δ*, *msl1Δ*, *cit2Δ*, *aco1Δ*, and *mdh3Δ*, are viable and do not exhibit growth defects (Lee et al., 2011). The two-carbon acetyl-CoA is converted to four-carbon dicarboxylic acids, including succinate and malate, which bypass oxidative decarboxylation and are transported to the mitochondria, where they are used to replenish intermediates of the TCA cycle (van Roermund et al., 1999).

The carnitine shuttle transfers acetyl units from the peroxisome (Fig. 3.2). Acetyl-CoA is converted to acetylcarnitine by carnitine acetyltransferase (*CAT2*) in the peroxisomes. Acetylcarnitine is transported into mitochondria by the carnitine-acetylcarnitine translocase (*CRC1*) and converted back to carnitine and acetyl-CoA by the mitochondrial *CAT2* (Palmieri et al., 1997; Van Roermund et al.,1995). Mitochondrial acetyl-CoA then enters the TCA cycle. Similarly, acetyl-CoA from the cytoplasm is shuttled into the mitochondria through the cytoplasmic carnitine acetyltransferase (*YAT1* and *YAT2*), which is associated with the mitochondrial outer membrane. The pool of acetyl-CoA inside the mitochondria is utilized by the TCA cycle, the central metabolic pathway in the mitochondrial matrix. The TCA cycle is also required for biosynthesis of amino acids and heme.

As discussed above, TCA cycle deficiencies may be replenished by the carnitine shuttle and the glyoxylate cycle, which complement each other by replenishing acetyl-CoA, citrate, malate, and succinate. Because *crd1Δ* cells exhibit deficiencies in the TCA

cycle and acetyl-CoA synthesis, I hypothesized that these cells require the carnitine shuttle and/or the glyoxylate cycle for cell survival. In this study, I report that both replenishing pathways are required for optimal growth of *crd1Δ* cells. Carnitine-acetylcarnitine translocase activity is decreased in the *crd1Δ* mutant, and carnitine rescues temperature sensitive growth. The glyoxylate cycle is essential in the CL mutant, as double mutants of *crd1Δ* and glyoxylate cycle mutants were not viable. Supplementation of carnitine, acetylcarnitine, or oleate rescued the growth defect of the *crd1Δ* mutant at elevated temperature. These results show for the first time that CL-deficient cells require the glyoxylate cycle to compensate for TCA cycle defects.

MATERIALS AND METHODS

Yeast strains and growth media

The yeast *S. cerevisiae* strains used in this study are listed in Table 3.1. Single deletion mutants were obtained from the yeast knockout deletion collection (Invitrogen). Double mutants were obtained by tetrad dissection. Synthetic complete (YNBD) medium contained adenine (20.25 mg/liter), arginine (20 mg/liter), histidine (20 mg/liter), leucine (60 mg/liter), lysine (200 mg/liter), methionine (20 mg/liter), threonine (300 mg/liter), tryptophan (20 mg/liter), uracil (20 mg/liter), yeast nitrogen base without amino acids (Difco), and glucose (2%) (YNBD) or sodium acetate (2%) (YNBA) or oleic acid (0.12%) and Tween 80 (0.2%) (YNBO). Synthetic dropout media contained all ingredients mentioned above but lacked the indicated amino acids. Sporulation medium contained potassium acetate (1%), glucose (0.05%), and the essential amino acids required for sporulation. Complex medium contained yeast extract (1%), peptone (2%), and glucose (2%) (YPD). Solid medium was prepared by adding 2% agar. The cells for carnitine, β-

oxidation, and enzyme assays were grown on minimal glucose medium (YNB with 2% glucose), inoculated at A_{600} 0.2 in YNB 0.3% glucose medium, and grown for 8 hours. Finally, the strains were inoculated into rich oleate medium (YPO; 2% peptone, 1% yeast extract, 0.12% oleic acid, 0.2% Tween 80) at an A_{600} of 0.005 and grown for 16 hours.

Measurement of acetyl-CoA

Cells were grown to the logarithmic growth phase and a sample (3 ml) of the culture was centrifuged at 1700 g. Pellets were resuspended in 1 ml ddH$_2$O and centrifuged for 1 min at 9300 g. The resulting cell pellet was subjected to cell lysis and the lysed samples were rapidly quenched with 130 µl of 45:45:10 acetonitrile / methanol / H2O + 0.1% glacial acetic acid and spiked with 10 µmol I^{-1} glutaryl-CoA as an internal standard. The resuspended extract was incubated on ice with intermittent vortexing for 15 min. An equal molar volume of ammonium hydroxide was added post incubation to neutralize the acetic acid, and each extract was centrifuged for 3 min at 15,700 g, transferred to a new 1.5 ml microfuge tube and centrifuged for 5 min at 15,700 g. The clarified extract (10 µl) was injected for HPLC-MS/MS analysis (Bennett et al., 2009; Armando et al., 2011). (Mass spectrometry was carried out by Krishna Rao Maddipati, Director, Lipidomics Core).

Measurement of respiration

Cells were grown to the logarithmic phase and pelleted. Protein concentration was determined using the Bradford assay. Cells were then washed and resuspended in YNBO to 2 mg/ml final protein concentration. Oxygen consumption was measured in a closed 500 µl chamber equipped with a micro Clark-type oxygen electrode (Oxygraph system, Hansatech) at 30°C and analyzed with Oxygraph software. 500 µM KCN was added to inhibit cytochrome c oxidase. Non-cytochrome *c* oxidase-based respiration was

subtracted to determine oxygen consumption rates. Respiration was defined as oxygen consumed (nmol)/min total protein (mg). (This experiment was carried out in collaboration with Dr. Maik Hüttemann, Center for Molecular Medicine and Genetics, WSU).

The following experiments were carried out by Dr. Carlo W. van Roermund, Department of Genetic Metabolic Diseases, Academic Medical Center, Amsterdam, The Netherlands

(a) β-oxidation assay

Oleate-grown cells were washed with water and resuspended in phosphate buffered saline (PBS) to an A_{600} of 2.5. Aliquots of 20 µl of cell suspension were used for fatty acid β-oxidation measurements in 200 µl medium containing PBS plus 10 µM [1-^{14}C]-palmitate or [1-^{14}C]-octanoate. Reactions were allowed to proceed for 6 or 12 min at 30°C, followed by termination of reactions by adding 100 µl of 1.3 M perchloric acid. Radiolabeled CO_2 was trapped overnight in 500 µl of 2 M NaOH. The ^{14}C-labelled β-oxidation products were subsequently collected after extracting the acidified material with chloroform/methanol/heptane as described (Heikoop et al., 1990) and quantified in a liquid scintillation counter. The β-oxidation capacity of wild-type cells grown on oleate in each experiment was taken as a reference (100%).

(b) Carnitine acetyltransferase (CAT2 assay)

Oleate-grown cells (20 ml) were washed twice and pelleted for carnitine acetyltransferase activity. The cell homogenate was prepared by disrupting the cell pellet in 500 µl of 0.9% NaCl with 200 µl of glass beads for 5 min by vortexing at 4°C. Cell debris was removed by centrifugation for 1 min at 13,000 rpm. For measurement of carnitine acetyltransferase, the assay mixture (final volume of 100 µl) was composed of 40 mM HEPES (2 M; pH 7.4), 0.1 % triton-x-100, 1 mM carnitine, 60 µM acetyl-CoA, 200,000

dpm [1-C^{14}]-acetyl-CoA, and 40 µl of homogenate. The reaction mixture was incubated for 10 min at 28°C. The reaction was stopped with 500 µl ice-cold EtOH on the AG11-8 column. The column was washed twice with 500 µl EtOH and we measured the [1-C^{14}]-acetyl-carnitine.

(c) Carnitine-acetylcarnitine translocase (CACT assay)

Carnitine acetylcarnitine translocase activity was measured in spheroplasts prepared from wild-type or mutant cells grown on oleate. Activity measurements were performed in a medium containing 1.2 M sorbitol, 50 mM KPi pH 7.5, 1 mM EDTA, 200,000 d.p.m. [1-^{14}C] acetylcarnitine (5 µM) and digitonized (20 µg/ml) spheroplasts (100 µg protein). This digitonine concentration selectively permeabilizes the plasma membrane, as demonstrated by complete release of the cytosolic marker enzyme phosphoglucose isomerase (PGI), whereas intracellular membranes of mitochondria and peroxisomes remain intact (Verleur et al., 1997). Reactions were allowed to proceed for 10 min at 28°C, and subsequently stopped by the addition of 100 µl 1.3 M perchloric acid. Radiolabeled CO_2 was trapped overnight in 500 µl of 2 M NaOH.

(d) Carnitine measurement

Oleate-grown cells (20 ml) were washed twice and disrupted by vigorously vortexing for 30 min at 4°C with ~200 µl glass beads in an end volume of 400 µl. Cell debris (75 µl) was mixed and subsequently deproteinized with 500 µl acetonitrile and centrifuged for 15 min at 12,000 rpm. The resulting supernatant was dried under nitrogen at 45°C and subsequently derivatized in 100 µl butanol–HCl for 15 min at 60°C. Samples were dried under nitrogen at 45°C and redissolved in 140 µl acetonitril. Free carnitine was measured as described by Vreken et al. (1999).

RESULTS

Perturbation of carnitine-acetylcarnitine translocase activity in *crd1Δ*

The data presented in the previous chapter showed that the loss of CL leads to decreased growth and acetyl-CoA levels on acetate medium. In *S. cerevisiae*, the glyoxylate cycle and the carnitine shuttle facilitate growth when acetate is the sole carbon source (Palmieri et al., 1997; Palmieri et al., 1999; Lee et al., 2011). Therefore, I hypothesized that growth defects of *crd1Δ* on acetate and at elevated temperature may be due to perturbation of either or both of these pathways. Consistent with my hypothesis, growth of *crd1Δ* on acetate medium and at elevated temperature are restored by supplementation of carnitine or acetylcarnitine (Fig. 3.3A and Fig. 3.8A). Acetylcarnitine was more effective than carnitine for rescue of *crd1Δ* growth defects. However, acetyl-CoA levels were not restored by supplementation of carnitine or acetylcarnitine on acetate medium (Fig. 3.3B).

Acetyl-CoA that is produced from acetate in the cytosol and fatty acid oxidation in the peroxisome must be transported across the mitochondrial membranes by carnitine-acetylcarnitine translocase. Defects in the carnitine shuttle lead to decreased carnitine levels, activity of carnitine acetyltransferase, and/or activity of carnitine-acetylcarnitine translocase (van der Leij et al., 2000; Franken et al., 2008; van Roermund et al., 1995). The observed rescue of decreased growth on acetate by carnitine or acetylcarnitine suggests that either carnitine levels, activity of carnitine acetyltransferase, and/or activity of carnitine-acetylcarnitine translocase are decreased in CL-deficient cells. To address this possibility, total free carnitine was quantified using tandem mass spectrometry and

found to be only marginally reduced (~14%) in *crd1Δ* cells (Fig. 3.4A). In addition, activity of the carnitine acetyltransferase was unaltered in the *crd1Δ* mutant (Fig. 3.4B).

Acetylcarnitine that is synthesized in the peroxisomes and cytosol is transported into the mitochondria by carnitine-acetylcarnitine translocase, which is a mitochondrial inner membrane protein. Noel and Pande (1986) reported that CL is required for carnitine-acetylcarnitine translocase activity. Impaired enzyme activity results in the inability to transport acetyl-CoA into mitochondria because acetylcarnitine cannot traverse through the mitochondrial membrane (McGarry and Brown, 1997; Hynes et al., 2011). Therefore, I addressed the possibility that decreased growth on acetate in *crd1Δ* cells may result from decreased carnitine-acetylcarnitine translocase activity. The *crd1Δ* mutant exhibited an ~35% decrease in activity of carnitine-acetylcarnitine translocase relative to wild-type (Fig. 3.5). Taken together, these experiments indicate that CL-deficient cells have a deficiency in transport of acetylcarnitine through the mitochondrial membrane due to decreased carnitine-acetylcarnitine translocase activity.

The glyoxylate cycle compensates for TCA cycle defects in *crd1Δ*

As discussed earlier, the glyoxylate cycle is an anaplerotic pathway that provides TCA cycle metabolites by an alternative route. If the TCA cycle is defective in *crd1Δ* cells, then perturbation of the glyoxylate cycle may exacerbate growth defects of *crd1Δ* cells, while up-regulation of the glyoxylate cycle may rescue *crd1Δ* growth defects. To test this prediction, I examined genetic interaction between *crd1Δ* and mutants in the glyoxylate cycle. As predicted, deletion of *MLS1* in *crd1Δ* cells leads to synthetic lethality at the optimal growth temperature of 30°C (Fig. 3.6). The other mutants of the glyoxylate cycle, including *CIT2*, *SDH1*, and *SFC1*, were synthetically lethal with *crd1Δ* cells at the elevated

temperature 37°C. (Fig. 3.7).

Growth of *crd1Δ* at elevated temperature was restored by supplementation of oleate (Fig. 3.8B). Fatty acids are converted to acetyl-CoA inside the peroxisome by β-oxidation. Acetyl-CoA thus generated enters the glyoxylate cycle to synthesize succinate, malate, and citrate. I explored the possibility that supplementation of oleate rescued growth of *crd1Δ* cells as a result of increased β-oxidation. O_2 consumption was measured in intact cells grown on oleate. The rate of O_2 uptake in the *crd1Δ* mutant was unaltered (Fig. 3.9A) and oxidation of oleate was marginally decreased (Fig. 3.9B). Therefore, the most likely mechanism underlying rescue of growth defects by oleate is up-regulation of the glyoxylate cycle to replenish TCA cycle intermediates. These findings suggest for the first time that the glyoxylate cycle is essential in CL-deficient cells.
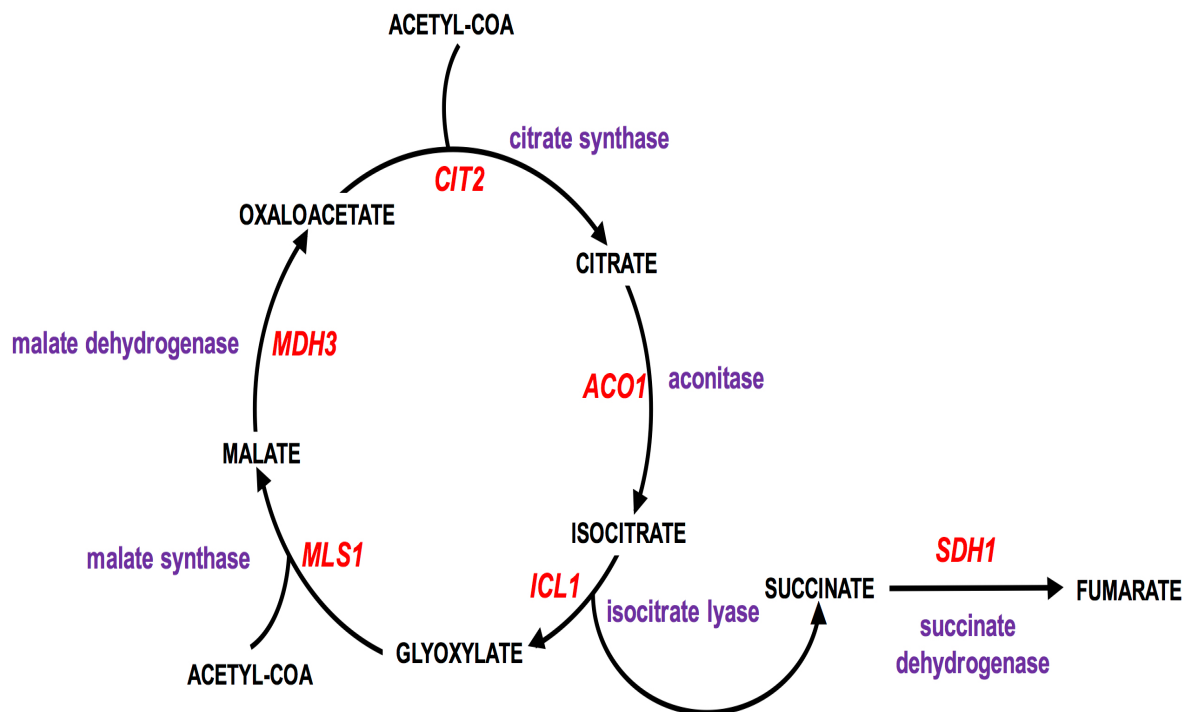
FIGURE 3.1. The glyoxylate cycle. Acetyl-CoA produced from β-oxidation of fatty acids in the peroxisomes is condensed with oxaloacetate to form citrate, which is converted into isocitrate. Isocitrate is converted to succinate and glyoxylate. Glyoxylate is condensed with another molecule of acetyl-CoA to form malate, which is converted to oxaloacetate. Enzymes are indicated in violet, genes encoding the respective enzymes are shown in red, and intermediates are represented in black.
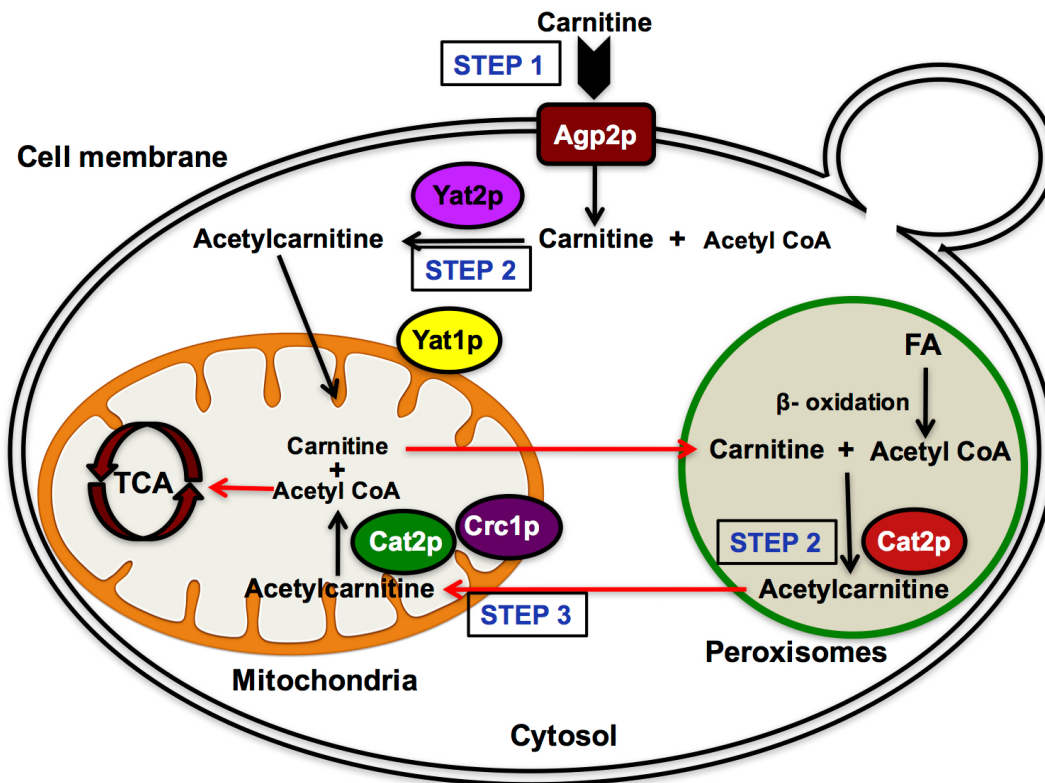
FIGURE 3.2. The carnitine shuttle (modified from Franken et al., 2008). Acetyl-CoA produced from β-oxidation of fatty acids in the peroxisomes is transported to the mitochondria in the form of acetylcarnitine, produced by the peroxisomal carnitine acetyltransferase Cat2p. This enzyme has two isoforms, one found in peroxisomes and the other in mitochondria. Translocation of acetylcarnitine across the mitochondrial membrane is mediated by the carnitine-acetylcarnitine translocase, Crc1p. The mitochondrial Cat2p converts acetylcarnitine to carnitine and acetyl-CoA. Two additional carnitine acetyltransferases include Yat1p, found on the outer mitochondrial membrane, and Yat2p, localized in the cytosol. Carnitine is imported into cells by the carnitine transporter, Agp2p.
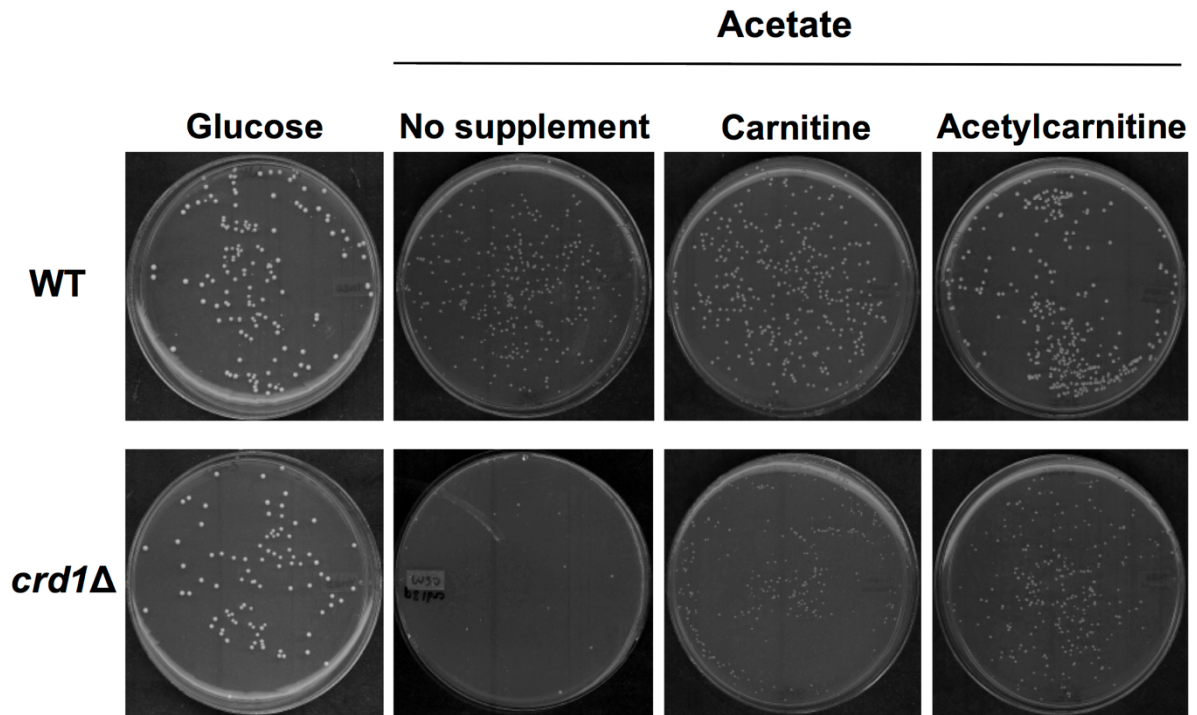
FIGURE 3.3A. Carnitine and acetylcarnitine restored the growth of *crd1Δ* on acetate. Cells were pre-cultured in YNBD overnight, serially diluted, plated on YNBA with or without carnitine or acetylcarnitine (500 mg/l), and incubated at 30°C for 4 days.
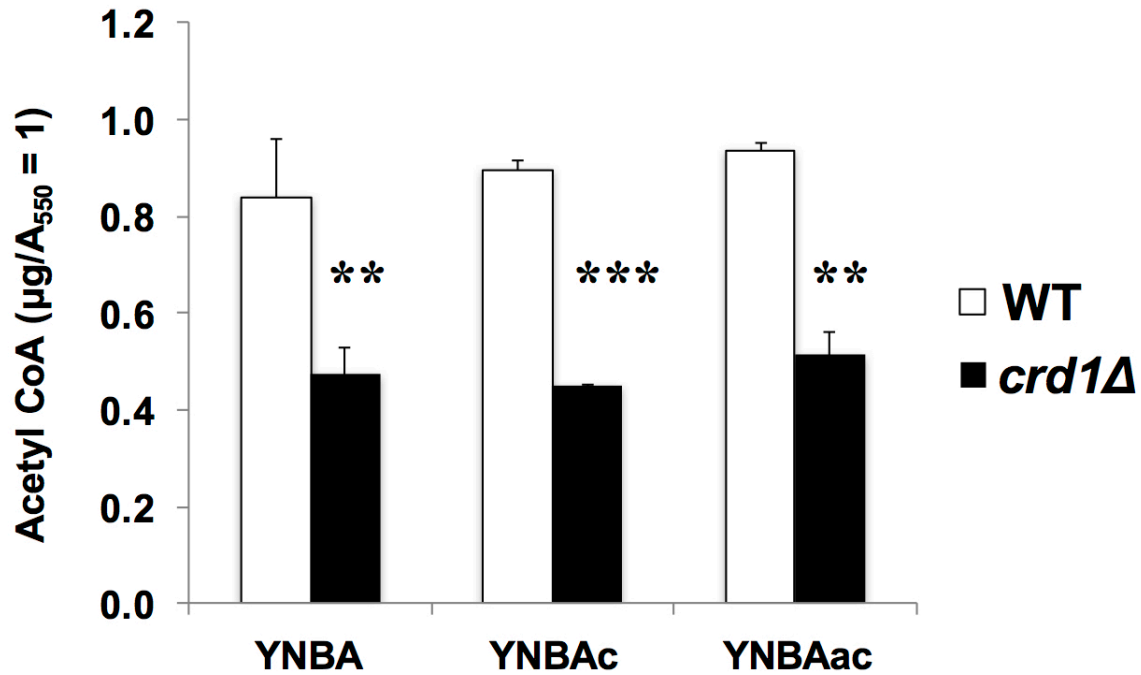
FIGURE 3.3B. Carnitine and acetylcarnitine do not rescue decreased acetyl-CoA levels in *crd1Δ* on acetate. Wild-type and *crd1Δ* cells were grown in YNBA with or without carnitine or acetylcarnitine (500 mg/l) until cells reach an A_{550} of 1. Cells were pelleted and acetyl-CoA was extracted using glutaryl-CoA as an internal standard. The clarified extract (10 μl) was analyzed by HPLC-MS/MS. Data shown are mean ± S.E. (n = 6) (**p<0.01, ***p<0.001).
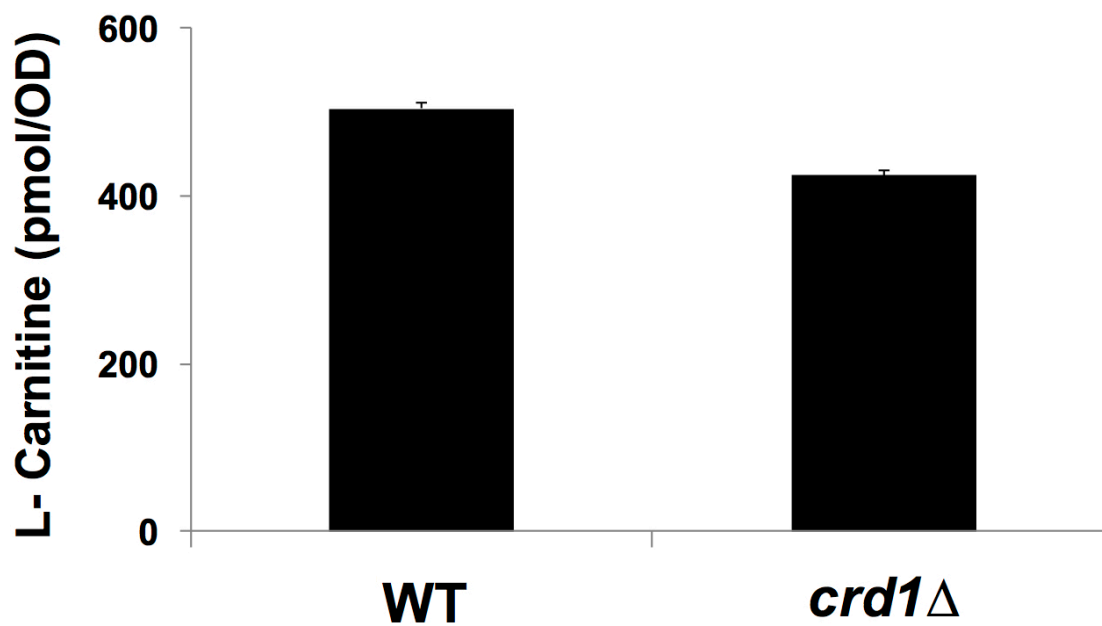
FIGURE 3.4A. Carnitine levels are marginally decreased in *crd1Δ*. Wild-type and *crd1Δ* cells were grown in YNBO. Total intracellular carnitine levels were determined by tandem mass spectrometry as described in the "Materials and Methods". Data shown are mean ± SE (n=6).
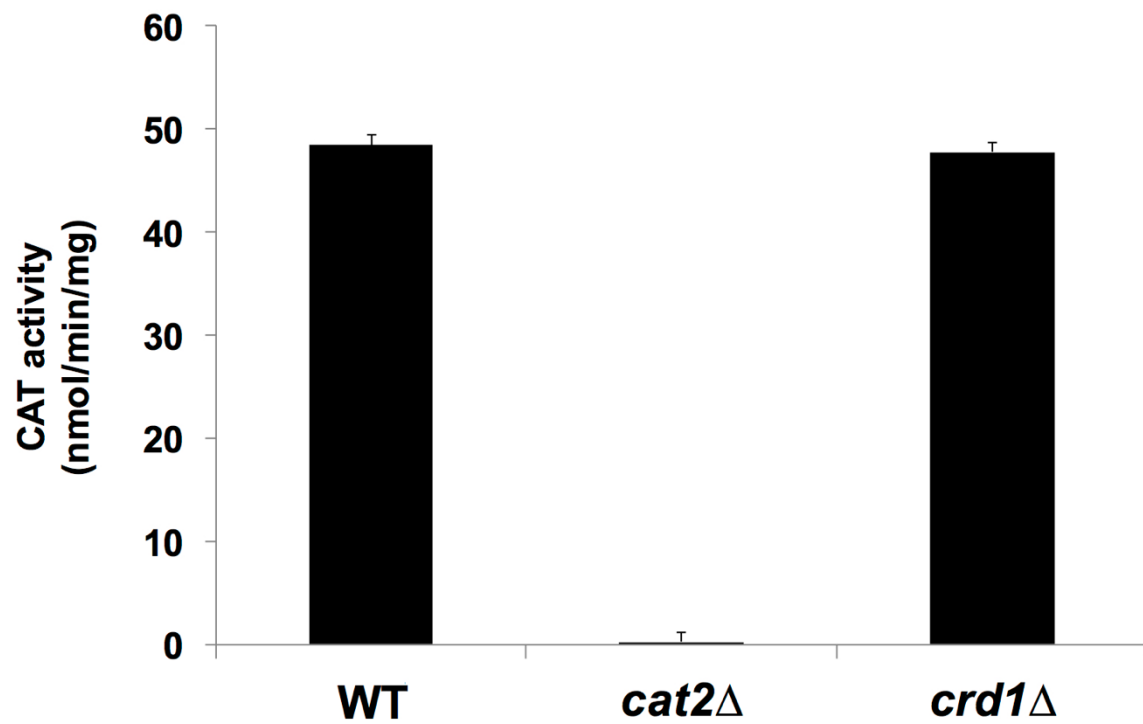
FIGURE 3.4B. Carnitine acetyltransferase activity is not decreased in *crd1Δ*. Wild-type and *crd1Δ* cells were grown in YNBO and carnitine acetyltransferase activity was measured as described in the "Materials and Methods". Data shown are mean ± SE (n=6).
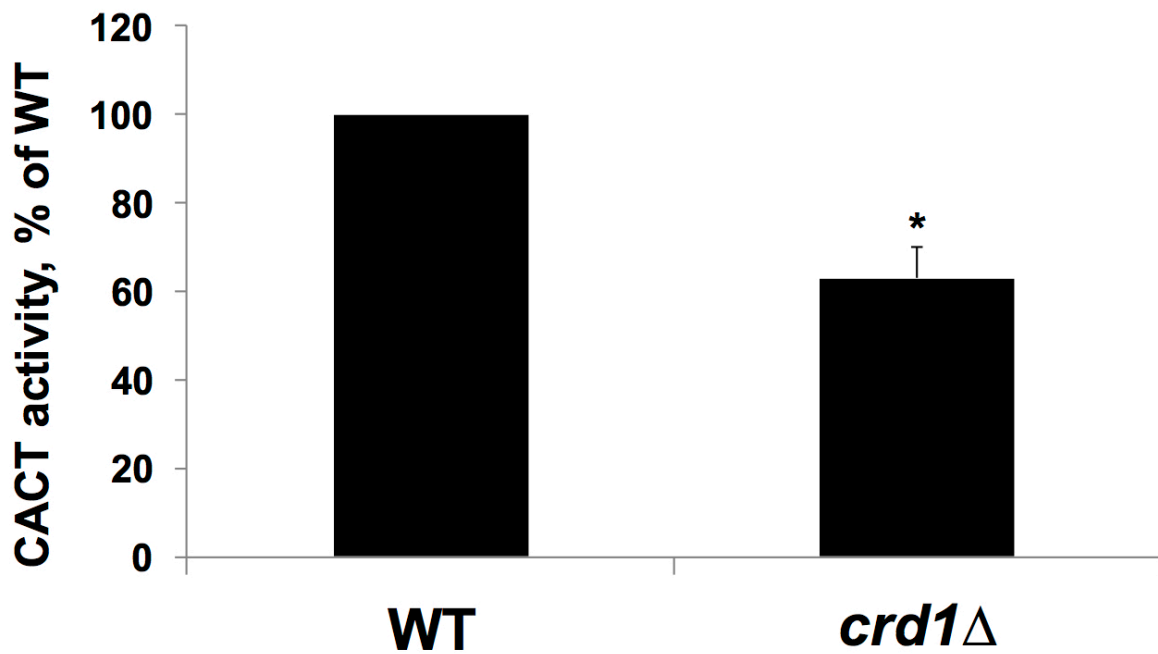
FIGURE 3.5. Carnitine-acetylcarnitine tranlocase activity is decreased in *crd1Δ*. Wild-type and *crd1Δ* cells were grown in YNBO and carnitine-acetylcarnitine tranlocase activity was measured as described in the "Materials and Methods". Data shown are mean ± S.E. (n = 6) (*p<0.05).
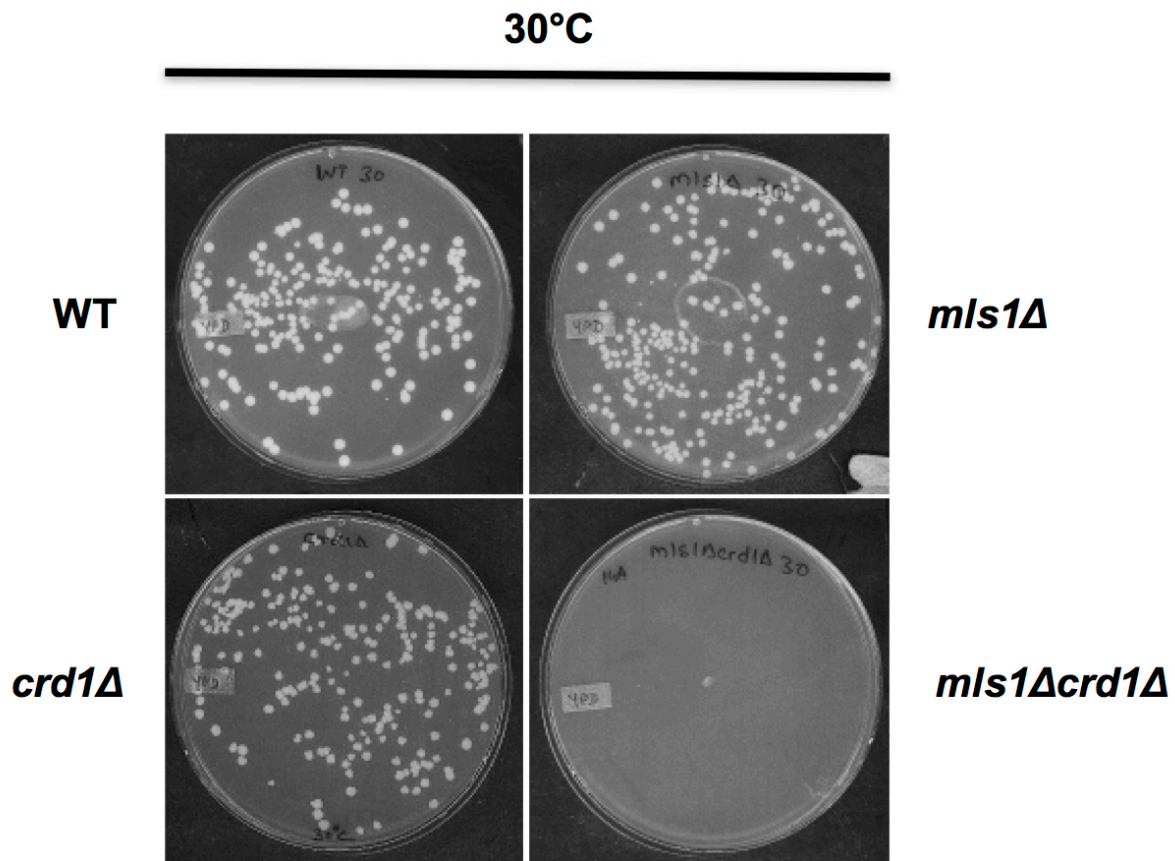
FIGURE 3.6. Genetic interaction between *crd1Δ* and *mls1Δ*. Cells were pre-cultured in YPD overnight, serially diluted, plated on YNBD, and incubated at 30°C for 4 days.

A
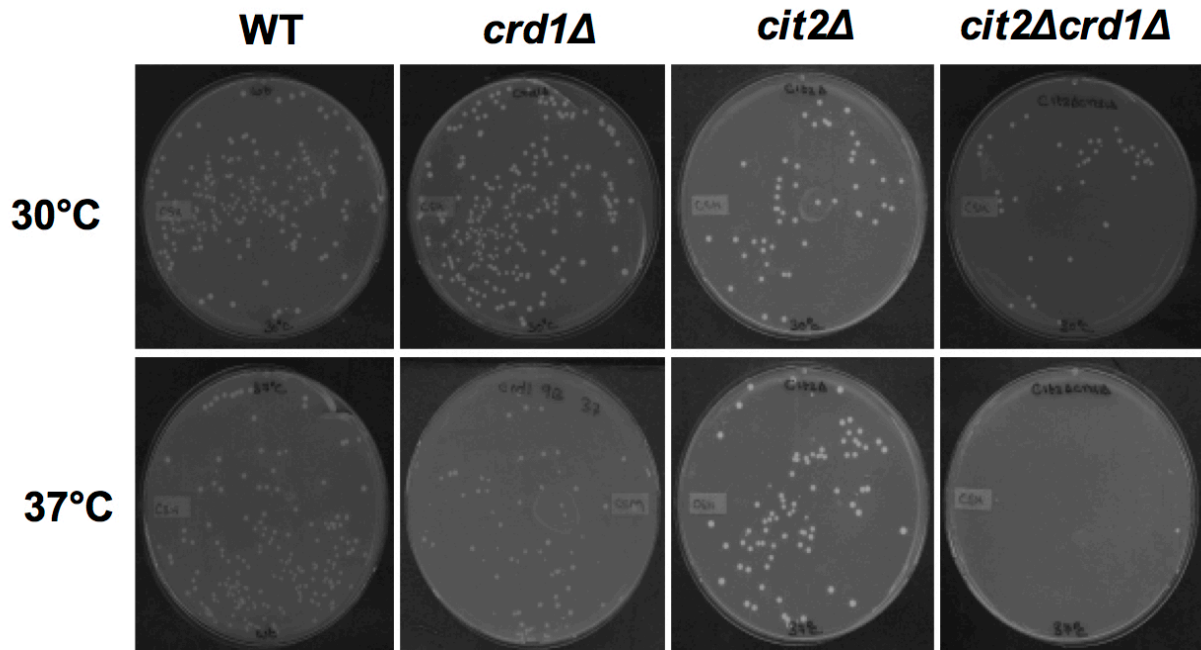
B
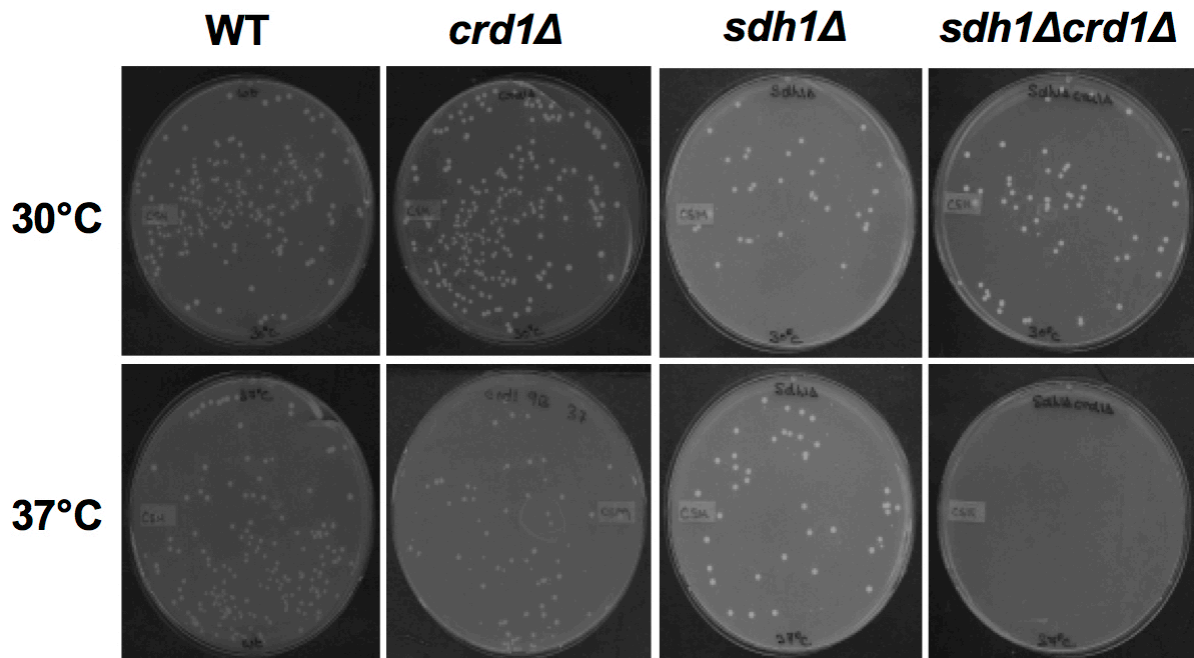
C
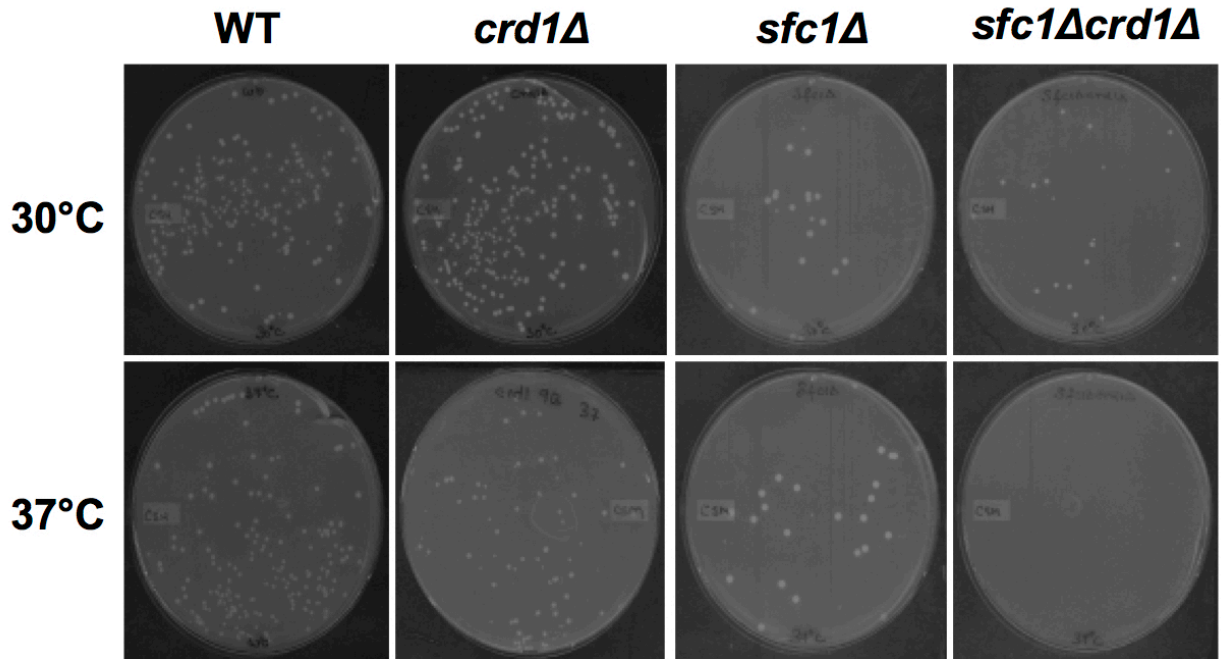
FIGURE 3.7. Genetic interaction between _crd1Δ_ and glyoxylate cycle mutants. Cells were pre-cultured in YPD overnight, serially diluted, plated on YNBD, and incubated at 30°C or 37°C for 4 days. Genetic interaction between _crd1Δ_ and (A) _cit2Δ_, (B) _sdh1Δ_, and (C) _sfc1Δ_ was determined.
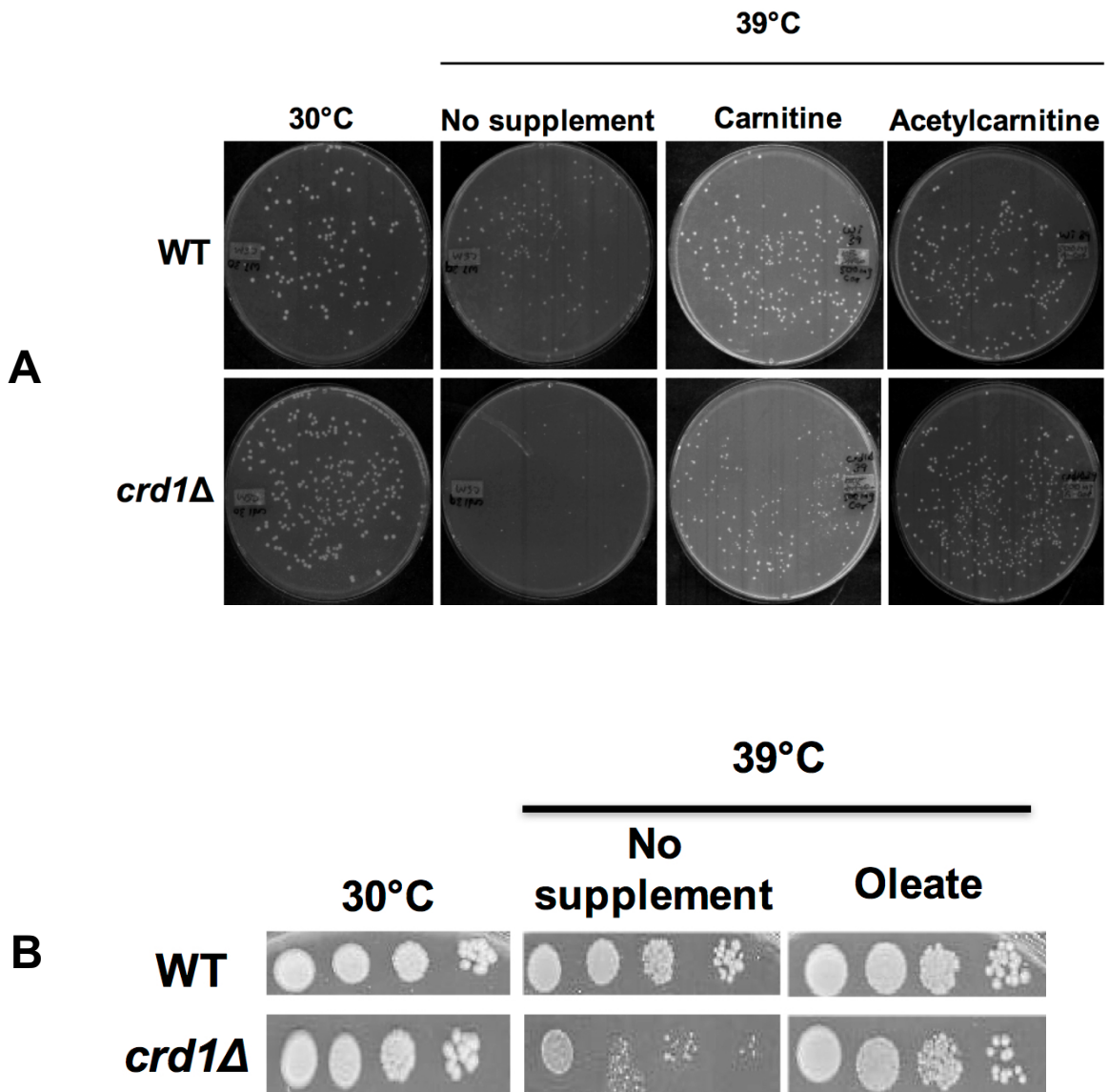
FIGURE 3.8. Supplementation of carnitine, acetylcarnitine, or oleate restored the growth of *crd1Δ* at elevated temperature. Cells were pre-cultured in YNBD overnight, serially diluted, and plated on YNBD with or without carnitine or acetylcarnitine (500 mg/l) (A) or oleate (B). Plates were incubated at 30°C or 39°C for 4 days.
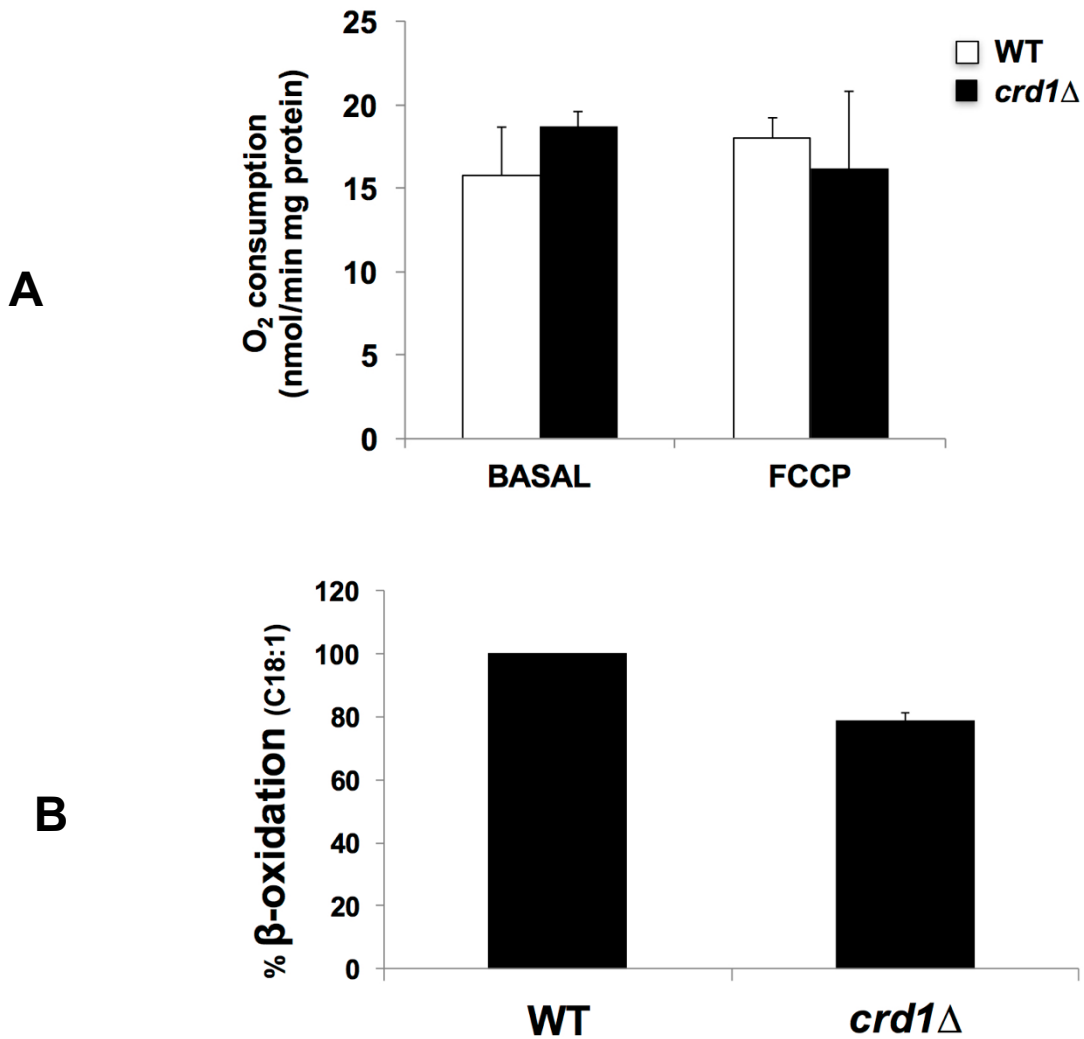
FIGURE 3.9A. β-oxidation is not significantly affected in *crd1Δ* cells. Wild-type and *crd1Δ* cells were grown in YNBO. (A) O_2 consumption and (B) β-oxidation of oleate were measured as described in the "Materials and Methods". Data shown are mean ± SE (n=6).

DISCUSSION

The studies in this chapter support the hypothesis that CL mutants require the carnitine shuttle and the glyoxylate cycle for optimal growth. The *crd1Δ* mutant exhibit decreased carnitine-acetylcarnitine translocase activity; supplementation of carnitine or acetylcarnitine restored growth on acetate and rescued the temperature sensitive phenotype of the mutant. The most striking finding was synthetic lethality between *crd1Δ* and glyoxylate cycle mutants. Furthermore, the temperature sensitivity phenotype of *crd1Δ* cells was restored by supplementation of oleate. The most likely explanation for this rescue is that the glyoxylate cycle is required to restore TCA cycle metabolites in CL-deficient cells.

How does the glyoxylate cycle compensate for TCA cycle defects in CL-deficient cells? The glyoxylate cycle synthesizes TCA cycle intermediates in the peroxisome, which are transported into the mitochondria. In *S.cerevisiae*, the peroxisomal membrane forms a pore-like structure that is permeable to acetylcarnitine (van Roermund et al., 1999; Kunze and Hartig, 2013). Supplementation of carnitine transports acetyl-CoA from the cytosol to the peroxisome as acetylcarnitine, which is converted to acetyl-CoA that is utilized in the glyoxylate cycle. The glyoxylate cycle may be up-regulated in *crd1Δ* cells. Alternatively, glyoxylate cycle enzyme activities may be increased in the mutant. Either of these responses could potentially replenish intermediates of the TCA cycle, including succinate, malate, and citrate.

How does CL deficiency lead to decreased carnitine-acetylcarnitine translocase activity? Crc1 is localized in the inner mitochondrial membrane, which contains CL in proximity to the CL-enriched membrane. CL was shown to activate Crc1 *in vitro* (Noel

and Pande, 1986) and may thus be required for Crc1 function *in vivo* as well. The stability

of Crc1 may also be decreased in CL-deficient membranes. An alternative possibility is

that import of Crc1 into the mitochondria of CL-deficient cells may be decreased, as CL

is required for optimal protein import (Jiang et al., 2000; Gebert et al., 2009).

Based on the data obtained, I propose the following model to elucidate the role of

CL in regulating the transport of acetyl-CoA (Fig. 3.10). Loss of CL leads to decreased

carnitine-acetylcarnitine translocase activity in the inner mitochondrial membrane, which

disrupts shuttling of acetyl-CoA to the mitochondria from cellular compartments.

Decreased movement of acetylcarnitine across the mitochondria reduces levels of the

precursor of the TCA cycle (acetyl-CoA) and perturbs synthesis of TCA cycle

intermediates. Therefore, CL-deficient cells depend on the glyoxylate cycle to replenish

intermediates of the TCA cycle.

How is the role of CL in transport of acetyl-CoA relevant to BTHS and other cardiac

disorders? The data presented here suggest for the first time that CL is a critical regulator

of intracellular transport of acetyl-CoA. Human disorders of carnitine deficiency have been

described, several of which lead to clinical outcomes similar to those seen in BTHS. The

deficiency of carnitine palmitoyltransferase (CPT II) is associated with exercise

intolerance, carnitine-acetylcarnitine translocase (CACT) deficiency leads to

cardiomyopathy with arrhythmia, and deficiency of the carnitine transporter (OCTN2)

results in cardiomyopathy and skeletal myopathy (Rinaldo et al., 2002; Ørngreen et al.,

2003; Longo et al., 2006; Wanders and Ruiter, 2010). In mammals, disruption of the TCA

cycle perturbs cardiac ATP production, which is essential for cell function and basal

cellular metabolism. The primary source of energy in the heart is ATP that is produced

entirely from oxidative phosphorylation using substrates (NADH and $FADH_2$) generated mainly in the TCA cycle (Kodde et al., 2007; Stanley et al., 2005). The results from my studies using yeast as a model system suggest that supplementation of deficient metabolites may alleviate some of the clinical presentation observed in BTHS and other disorders due to CL deficiencies.
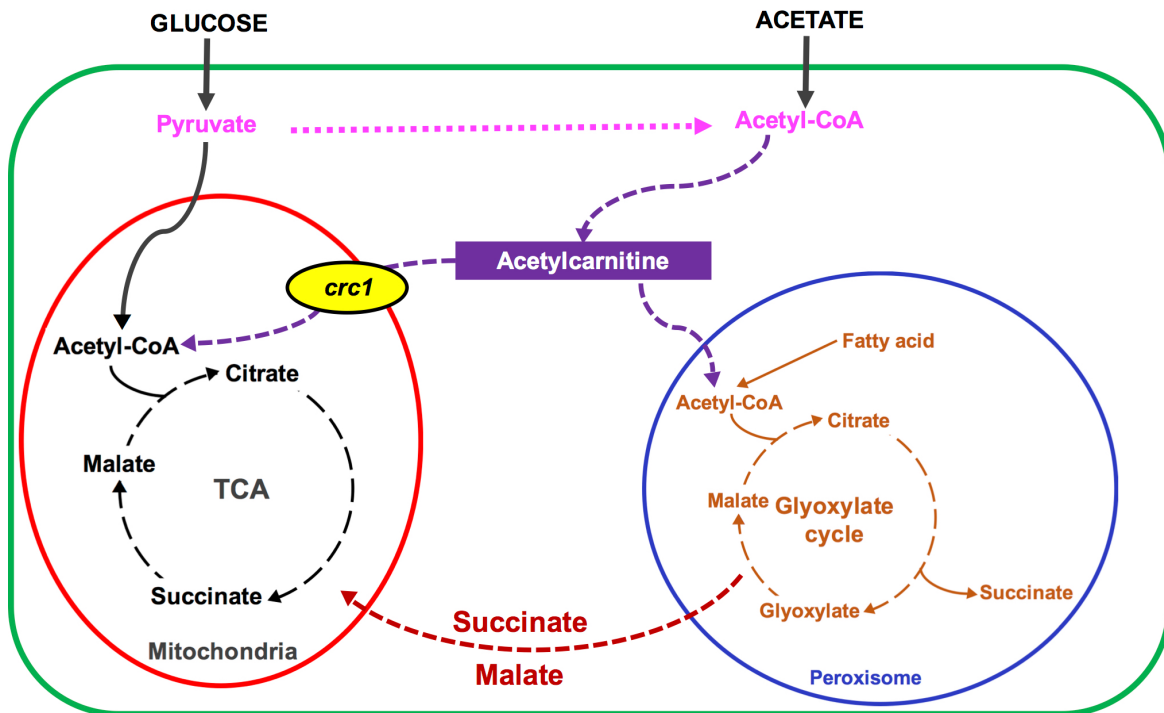
FIGURE 3.10. Model: Glyoxylate cycle-dependent transport of metabolites in CL-deficient cells. Loss of CL leads to decreases in acetyl-CoA (Chapter 2) and carnitine-acetylcarnitine translocase activity, causing perturbation of acetylcarnitine transport into mitochondria. Translocase deficiency may result in reduced synthesis of TCA cycle intermediates due to decreased acetyl-CoA. Intermediates of the TCA cycle supplied by the glyoxylate cycle replenish these deficiencies.

TABLE 3.1. Yeast strains used in this study.

Strains	Genotype	Source or Ref.
BY4741	*MATα, his3Δ1, leu2Δ0, ura3Δ0, met15Δ0*	Invitrogen
BY4742	*MATα, his3Δ1, leu2Δ0, ura3Δ0, lys2Δ0*	Invitrogen
VGY1	*MATα, his3Δ1, leu2Δ0, lys2Δ0, ura3Δ0, crd1Δ::URA3*	Gohil et al., 2005
CG922-a	*MATa, lys2-801, ade2-101, trp1Δ1, his3Δ200, leu2Δ1, crd1Δ::URA3*	
CG923-α	*MATα, lys2-801, ade2-101, trp1Δ1, his3Δ200, leu2Δ1, crd1Δ::URA3*	
mls1Δ	*MATa, his3Δ1, leu2Δ0, met15Δ0, ura3Δ0, mls1Δ::KanMX4*	Invitrogen
cit2Δ	*MATa, his3Δ1, leu2Δ0, met15Δ0, ura3Δ0, cit21Δ::KanMX4*	Invitrogen
sdh1Δ	*MATa, his3Δ1, leu2Δ0, met15Δ0, ura3Δ0, sdh1Δ::KanMX4*	Invitrogen
sfc1Δ	*MATa, his3Δ1, leu2Δ0, met15Δ0, ura3Δ0, sfc1Δ::KanMX4*	Invitrogen
mls1Δcrd1Δ	*MATa, his3Δ1, leu2Δ0, met15Δ0, ura3Δ0, mls1Δ::KanMX4, crd1Δ::KanMX4*	This study
cit2Δcrd1Δ	*MATa, his3Δ1, leu2Δ0, met15Δ0, ura3Δ0, cit2Δ::KanMX4, crd1Δ::KanMX4*	This study
sdh1Δcrd1Δ	*MATa, his3Δ1, leu2Δ0, met15Δ0, ura3Δ0, sdh1Δ::KanMX4, crd1Δ::KanMX4*	This study
sfc1Δcrd1Δ	*MATa, his3Δ1, leu2Δ0, met15Δ0, ura3Δ0, sfc1Δ::KanMX4, crd1Δ::KanMX4*	This study

CHAPTER 4 IDENTIFICATION OF PHYSIOLOGICAL MODIFIERS THAT EXACERBATE THE LOSS OF TAFFAZIN

INTRODUCTION

Barth syndrome (BTHS), a rare X-linked genetic disorder, is caused by mutations in the gene tafazzin (TAZ). TAZ is involved in remodeling cardiolipin (CL), the signature phospholipid of the mitochondrial membranes. The clinical symptoms that characterize BTHS vary widely, even among patients with the identical mutation, and the mechanism underlying the pathology of BTHS has not been identified. We hypothesize that physiological modifiers exacerbate the tafazzin defect and, hence, account for the diversity in symptoms. Identification of such physiological modifiers will elucidate the cellular role of tafazzin and may shed light on the mechanisms underlying the diverse clinical symptoms in BTHS patients.

Previous studies have reported that tafazzin is conserved from yeast to humans and suggest the feasibility of identifying synthetic interactions in yeast that may be relevant to BTHS. The yeast *TAZ1* gene shares homology with the human TAZ gene, G4.5. Our lab constructed a null mutant of this gene, *taz1Δ*, by removing 91% of the coding sequence (Gu et al., 2004). Phospholipid analysis of the null mutant showed a reduced level of total CL and accumulation of MLCL (monolysocardiolipin), consistent with defective CL remodeling, as seen in BTHS cells. The predominant acyl species found in wild type CL were markedly reduced in *taz1Δ*, and CL molecules contained more saturated fatty acids than those in the wild type (Gu et al., 2004). In addition, CL in the *taz1Δ* mutant contained multiple fatty acyl species, and these lacked molecular symmetry, similar to the finding in BTHS cells (Schlame et al., 2005). These defects in yeast are complemented by expression of the human TAZ cDNA (Ma et al., 2004). Our lab has

characterized several CL mutants that may be used to assess the role of CL in cell functions. The current study utilizes the *taz1Δ* mutant, which cannot remodel CL. Functional conservation of CL mutants from yeast to humans increases the probability that synthetic interactions that occur with yeast CL mutants will also be observed in mammalian cells. To identify these physiological factors, we used the powerful genetic tool Synthetic Genetic Analysis (SGA) to identify synthetic interactions of tafazzin, which are likely to identify genes that affect its phenotypic expression.

Synthetic analysis exploits the possibility that two non-lethal mutations in genes providing overlapping / essential functions lead to an inviable cell when present together (Hartman et al., 2001). Synthetic lethal interaction may suggest that the gene products carry out similar functions, possibly by alternative pathways. In the yeast *S. cerevisiae*, synthetic lethal screens traditionally have been based on a plasmid dependence assay, in which mutagenized cells are screened for the inability to lose a plasmid carrying the gene of interest. More recently, SGA methodology (Tong et al., 2004) has made it possible to evaluate double mutants containing a mutation in a specific gene of interest and in each of 4,800 non-essential yeast genes. Synthetic lethal screens have elucidated gene function as well as interactions in pathways as diverse as DNA replication (Grossi et al., 2004; Suter et al., 2004), the MAP kinase cell integrity pathway (Green et al., 2003), endocytosis (Care et al., 2004), DNA damage tolerance (Hishida et al., 2002), nuclear migration (Fujiwara et al., 1999), the spindle checkpoint (Lee and Spencer, 2004), and phospholipid synthesis (Birner et al., 2003). Previous studies in our lab have identified a synthetic lethal interaction between the genes for CL synthase and mitochondrial phosphatidylethanolamine (PE) synthesis (Gohil et al., 2005). We expect that the

synthetic lethality screen will facilitate the identification of physiological factors that exacerbate the loss of tafazzin.

The SGA screen offers two important advantages over classical genetic approaches: (a) An existing collection of yeast deletion mutants of all 4,800 non-essential yeast genes can be screened, and (b) the identity of the mutant is known immediately. We implemented the SGA screen (Fig. 4.1) to identify mutants that synthetically interact with *taz1Δ* in order to obtain a global idea of pathways that have overlapping function with CL remodeling. In the study described here, seventy synthetic lethal mutants and one hundred and two synthetic sick mutants were identified by the SGA and are grouped based on biological function. Among these, interaction with genes for phospholipid deacylation, arginine metabolism, iron homeostasis, and vacuolar protein sorting were validated.

MATERIALS AND METHODS

Yeast strains and growth media

The yeast *S. cerevisiae* strains used in this study are listed in Table 4.1. Single deletion mutants were obtained from the yeast knockout deletion collection (Invitrogen). Double mutants were obtained by tetrad dissection. Synthetic complete (YNB) medium contained adenine (20.25 mg/liter), arginine (20 mg/liter), histidine (20 mg/liter), leucine (60 mg/liter), lysine (200 mg/liter), methionine (20 mg/liter), threonine (300 mg/liter), tryptophan (20 mg/liter), uracil (20 mg/liter), yeast nitrogen base without amino acids (Difco), and glucose (2%) (YNBD) or sodium acetate (2%) (YNBA). Synthetic dropout media contained all ingredients mentioned above but lacked specific compounds required for selection. Sporulation medium contained potassium acetate (1%), glucose (0.05%),

and the essential amino acids required for sporulation. Complex medium contained yeast extract (1%), peptone (2%), and glucose (2%) (YPD). Solid medium was prepared by adding 2% agar.

DNA and strain manipulation

To construct the *taz1Δcan1Δ* starting strain, a 1.8 kb *CAN1* deletion cassette was amplified from Y5563 (kindly provided by Dr. Charles Boone) by sense primer (5'-TAGGGCGAACTTGAAGAATAACC-3') and antisense primer (5'-ACGAAAAATGAGTAAAAATTATCTT-3') and inserted into the genome of BY4741 *(MATa)* with the disruption confirmed by PCR. The *can1Δ* mutant was then crossed to BY4742 *(MATα)* to obtain a *MATα can1Δ* strain by tetrad analysis. The *TAZ1* gene in the *can1Δ* mutant *(MATα)* was disrupted by a 1.8 kb *URA3* fragment released from the PUC19 plasmid digested using PvuII. The disruption of *TAZ1* was confirmed by PCR, Southern blot, and phospholipid analysis.

Synthetic genetic array (SGA)

The *MATα can1Δtaz1Δ* mutant was crossed to the array of deletion mutants in the *MATa* background, in which the deletions are linked to the dominant selectable marker for geneticin resistance, *KanMX4*. Diploids were selected and sporulation was induced. Haploid spore progeny were transferred to synthetic medium lacking histidine, which allowed for selective germination of *MATa* cells (by virtue of the *MFA1pr-HIS3* reporter). Following two rounds of selection in His- synthetic medium, double mutant *MATa* progeny were selected in Ura- medium supplemented with geneticin. Independent confirmation of synthetic lethality was carried out to rule out false positives and false negatives (Tong et al., 2001).

Construction of double mutants by tetrad dissection

The CL mutant *taz1Δ::URA3 MATα* was crossed with mutants of opposite mating type obtained from the yeast deletion collection. The heterozygous diploids were selected on dropout medium lacking methionine and lysine, sporulated, and tetrads were dissected. The synthetic interaction between CL and deletion mutants was determined by examining the growth of the double mutant compared to isogenic parent strains and wild type on YPD.

Colony formation analysis

Cells were pre-cultured in YPD at 30˚C to the mid-log phase. The absorbance at 550nm (A_{550}) of the liquid culture was determined using a spectrophotometer (Beckman). Cell aliquots were centrifuged and pellets were re-suspended in YPD to adjust the A_{550} value to 10 units per mL. 10 µL of the above sample were added to 990 µL of water. 10 µL of the 100X diluted sample were placed on a hemocytometer for cell counting using light microscopy at a magnification of 1000X. Based on cell number, cell aliquots with A_{550} of 10 were adjusted again and diluted to 2000 cells/mL, from which 100 µL suspension that contained about 200 cells were plated on a YPD plate and incubated at 30˚C or 39˚C for 3 days. The ability of single cells to form colonies was evaluated at 30˚C or 39˚C.

FM 4-64 staining

FM 4-64 staining was performed as previously described (Conboy and Cyert, 2000) with minor modification. Cell aliquots equivalent to an A_{550} of 1.0 were harvested by centrifugation, resuspended in 100 µL YPD, and incubated at 37˚C or 39˚C with 0.16 mM FM4-64 for 15 min. Cells were pelleted and washed once with 37˚C YPD or 39˚C YPD and then resuspended in 500 µL YPD of the same temperature for 30 min. The cell

suspension was centrifuged and the supernatants were discarded. The cell pellets were resuspended in 100 μL YPD, from which 3 μL were applied to the microscope slide and observed using epifluorescence microscopy using the filter for red fluorescence.

RESULTS AND DISCUSSION

Construction of the starting strain for the synthetic lethal screen

The starting strain was constructed in four steps: disruption of *TAZ1* in *can1Δ*, confirmation of disruption by PCR, genetic analysis of phenotypes, and phospholipid analysis. The *CAN1* deletion cassette was amplified from Y5563 and inserted into BY4741 *(MATa)*, which was further crossed with BY4742 *(MATα)* to obtain *MATα can1Δ* by tetrad analysis (as explained in Tong et al., 2001). The yeast chromosomal *TAZ1* gene in the *can1Δ* mutant *(*BY4742 *MATα)* was disrupted by the deletion cassette as shown in Fig. 4.2, and amplified by PCR to construct the *can1Δtaz1Δ* mutant *(*BY4742 *MATα)*. The disruption of *CAN1* and *TAZ1* was confirmed by PCR and phospholipid analysis. To confirm mating type, the starting strain *can1Δcrd1Δ* was crossed to test strains CG922 *(MATa)* and CG923 *(MATα)* and replica plated on minimal medium. The selective markers of BY4742 *MATα can1Δtaz1Δ* mutant were confirmed on synthetic dropout medium. The starting strain BY4742 *MATα can1Δtaz1Δ*, thus constructed, was further used to carry out the synthetic lethal screen.

Genome-wide synthetic lethality screen with *can1Δtaz1Δ*

The query strain, in which the *taz1Δ* mutation was linked to the dominant selectable marker *URA3* and the reporter construct *MFA1pr-HIS3*, which is expressed only in *MATa* cells was crossed with the array of 4,800 deletion mutants in the *MATa* background, in which the deletion is linked to the dominant selectable marker for geneticin

(kanamycin) resistance, *KanMX*. The *MATα* strain was lys⁻met⁺, and the *MATa* strain was met⁻ lys⁺. Diploids were selected on plates lacking both lysine and methionine, and sporulation was induced. Haploid spore progeny were transferred to synthetic medium lacking histidine, which allows for selective germination of *MATa* cells (by the *MFA1pr-HIS3* reporter). Following two rounds of selection, the *MATa* cells were transferred to medium lacking uracil and containing geneticin. Synthetic interaction was indicated by decreased growth of the haploid double mutant progeny.

As expected, the SGA screen identified a large number of synthetic interactions that included 70 potential synthetic lethal interactions (Table 4.2 and 4.3) and 102 potential sick interactions (Table 4.4 and 4.5), which were grouped based on biological function (Fig. 4.3 and 4.4). These genes define many biological functions, including hydrolase activity, transferase activity, structural molecule activity, DNA binding, structural constituent of ribosome, cytoskeleton protein binding, oxidoreductase activity, transporter activity, ATPase activity, methyltransferase activity, ion binding, lyase activity, signal transducer activity, phosphatase activity, and others.

Biological processes required for fitness of the *taz1Δ* mutant

The screen identified two mutants, *arg3Δ* and *isa2Δ*, previously shown to be synthetically lethal with *taz1Δ* (Gaspard et al., 2015). However, two genes previously shown to be synthetically lethal with *taz1Δ*, *yme1Δ* and *tom5Δ*, were not identified. This outcome is consistent with the large number of false positives and false negatives that commonly result from this screen. The SGA screen has large number of false positive and false negative due to following reasons: (a) the selection of double mutants may not be stringent enough, (b) the genetic background of the deletion collection was constructed

in the BY4741 or BY4742 background and the *taz1Δ* mutant exhibits less severe phenotype in this particular background, and (c) SGA involves several steps such as mating, selection on drop out media, and meiotic sporulation. If growth of mutants is affected in these process, double mutants may not be identified, demonstrating the need for follow-up studies to verify findings independently. Follow up studies were carried out with mutants of phospholipase B metabolism, arginine metabolism, mitochondrial iron metabolism, and vacuolar protein sorting.

a. Phospholipase B and phospholipid metabolism. The screen revealed that *taz1Δ* is synthetically sick with *plb3Δ*. *PLB3* encodes phospholipase B (lysophospholipase), which hydrolyzes phosphatidylinositol and phosphatidylserine (Merkel et al., 1999; Merkel et al., 2005; Byrne and Wolfe, 2005). This was especially interesting because Taz1 is a transacylase that transfers acyl groups from phospholipids (independent of CoA). Synthetic lethality with phospholipases suggests that Taz1 may affect cellular functions as a result of affecting lysolipids other than those derived from CL. It remains unclear why *taz1Δ* is synthetically sick with *plb3Δ*. To determine if other phospholipase B mutants (*plb1Δ* and *plb2Δ*) interact with *taz1Δ*, I constructed double mutants with *taz1Δ* and checked for growth at elevated temperatures by the colony formation assay (Table 4.6). I also tested synthetic interaction with *crd1Δ* to distinguish between the role of CL depletion vs CL remodeling in the synthetic interaction. The *taz1Δ* mutant in this genetic background can grow at temperatures up to 39°C, while the *crd1Δ* mutant can grow at temperature only up to 37°C. As seen in Table 4.6, mutants *plb1Δ* and *plb3Δ*, but not *plb2Δ*, showed genetic interaction with *taz1Δ*. Interestingly, the phospholipase B mutants did not genetically interact with *crd1Δ*, suggesting that the

function that was affected in the double mutant was not CL deficiency, but probably more related to CL remodeling.

Previous studies have shown that the only phospholipase that deacylates CL is cardiolipin-specific deacylase (*CLD1*), although the possibility that enzymes with phospholipase A or B activity could also catalyze deacylation of CL was not ruled out (Beranek et al., 2009). In *Penicillium notatum*, purified phospholipase B catalyzed deacylation of 1,2-diacylphospholipid and lysophospholipids at the sn-1 and sn-2 positions of fatty acids, and CL acts as a lipid activator of catalysis (Saito., 2014). Witt et al. (1984) reported that phospholipase B exhibits transacylase activity in *S. cerevisiae*. Based on these studies, I hypothesize that tafazzin plays a role not only in the acylation of MLCL to CL, but also in regulating lysolipid formation from other cellular lipids.

b. Arginine metabolism. *ARG3* encodes an enzyme that catalyzes the biosynthesis of arginine from ornithine, thereby participating in the aspartate-argininosuccinate shunt (Crabeel et al., 1981). The role of the aspartate-argininosuccinate shunt is to break down ornithine into intermediates of the TCA cycle, including fumarate and malate. Recent studies demonstrated that *taz1Δ* is synthetically lethal with *arg3Δ* (Beranek et al., 2009). My observation that *arg3Δ* is synthetically sick with *taz1Δ* confirms the previous finding and suggests that the aspartate-argininosuccinate shunt is required for cells to survive in the absence of tafazzin. There are at least two possible explanations for this synthetic interaction. First, *taz1Δ* cells may be deficient in TCA cycle intermediates fumarate and malate, which can be supplied by the aspartate-argininosuccinate shunt. This is consistent with the observed decrease in aconitase and succinate dehydrogenase activities in CL deficient cells, suggesting that

the TCA cycle is perturbed (Patil et al., 2013). Second, synthetic lethality may reflect an increased need for glutamine. In yeast, glutamate is converted to glutamine by glutamine synthetase. Decreased growth of the *crd1Δ* mutant is rescued by supplementation of glutamate (Vinay A. Patil, unpublished data). This deficiency may be exacerbated by perturbation of the aspartate-argininosuccinate shunt, which converts glutamate to glutamine and other intermediates of the TCA cycle.

c. Mitochondrial iron metabolism. The SGA screen identified *isa2Δ* as synthetically lethal with *taz1Δ*. *ISA2* encodes a protein required for the maturation of mitochondrial Fe-S clusters. Patil et al. (2013) showed that *crd1Δ* cells exhibit defective Fe-S biogenesis, resulting in perturbation of iron homeostasis. The synthetic lethality finding suggests that the *taz1Δ* mutant may also exhibit Fe-S defects. The phenotypes observed due to perturbation of Fe-S biogenesis in humans include heart failure and hypertrophic cardiomyopathy (Tsai et al., 2010), and may also be relevant in BTHS. It is unclear how CL synthesis is linked to Fe-S biogenesis. Decreased import of proteins required for Fe-S biogenesis has been suggested (Patil et al., 2013), which may explain a defect in both *crd1Δ* and *taz1Δ* cells.

d. Vacuole protein sorting. *APM3* encodes the Mu3-like subunit of the AP-3 clathrin associated protein complex, which functions in the alkaline phosphatase pathway (ALP) (Yeung et al., 1999; Odorizzi et al., 1998; Cowles et al., 1997). The ALP pathway bypasses endosomal intermediates and transports alkaline phosphatase to the vacuole (Piper et al., 1997; Cowles et al., 1997; Odorizzi et al., 1998). The screen revealed that *apm3Δ* is synthetically sick with *taz1Δ*, but validation did not confirm genetic interaction with *taz1Δ* or *crd1Δ*. In fact, follow up experiments indicated that *apm3Δ* rescued *crd1Δ*

defects. Previous studies have shown that the loss of CL leads to vacuolar defects, including enlarged vacuole and decreased vacuole acidification at elevated temperature (Chen et al., 2008b). These phenotypes suggested that endocytic trafficking may be perturbed in the CL mutant. Interestingly, *apm3Δ* rescued decreased cell growth (Figs. 4.5 and 4.6), as well as vacuolar morphology defects of *crd1Δ* at elevated temperature (Fig. 4.7). One possible explanation for rescue by *apm3Δ* is that the ALP pathway may be up-regulated or overactive in CL-deficient cells. This would result in excessive transport of alkaline phosphatase and the vacuolar t-SNARE Vam3p to the vacuole, which is deleterious to cells (Stepp et al., 1997). These findings suggest that overactive the ALP pathway or increased alkaline phosphatase in the vacuole may be deleterious to CL-deficient cells.

Conclusion

The SGA screen described here identified many genetic interactions with *taz1Δ*, suggesting that many cellular pathways are affected by tafazzin. Interesting interactions were observed with genes affecting phospholipase B, the argininosuccinate shunt, mitochondrial iron homeostasis, and vacuolar protein sorting. The interaction with phospholipase B suggests that taffazin may be involved in remodeling phospholipids other than CL. Previous studies reported that Fe-S biogenesis is perturbed in *crd1Δ* (Patil et al., 2013). The genetic interaction studies in this chapter suggest that Fe-S biogenesis may also be perturbed in *taz1Δ*. The aspartate-argininosuccinate shunt functions in the synthesis of the TCA cycle intermediates, and synthetic lethality with mutants in this pathway suggests that the aspartate-argininosuccinate is required for tafazzin deficient

cells. Understanding the role of tafazzin in Fe-S biogenesis and the aspartate-argininosuccinate shunt may have implication for BTHS.
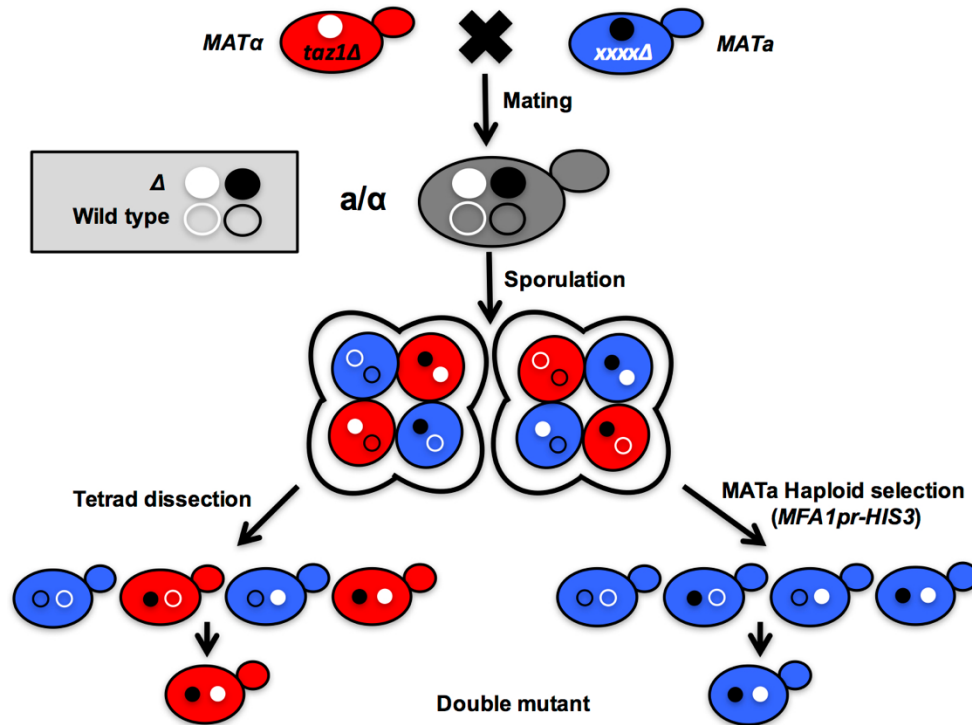
FIGURE 4.1. Synthetic genetic array (SGA) screen identifies mutants synthetically lethal with _taz1Δ_ (modified from Tong et al., 2001). A _MATα_ (lys-) query strain carrying the mutations (_taz1Δ::URA3_ and _can1Δ::MFA1pr-HIS3_) was crossed to an ordered array of _MATa_ (met-) viable yeast deletion mutants, each carrying a gene deletion mutation linked to a kanamycin-resistance marker (KanMX) to form diploids. The haploid meiotic spore progeny are formed when heterozygous diploids are transferred to the sporulation media. Haploid spore progeny were transferred to synthetic medium lacking histidine, which allows for selective germination of _MATa_ cells which express the _MFA1pr-HIS3_ reporter specifically. The selected _MATa_ meiotic progeny were transferred to the medium that lacks uracil and contains kanamycin. Uracil auxotrophy and kanamycin resistance markers were used to identify the double mutant meiotic progeny.
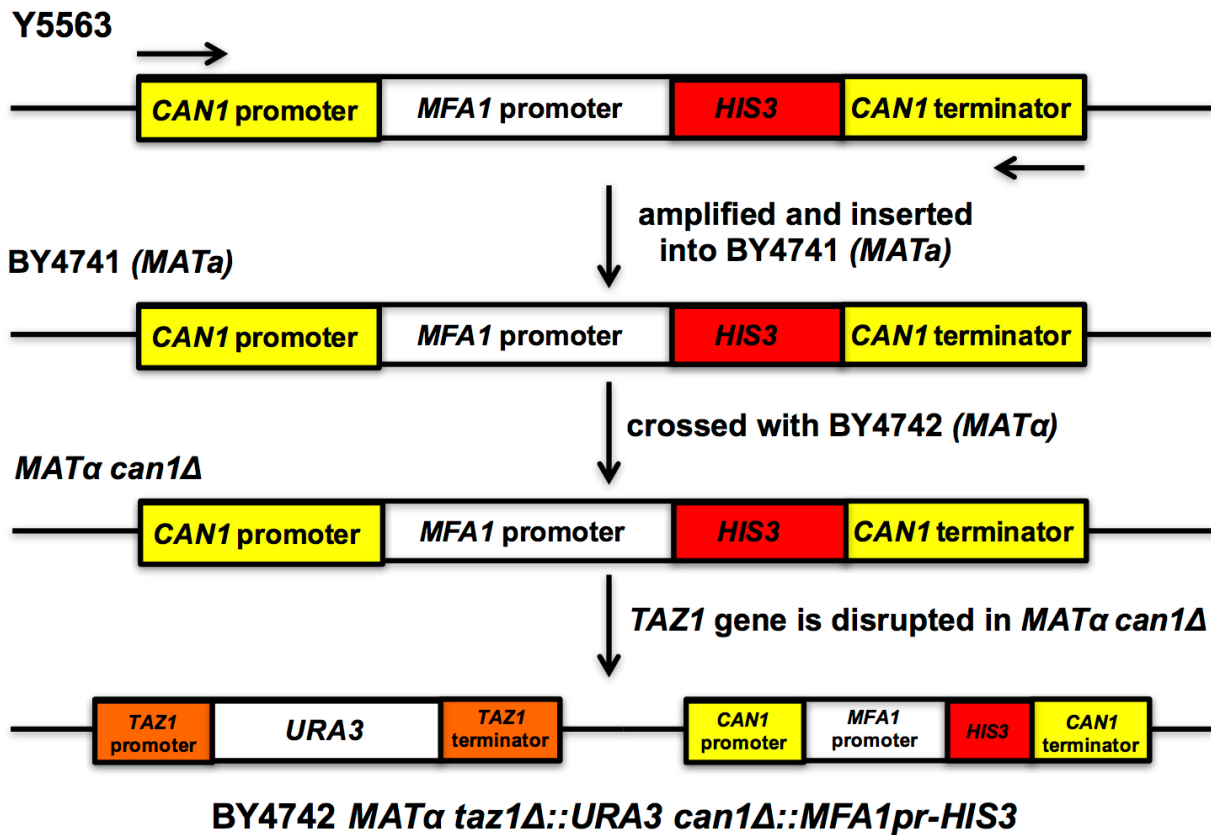
FIGURE 4.2. Disruption of the chromosomal *TAZ1* gene by *URA3* to obtain BY4742 *MATα taz1Δ::URA3 can1Δ::MFA1pr-HIS3* (modified from Tong et al., 2001). Construction of the starting strain (*taz1Δ::URA3 can1Δ::MFA1pr-HIS3*) involved two steps. First, the *mfa1Δ::MFA1pr-HIS3* open reading frame (ORF) was integrated at the *CAN1* locus such that its expression is regulated by the MFA1 promoter (MFA1pr), *mfa1Δ::MFA1pr-HIS3*. Second, the *TAZ1* gene in the *can1Δ::MFA1pr-HIS3* strain was disrupted by a 1.8 kb URA3 fragment generated from construct DR2 to obtain *MATα taz1Δ::URA3 can1Δ::MFA1pr-HIS3*.
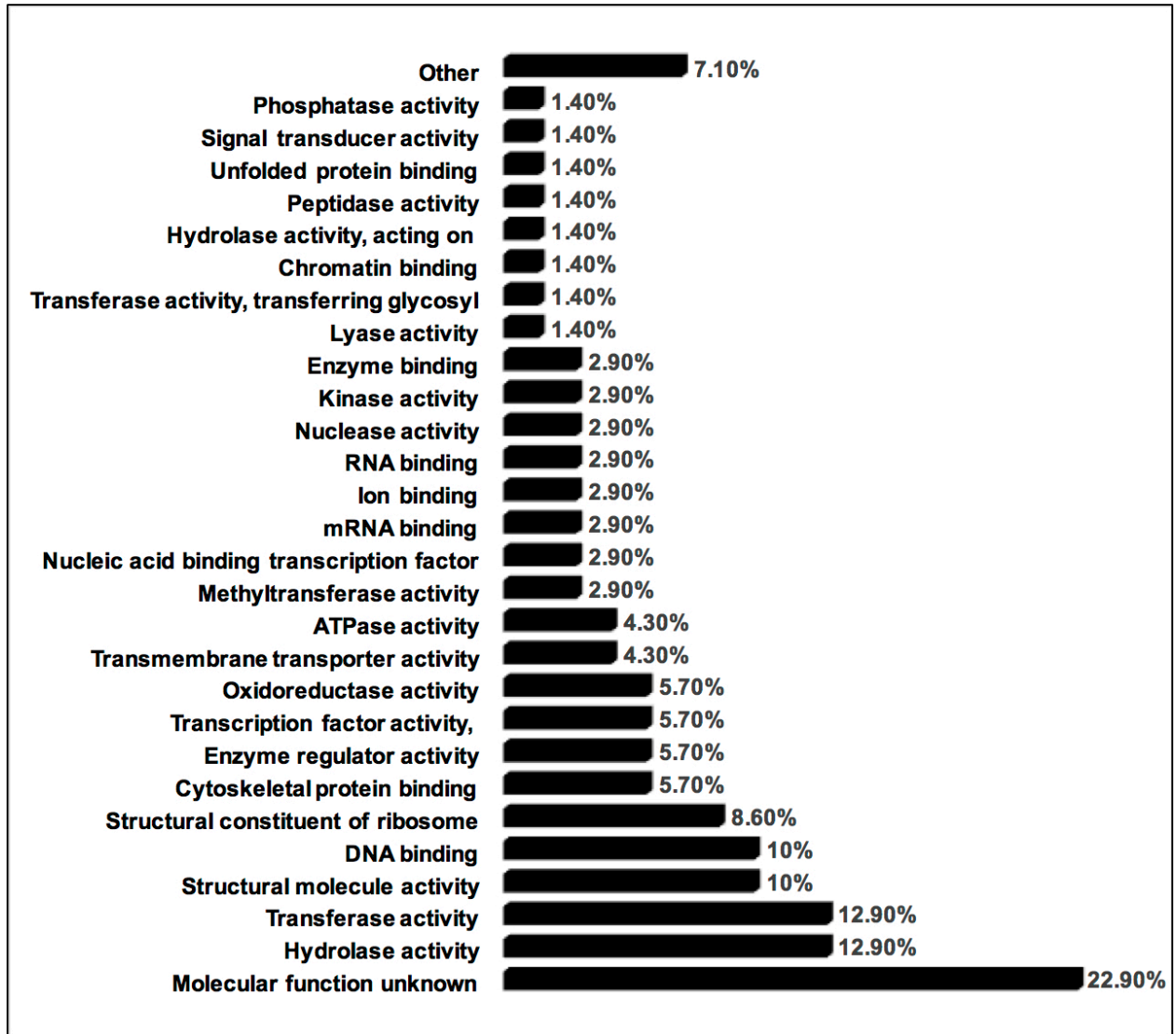
FIGURE 4.3. Functional classification of genes exhibiting synthetic lethal interaction with *taz1Δ*. Synthetic lethal interactions identified by SGA were classified by biological process based on gene ontology. The percentage of genes representing the specific processes are indicated.
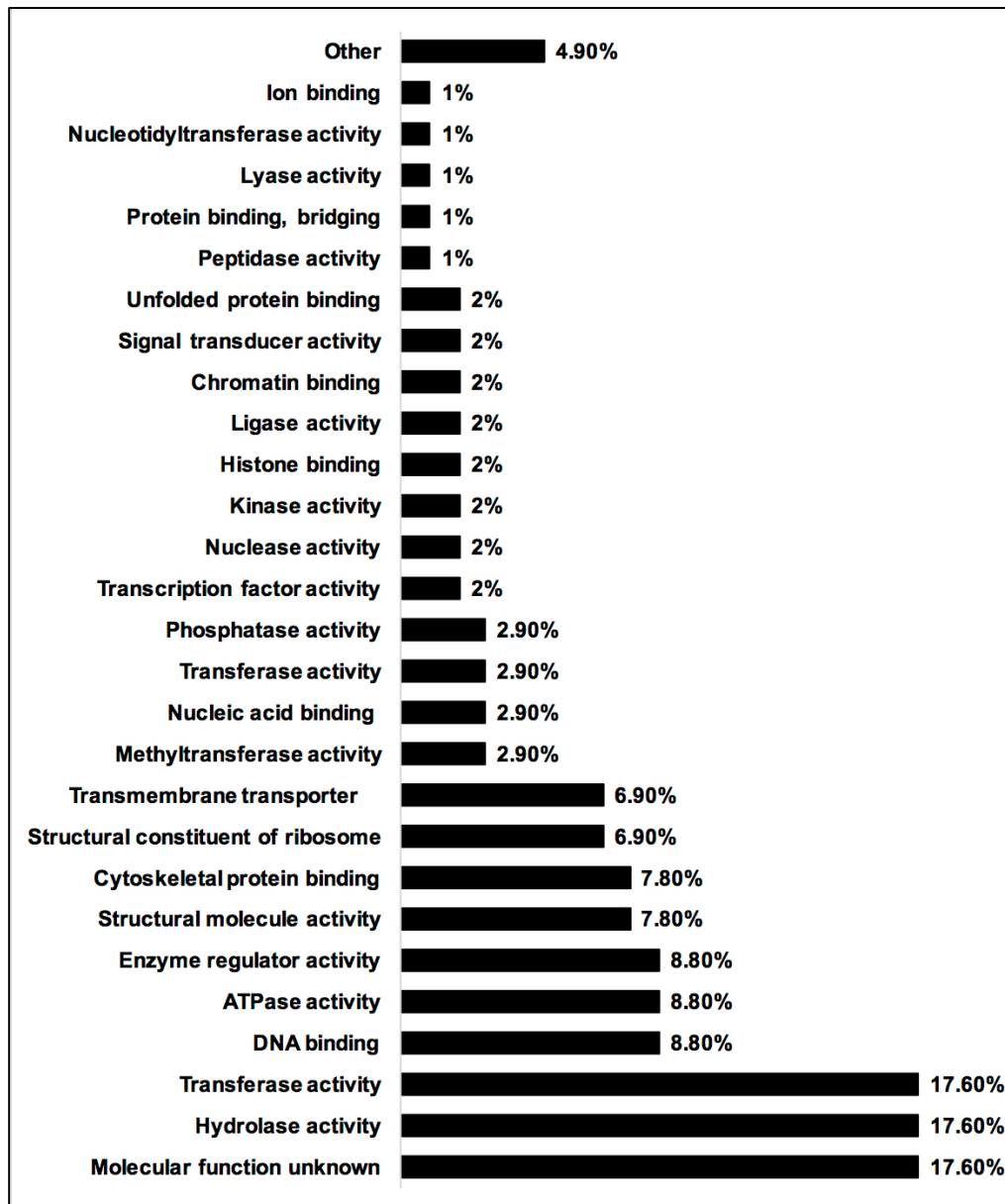
FIGURE 4.4. Functional classification of genes exhibiting synthetic sick interaction with *taz1Δ*. Synthetic sick interactions identified by SGA were classified by biological process based on gene ontology. The percentage of genes representing the specific processes are indicated.
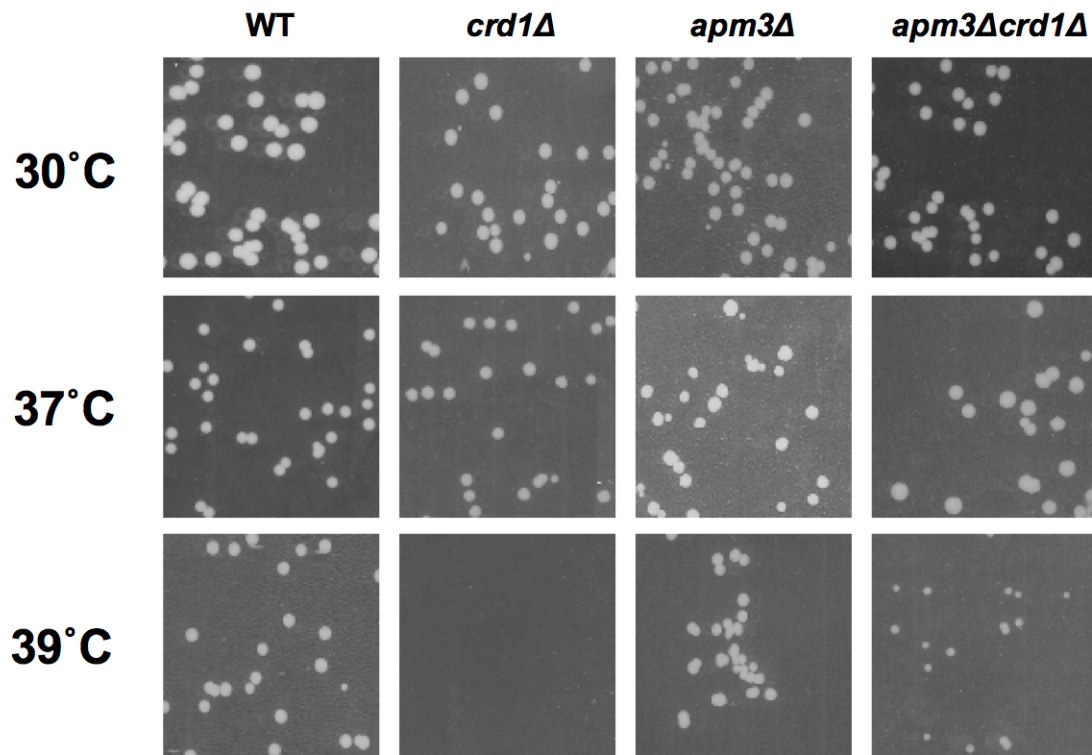
FIGURE 4.5. *apm3Δ* **suppresses the growth defect of** *crd1Δ* **at elevated temperature.** Cells were pre-cultured in YPD overnight, serially diluted, plated on YPD, and incubated at the indicated temperature for 3-5 days.
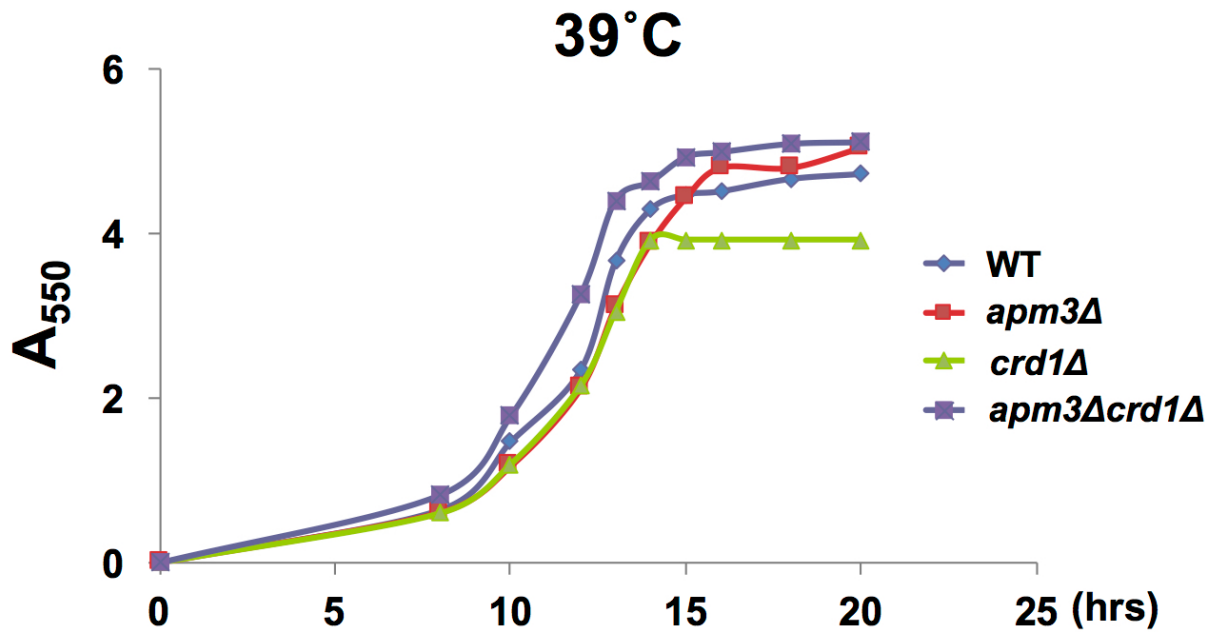
FIGURE 4.6. *apm3Δ* suppresses the growth defect of *crd1Δ* at elevated temperature. Cells were inoculated in YPD at 39°C at an initial A_{550} of 0.05, and A_{550} was measured at the indicated times. The growth curves shown in the figure are representative of three experiments.
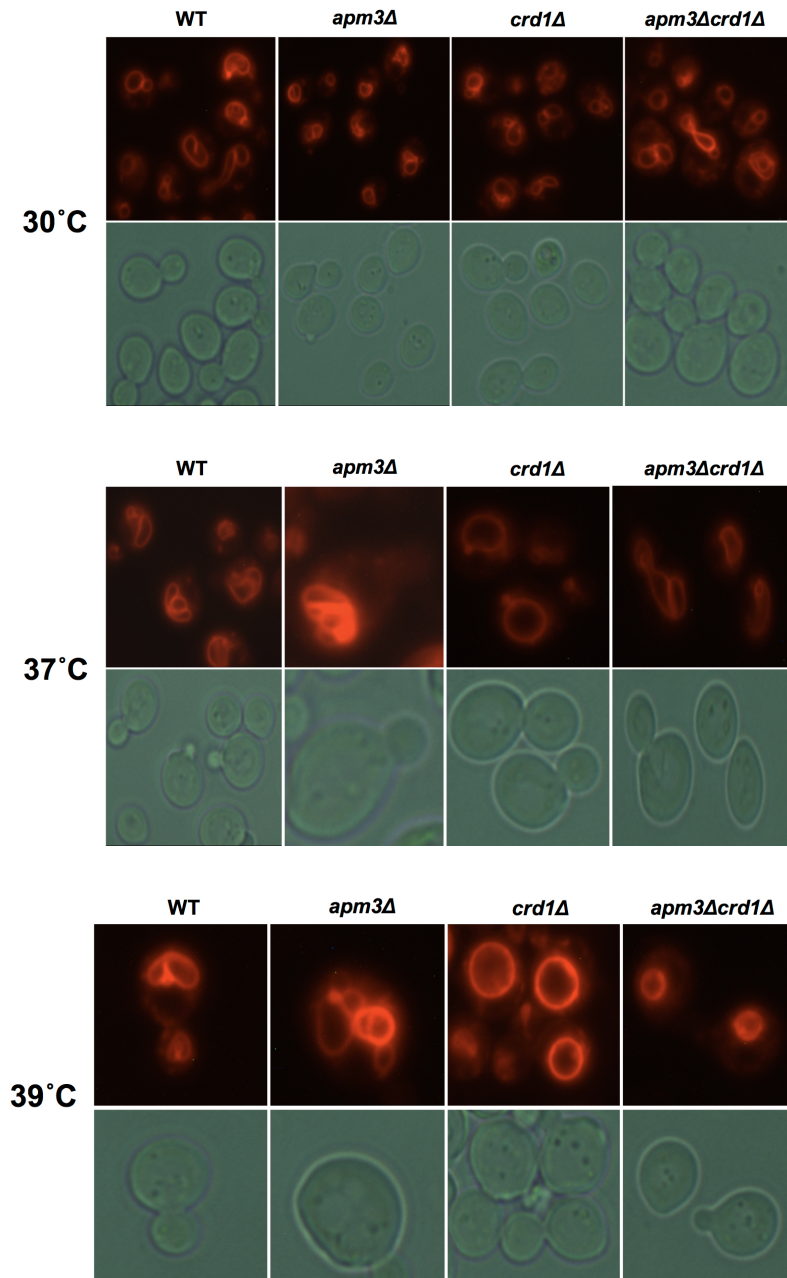
FIGURE 4.7. *apm3Δ* rescues the vacuole morphology defect of *crd1Δ* at elevated temperature. Cells were pre-cultured in YPD to the early log phase at 30°C and then transferred to 37°C or 39°C for 8 hours. Vacuoles were visualized by staining with FM4-64 and cells were observed using fluorescence microscopy. All images were taken at the same magnification (1000x).

TABLE 4.1. Yeast strains used in this study.

Strains	Genotype	Source or Ref.
Y5563	MATα, his3Δ1, leu2Δ0, ura3Δ0, met15Δ0, LYS2$^+$, lyp1Δ, can1Δ::MFA1pr-HIS3	Tong et al., 2001
BY4742	MATα, his3Δ1, leu2Δ0, ura3Δ0, lys2Δ0	Invitrogen
taz1Δcan1Δ	MATα, his3Δ1, leu2Δ0, lys2Δ0, ura3Δ0, taz1Δ::URA3, can1Δ::MFA1pr-HIS3	This study
VGY1	MATα, his3Δ1, leu2Δ0, lys2Δ0, ura3Δ0, crd1Δ::URA3	Gohil et al., 2005
taz1Δ	MATα, his3Δ1, leu2Δ0, lys2Δ0, ura3Δ0, taz1Δ::URA3	Invitrogen
CG922-a	MATa, lys2-801, ade2-101, trp1Δ1, his3Δ200, leu2Δ1, crd1Δ::URA3	Invitrogen
CG923-α	MATα, lys2-801, ade2-101, trp1Δ1, his3Δ200, leu2Δ1, crd1Δ::URA3	Invitrogen
plb11Δ	MATa, his3Δ1, leu2Δ0, met15Δ0, ura3Δ0, plb1Δ::KanMX4	Invitrogen
plb2Δ	MATa, his3Δ1, leu2Δ0, met15Δ0, ura3Δ0, plb2Δ::KanMX4	Invitrogen

plb3Δ	*MATa, his3Δ1, leu2Δ0, met15Δ0, ura3Δ0, plb3Δ::KanMX4*	Invitrogen
apm3Δ	*MATa, his3Δ1, leu2Δ0, met15Δ0, ura3Δ0, amp3Δ::KanMX4*	Invitrogen
plb1Δcrd1Δ	*MATa, his3Δ1, leu2Δ0, met15Δ0, ura3Δ0, plb1Δ::KanMX4, crd1Δ::KanMX4*	This study
plb2Δcrd1Δ	*MATa, his3Δ1, leu2Δ0, met15Δ0, ura3Δ0, plb2Δ::KanMX4, crd1Δ::KanMX4*	This study
plb3Δcrd1Δ	*MATa, his3Δ1, leu2Δ0, met15Δ0, ura3Δ0, plb3Δ::KanMX4, crd1Δ::KanMX4*	This study
apm3Δcrd1Δ	*MATa, his3Δ1, leu2Δ0, met15Δ0, ura3Δ0, amp3Δ::KanMX4, crd1Δ::KanMX4*	This study
plb1Δtaz1Δ	*MATa, his3Δ1, leu2Δ0, met15Δ0, ura3Δ0, plb1Δ::KanMX4, taz1Δ::KanMX4*	This study
plb2Δtaz1Δ	*MATa, his3Δ1, leu2Δ0, met15Δ0, ura3Δ0, plb2Δ::KanMX4, taz1Δ::KanMX4*	This study
plb3Δtaz1Δ	*MATa, his3Δ1, leu2Δ0, met15Δ0, ura3Δ0, plb3Δ::KanMX4, taz1Δ::KanMX4*	This study
apm3Δtaz1Δ	*MATa, his3Δ1, leu2Δ0, met15Δ0, ura3Δ0, amp3Δ::KanMX4, taz1Δ::KanMX4*	This study

TABLE 4.2. Synthetic lethal interaction with *taz1Δ*. Summary of genes identified as synthetically lethal with the *taz1Δ* mutant. The identified genes are grouped based on biological function.

GO term	Frequency	Gene(s)
Molecular function unknown	16 out of 70 genes, 22.9%	DEP1, NPL4, SOL2, AHC2, CSM1, FIG2, OCA4, IES6, BUD13, ICE2, PET130, VPS53, DID2, SOV1, CAF120
Hydrolase activity	9 out of 70 genes, 12.9%	NPP1, RAD18, TPS2, PDR11, SDS3, IMP2, HNT3, TAF14, KRE6
Transferase activity	9 out of 70 genes, 12.9%	RBK1, BUD23, ARE1, SSK22, GSC2, SSM4, TRM9, SER1, LOA1
Structural molecule activity	7 out of 70 genes, 10%	MRPS9, RPL21A, RPS14A, IMG1, RPS21B, CSE2, RPS12
DNA binding	7 out of 70 genes, 10%	RIM1, HCM1, RAD18, SPT4, GON7, SSN8, THO2
Structural constituent of ribosome	6 out of 70 genes, 8.6%	MRPS9, RPL21A, RPS14A, IMG1, RPS21B, RPS12
Enzyme regulator activity	6 out of 70 genes, 8.6%	SLI15, SYP1, SED4, SSN8, RBK1, SSK22
Transcription factor activity, protein binding	4 out of 70 genes, 5.7%	SRB8, SPT4, CSE2, TAF14
Cytoskeletal protein binding	4 out of 70 genes, 5.7%	ABP1, YKE2, HOF1, PAC1
Oxidoreductase activity Isomerase activity	4 out of 70 genes, 5.7%	TRX3, DFG10, CPR4, DEG1
Transmembrane transporter activity	3 out of 70 genes, 4.3%	ERS1, PDR11, QDR2
ATPase activity	3 out of 70 genes, 4.3%	RAD18, PDR11, TAF14

Methyltransferase activity	2 out of 70 genes, 2.9%	BUD23, TRM9
Nucleic acid binding transcription factor	2 out of 70 genes, 2.9%	HCM1, TAF14
mRNA binding	2 out of 70 genes, 2.9%	RPS14A, THO2
Ion binding	2 out of 70 genes, 2.9%	RBK1, ISA2
RNA binding	2 out of 70 genes, 2.9%	RPS14A, THO2
Nuclease activity	2 out of 70 genes, 2.9%	NPP1, HNT3
Enzyme binding	2 out of 70 genes, 2.9%	SPT4, RLF2
Lyase activity, Phosphatase activity	2 out of 70 genes, 2.9%	THR4, TPS2
Unfolded protein binding Signal transducer activity	2 out of 70 genes, 2.9%	VMA22, SSK22
Transferase activity, transferring glycosyl	1 out of 70 genes, 1.4%	GSC2
Chromatin binding	1 out of 70 genes, 1.4%	GON7
Hydrolase activity, glycosyl bonds	1 out of 70 genes, 1.4%	KRE6
Peptidase activity	1 out of 70 genes, 1.4%	IMP2
Other	5 out of 70 genes, 7.1%	TAH1, CBS1, VTH1, SAG1, PDR17

TABLE 4.3. Genes identified by SGA as synthetically lethal with *taz1Δ*.
(Ref: Gene description from Saccharomyces genome database)

Genes	SGD gene description
ABP1	Actin-binding protein of the cortical actin cytoskeleton
ARE1	Acyl-CoA sterol acyltransferase, isozyme of Are2p
BUD13	Subunit of the RES complex
BUD23	Protein involved in bud-site selection
CAF120	Part of the evolutionarily conserved CCR4-NOT transcriptional
CBS1	Mitochondrial translational activator of the COB mRNA
CPR4	Peptidyl-prolyl cis-trans isomerase (cyclophilin)
CSE2	Subunit of the RNA polymerase II mediator complex
CSM1	Nucleolar protein that forms a complex with Lrs4p
DEG1	Non-essential tRNA pseudouridine synthase
DEP1	Transcriptional modulator involved in phospholipid biosynthesis
DFG10	Protein of unknown function, involved in filamentous growth
DID2	Class E protein of the vacuolar protein-sorting (Vps) pathway
ERS1	Protein with similarity to human cystinosin
FIG2	Cell wall adhesin
FYV10	Protein of unknown function
GON7	Protein proposed to be involved in the modification
GSC2	Catalytic subunit of 1,3-beta-glucan synthase
HCM1	Forkhead transcription factor that drives S-phase
HNT3	Member of the third branch of the histidine triad (HIT) superfamily
HOF1	Bud neck-localized
ICE2	Integral ER membrane protein with type-III transmembrane domains
IES6	Protein that associates with the INO80 chromatin remodeling complex
IMG1	Mitochondrial ribosomal protein of the large subunit
IMP2	Transcriptional activator involved in maintenance of ion homeostasis
ISA2	Protein required for maturation of mitochondrial and cytosolic Fe/S

KRE6	Protein required for beta-1,6 glucan biosynthesis
LUG1	Putative protein of unknown function
MRPS9	Mitochondrial ribosomal protein of the small subunit
NPL4	Endoplasmic reticulum and nuclear membrane protein
NPP1	Nucleotide pyrophosphatase/phosphodiesterase family member
OCA4	Cytoplasmic protein required for replication of Brome mosaic virus
PAC1	Protein involved in nuclear migration
PDR11	ATP-binding cassette (ABC) transporter
PDR17	Phosphatidylinositol transfer protein (PITP)
PET130	Protein required for respiratory growth
QDR2	Multidrug transporter of the major facilitator superfamily
RAD18	Protein involved in postreplication repair
RBK1	Putative ribokinase
RIM1	Single-stranded DNA-binding protein
RLF2	Largest subunit (p90) of the Chromatin Assembly Complex (CAF-1)
RPL21A	Protein component of the large (60S) ribosomal subunit
RPS12	Protein component of the small (40S) ribosomal subunit
RPS14A	Ribosomal protein 59 of the small subunit
RPS21B	Protein component of the small (40S) ribosomal subunit
SAG1	Alpha-agglutinin of alpha-cells, binds to Aga1p during agglutination
SDS3	Component of the Rpd3p/Sin3p deacetylase complex
SED4	Integral endoplasmic reticulum membrane protein
SER1	3-phosphoserine aminotransferase
SLI15	Subunit of the conserved chromosomal passenger complex
SOL2	Protein with a possible role in tRNA export
SOV1	Mitochondrial protein of unknown function
SPT4	Protein involved in the regulating Pol I and Pol II transcription
SRB8	Subunit of the RNA polymerase II mediator complex
SSK22	MAP kinase kinase kinase of the HOG1
SSM4	Ubiquitin-protein ligase involved in ER-associated protein degradation
SSN8	Cyclin-like component of the RNA polymerase II holoenzyme

SYP1	Protein of unknown function
TAF14	Subunit of TFIID, TFIIF, INO80, SWI/SNF, and NuA3 complexes
TAH1	HSP90 cofactor; interacts with Hsp82p, Pih1p, Rvb1 and Rvb2
THO2	Subunit of the THO complex
THR4	Threonine synthase
TPS2	Phosphatase subunit of the trehalose-6-phosphate synthase
TRM9	tRNA methyltransferase
TRX3	Mitochondrial thioredoxin
VMA22	Peripheral membrane protein that is required for vacuolar H+-ATPase
VPS53	Component of the GARP (Golgi-associated retrograde protein)
VPS66	Cytoplasmic protein of unknown function
VTH1	Putative membrane glycoprotein
WHI3	RNA binding protein that sequesters CLN3 mRNA in cytoplasmic foci
YKE2	Subunit of the heterohexameric Gim/prefoldin protein complex

TABLE 4.4. Synthetic sick interaction with *taz1Δ*. Summary of genes identified as synthetically sick with the *taz1Δ* mutant. The identified genes are grouped based on biological function.

GO term	Frequency	Gene(s)
Molecular function unknown	18 out of 102 genes, 17.6%	AIM4, APM3, RXT3, MSH5, KRE28, RMD6, NIF3, EFG1, PEX28, GVP36, VPS70, VPS65, PEX30, OPI9, MPA43, ZEO1, RTT10, NCA2
Hydrolase activity	18 out of 102 genes, 17.6%	MMS4, PCA1, RRT12, GUD1, IRC3, PTP3, RTR1, DNF1, RSC1, RSR1, TES1, SNO1, ADE17, RNH201, PLB3, MET22, ARP8, ELP4
Transferase activity	18 out of 102 genes, 17.6%	PMT2, GAL1, RKM3, HSL7, SHM1, ARE1, ARG3, RKM4, GSC2, RPA12, UFD4, CST9, VAN1, ADE17, SAS2, HRD1
DNA binding **RNA binding**	9 out of 102 genes, 8.8%	RIM1, PHO2, CMR1, MET32, ADE12, HAP5, BEM2, WHI3, ARP8, ELP4
ATPase activity **Oxidoreductase activity**	9 out of 102 genes, 8.8%	PCA1, IRC3, DNF1, RSC1, ARP8, ELP4, SOD2, BNA1, CAT5
Enzyme regulator activity	9 out of 102 genes, 8.8%	GCS1, BEM2, GCN1, BUD6, GAL80, VPS75, PCL1, CLN2, CLB5
Structural molecule activity	8 out of 102 genes, 7.8%	RPS9B, RPS11A, SWR1, RPL29, RPL7A, RPS27B, RPS27A, RPS17A
Cytoskeletal protein binding **Transcription factor binding**	8 out of 102 genes, 7.8%	GCS1, YKE2, BUD6, RBL2, MET32, GAL80, SIN4, CTI6
Structural constituent of ribosome	7 out of 102 genes, 6.9%	RPS9B, RPS11A, RPL29, RPL7A, RPS27B, RPS27A, RPS17A
Transmembrane transporter	7 out of 102 genes, 6.9%	PCA1, DNF1, MPC1, MNR2, GAP1, TAT2, HUT1

Methyltransferase activity	3 out of 102 genes, 2.9%	RKM3, HSL7, RKM4
Nucleic acid binding transcription factor	3 out of 102 genes, 2.9%	PHO2, MET32, HAP5
Transferase activity, transferring glycosyl	3 out of 102 genes, 2.9%	PMT2, GSC2, VAN1
Phosphatase activity	3 out of 102 genes, 2.9%	PTP3, RTR1, MET22
Transcription factor activity, protein binding	2 out of 102 genes, 2%	MET32, SRB2
Nuclease activity	2 out of 102 genes, 2%	MMS4, RNH201
Kinase activity	2 out of 102 genes, 2%	GAL1, ADO1
Histone binding	2 out of 102 genes, 2%	VPS75, CTI6
Ligase activity	2 out of 102 genes, 2%	ADE5,7, ADE12
Chromatin binding	2 out of 102 genes, 2%	LIF1, CST9
Signal transducer activity GTPase activity	2 out of 102 genes, 2%	RSR1, SLG1
Unfolded protein binding	2 out of 102 genes, 2%	VMA22, SSQ1
Peptidase activity	1 out of 102 genes, 1%	RRT12
Protein binding, bridging	1 out of 102 genes, 1%	PEX14
Lyase activity	1 out of 102 genes, 1%	MDE1

Nucleotidyltransferase activity	1 out of 102 genes, 1%	RPA12
Ion binding	1 out of 102 genes, 1%	PCA1
Other	5 out of 102 genes, 4.9%	GAL3,MAM33,TLG2,MCH5,VPS28

TABLE 4.5. Genes identified by SGA as synthetically sick with *taz1Δ*.
(Ref: Gene description from Saccharomyces genome database)

Genes	SGD gene description
ADE12	Adenylosuccinate synthase
ADE5,7	Bifunctional enzyme of the 'de novo' purine nucleotide biosynthetic
ADO1	Adenosine kinase, required for the utilization of S-adenosylmethionine
AIM4	Protein proposed to be associated with the nuclear pore complex
APM3	Mu3-like subunit of the clathrin associated protein complex (AP-3)
ARE1	Acyl-CoA sterol acyltransferase, isozyme of Are2p
ARG3	Ornithine carbamoyltransferase
ARP8	Nuclear actin-related protein involved in chromatin remodeling
BEM2	Rho GTPase activating protein (RhoGAP)
BNA1	hydroxyanthranilic acid dioxygenase
BUD6	Actin- and formin-interacting protein
CAT5	Protein required for ubiquinone (Coenzyme Q) biosynthesis
CLB5	B-type cyclin involved in DNA replication during S phase
CLN2	G1 cyclin involved in regulation of the cell cycle
CST9	SUMO E3 ligase
CTI6	Protein that relieves transcriptional repression
CUE4	Protein of unknown function; has a CUE domain that binds ubiquitin
DFG10	Protein of unknown function, involved in filamentous growth
DNF1	Aminophospholipid translocase (flippase)
EFG1	Essential protein required for maturation of 18S rRNA
ELP4	Subunit of Elongator complex
FMP37	Putative protein of unknown function
GAL1	Galactokinase
GAL3	Transcriptional regulator involved in activation of the GAL genes
GAL80	Transcriptional regulator involved in the repression of GAL genes
GAP1	General amino acid permease

GCN1	Positive regulator of the Gcn2p kinase activity
GCS1	ADP-ribosylation factor GTPase activating protein (ARF GAP)
GSC2	Catalytic subunit of 1,3-beta-glucan synthase
GUD1	Guanine deaminase
GUP2	Probable membrane protein
GVP36	BAR domain-containing protein that localizes to Golgi vesicles
HAP5	Subunit of the heme-activated
HRD1	Ubiquitin-protein ligase required for endoplasmic reticulum
HSL7	Protein arginine N-methyltransferase
HUT1	Protein with a role in UDP-galactose transport to the Golgi lumen
IRC3	Putative protein of unknown function
JLP2	Protein of unknown function
KRE28	Protein of unknown function that localizes to the nuclear
LIF1	Component of the DNA ligase IV complex
LRC3	Putative protein of unknown function
MAM33	Acidic protein of the mitochondrial matrix
MCH5	Plasma membrane riboflavin transporter
MDE1	5'-methylthioribulose-1-phosphate dehydratase
MET22	Bisphosphate-3'-nucleotidase
MET32	Zinc-finger DNA-binding protein
MMS4	Subunit of the structure-specific Mms4p-Mus81p endonuclease
MNR2	Putative magnesium transporter
MPA43	Putative protein of unknown function
MSH5	Protein of the MutS family
NCA2	Protein involved in regulation of mitochondrial ATP synthase
OCA2	Putative protein with similarity to predicted tyrosine phosphatases
OPI9	Dubious open reading frame unlikely to encode a protein
OSW3	Putative protein of unknown function
PCA1	Cadmium transporting P-type ATPase
PCL1	Pho85 cyclin of the Pcl1,2-like subfamily
PEX14	Peroxisomal membrane peroxin

PEX28	Peroxisomal integral membrane peroxin
PEX30	Peroxisomal integral membrane protein
PHO2	Homeobox transcription factor
PLB3	Phospholipase B (lysophospholipase)
PMT2	Protein O-mannosyltransferase
PTP3	Phosphotyrosine-specific protein phosphatase
RBL2	Protein involved in microtubule morphogenesis
RIM1	Single-stranded DNA-binding protein
RKM3	Ribosomal lysine methyltransferase
RKM4	Ribosomal lysine methyltransferase
RLF2	Largest subunit (p90) of the Chromatin Assembly Complex (CAF-1)
RMD6	Protein required for sporulation
RNH201	Ribonuclease H2 catalytic subunit
RPA12	RNA polymerase I subunit A12.2
RPL29	Protein component of the large (60S) ribosomal subunit
RPL7A	Protein component of the large (60S) ribosomal subunit
RPS11A	Protein component of the small (40S) ribosomal subunit
RPS17A	Ribosomal protein 51 (rp51) of the small (40s) subunit
RPS27A	Protein component of the small (40S) ribosomal subunit
RPS27B	Protein component of the small (40S) ribosomal subunit
RPS9B	Protein component of the small (40S) ribosomal subunit
RSC1	Component of the RSC chromatin remodeling complex
RSR1	GTP-binding protein of the ras superfamily
RTR1	Protein with a role in transcription
RTT10	Cytoplasmic protein with a role in regulation of Ty1 transposition
RXT3	Subunit of the RPD3L complex
SAS2	Histone acetyltransferase (HAT) catalytic subunit of the SAS complex
SEC66	Non-essential subunit of Sec63 complex
SHM1	Mitochondrial serine hydroxymethyltransferase
SIN4	Subunit of the RNA polymerase II mediator complex
SLG1	Sensor-transducer of the stress-activated PKC1-MPK1

SNO1	Protein of unconfirmed function
SOD2	Mitochondrial superoxide dismutase
SRB2	Subunit of the RNA polymerase II mediator complex
SSQ1	Mitochondrial hsp70-type molecular chaperone
SWR1	Swi2/Snf2-related ATPase
TAT2	High affinity tryptophan and tyrosine permease
TDH2	Glyceraldehyde-3-phosphate dehydrogenase
TES1	Peroxisomal acyl-CoA thioesterase
TLG2	Syntaxin-like t-SNARE that forms a complex with Tlg1p and Vti1p
UFD4	Ubiquitin-protein ligase (E3) that interacts with Rpt4p and Rpt6p
VAN1	Component of the mannan polymerase I
VMA22	Peripheral membrane protein that is required for vacuolar H+-ATPase
VPS28	Component of the ESCRT-I complex
VPS65	Dubious open reading frame
VPS70	Protein of unknown function involved in vacuolar protein sorting
VPS75	NAP family histone chaperone; binds to histones and Rtt109p
WHI3	RNA binding protein that sequesters CLN3 mRNA in cytoplasmic foci
YKE2	Subunit of the heterohexameric Gim/prefoldin protein complex
ZEO1	Peripheral membrane protein of the plasma membrane

TABLE 4.6. Genetic interaction of CL mutants with phospholipase B mutants. The phospholipase B mutants were crossed with the CL mutants to obtain double mutants. Genetic interaction was determined based on the viability of the double mutants.
Key: (-): no growth; (+/-): poor growth; (+): good growth.

Phospholipase B mutants	Growth of double mutants			
	taz1△		*crd1△*	
	30°C	**39°C**	**30°C**	**37°C**
plb1△	+	+/-	+	+
plb2△	+	+	+	+
plb3△	+	+/-	+	+

CHAPTER 5 FUTURE DIRECTIONS

The studies described in this thesis identified the fascinating new role of CL in acetyl-CoA metabolism, which interconnects metabolic pathways crucial for energy metabolism. The powerful SGA tool was used to identify cellular and biochemical processes in which CL may play a role. The data presented in Chapters 2 and 3 indicate that the loss of CL leads to perturbation of synthesis and transport of acetyl-CoA, which very likely results in perturbation of the TCA cycle and metabolic deficiencies observed in the CL mutant. However, the mechanism underlying defective acetyl-CoA homeostasis and TCA cycle defects in CL-deficient cells is not understood. Chapter 4 identifies potential physiological modifiers that exacerbate the loss of tafazzin. Characterization of these may contribute to our understanding of the basis for the variation in symptoms in BTHS. In this chapter, I suggest exciting future studies that would push our knowledge of the role of CL in cellular functions to interesting new directions by addressing the following questions.

1. What is the role of CL in acetate utilization?

The studies presented in Chapter 2 show that the loss of CL leads to defective acetate utilization, which results in perturbation of the PDH-bypass pathway. This is the first report to show that a phospholipid might be required for synthesis of acetyl-CoA. As an indication of defective acetate utilization, the growth and acetyl-CoA levels of *crd1Δ* were decreased when acetate was provided as the sole carbon source (Fig. 2.4 & 2.5). However, it is unclear how CL in the mitochondrial membrane is involved in acetate utilization, which is largely carried out in the mitochondrial outer membrane and cytosol. Future experiments to elucidate the mechanism underlying the role of CL in conversion

of acetate to acetyl-CoA should determine if gene expression, enzyme activity, import into the mitochondria, and/or stability of acetyl-CoA synthetase (*ACS1* and *ACS2*) are decreased in *crd1Δ*. This study may uncover a novel mechanism whereby synthesis of acetyl-CoA in different organelles is controlled by CL, which is predominantly in the mitochondria.

2. Is CL required for acetyl-CoA synthesis in mammals?

In chapter 2, I showed that acetyl-CoA levels are decreased in CL-deficient cells due to perturbation of the PDH-bypass. This identifies a novel role of CL in acetyl-CoA synthesis in yeast cells. I suggest future experiments to determine acetyl-CoA levels, acetate utilization, and activity of acetyl-CoA synthetase and PDH in mammalian cells. If experiments reveal that CL is required for acetyl-CoA synthesis in mammals as in yeast, this may suggest that the synthesis of acetyl-CoA is a physiological modifier that may contribute to the disparities in the clinical phenotypes observed in BTHS patients and other cardiac disorders. These experiments may shed light on treatments for BTHS that are targeted to these deficiencies.

3. Why is carnitine acetylcarnitine translocase activity decreased in *crd1Δ*?

The experiment illustrated in Fig. 3.5 indicates that activity of carnitine-acetylcarnitine translocase is decreased in *crd1Δ*, although carnitine levels and carnitine acetylcarnitine transferase activity are not altered. What is the cause of decreased translocase activity in *crd1Δ*? At least three possibilities could explain this decrease. First, the mRNA levels of *CRC1* may be decreased in *crd1Δ*. Second, based on studies showing that CL is required for optimal mitochondrial protein import (Jiang et al., 2000; Gebert et al., 2009; Kutik et al., 2008), import of mitochondrial Crc1 may be decreased

due to CL deficiency. Third, the stability of Crc1 may depend on interaction with CL. Based on these experiments, it will be interesting to determine if mammalian cells exhibit similar carnitine-acetylcarnitine translocase defects, and if supplementation of acetylcarnitine rescues some phenotypes observed in BTHS.

4. How does the glyoxylate cycle rescue *crd1Δ* mutant defects?

The data presented in Chapter 3 show that the glyoxylate cycle is essential in CL-deficient cells. My studies revealed that *crd1Δ* is synthetically lethal with mutants in the glyoxylate cycle, suggesting that intermediates of the glyoxylate cycle may compensate for *crd1Δ* deficiencies. However, the mechanism by which the glyoxylate cycle rescues *crd1Δ* mutant defects is not known. At least two possibilities could explain rescue by the glyoxylate cycle. First, the mRNA levels of glyoxylate cycle genes may be up-regulated in *crd1Δ*. Second, the activity of citrate synthase (CS), aconitase (ACO), malate dehydrogenase (MDH), isocitrate lyase (ICL), and malate synthase, enzymes that synthesize TCA cycle intermediates through the glyoxylate cycle, may be increased in *crd1Δ*. This may result in increased synthesis of succinate, malate, and citrate, which are expected to replenish deficiencies resulting from perturbed acetyl-CoA synthesis.

5. What is the role of CL in the cell integrity pathway?

In order to identify physiological modifiers that exacerbate the loss of CL, I performed a genome wide SGA screen with *crd1Δ* and *taz1Δ*, as described in Chapters 2 and 4. Among the genetic interactions uncovered in these screens, I would draw attention of future students to the cell integrity pathway. Previous studies have reported that the PKC-Slt2 pathway is defective in *pgs1Δ* cells, which exhibit decreased viability at high temperatures and a defective cell integrity pathway due to decreased Slt2p

phosphorylation (Zhong et al.,2007). The mechanism underlying decreased Slt2p phosphorylation in the CL mutant is unknown.

SDP1 encodes stress-inducible dual-specificity MAP kinase phosphatase that dephosphorylates Slt2p (Hahn et al., 2002; Byrne et al., 2005; Collister et al., 2002). During heat shock, Sdp1p is localized to mitochondria and cytosolic puncta, and is sequestered from Slt2p. When cells undergo heat stress adaptation, Sdp1p is released from cytoplasmic and mitochondrial puncta and is thus accessible to carry out Slt2p dephosphorylation and inactivation (Kuravi et al., 2011). Defective Slt2p phosphorylation in the *pgs1Δ* mutant could result from release of Sdp1p from sequestration, resulting in increased Sdp1p phosphatase levels in the cytosol and dephosphorylation of Slt2p before it moves into the nucleus. At least two possibilities could explain this decrease. First, CL mutants may exhibit increased activity of Sdp1p. Second, upstream effectors of the PKC-Slt2 pathway may not be activated in CL-deficient cells. Future experiments should address these possibilities.

In conclusion, one of the enigmas of BTHS (and other monogenic disorders) is that the disorder is characterized by a wide disparity of symptoms ranging from asymptomatic to newborn death, even in the presence of identical tafazzin mutations. This indicates that physiological modifiers affect the clinical outcome. The underlying pathology of BTHS and the physiological modifiers that affect the clinical outcome of this disorder remain to be identified. The studies described in Chapters 2 and 3 show, for the first time, that CL is required for optimal acetyl-CoA metabolism, which is essential for basal functioning of the TCA cycle. I invite my colleagues in the Greenberg lab to discover the mechanisms whereby CL participates in acetyl-CoA metabolism. I anticipate that the results will lead

to breakthroughs that will pave the way for a better understanding of cellular pathways that might be perturbed in BTHS patients.

REFERENCES

Abo Alrob, O. and G. D. Lopaschuk (2014). "Role of CoA and acetyl-CoA in regulating cardiac fatty acid and glucose oxidation." Biochem Soc Trans 42(4): 1043-1051.

Armando, J. W., B. A. Boghigian and B. A. Pfeifer (2012). "LC-MS/MS quantification of short-chain acyl-CoA's in Escherichia coli demonstrates versatile propionyl-CoA synthetase substrate specificity." Lett Appl Microbiol 54(2): 140-148.

Avidan, O. and U. Pick (2015). "Acetyl-CoA synthetase is activated as part of the PDH-bypass in the oleaginous green alga Chlorella desiccata." J Exp Bot 66(22): 7287-7298.

Balk, J., Aguilar Netz, D.J., Tepper, K., Pierik, A.J. & Lill, R. The essential WD40 protein Cia1 is involved in a late step of cytosolic and nuclear iron-sulfur protein assembly. *Molecular and cellular biology* 25, 10833-41 (2005).

Balk, J., Pierik, A.J., Netz, D.J., Muhlenhoff, U. & Lill, R. The hydrogenase-like Nar1p is essential for maturation of cytosolic and nuclear iron-sulphur proteins. *The EMBO journal* 23, 2105-15 (2004).

Barja, G. Mitochondrial oxygen radical generation and leak: sites of production in states 4 and 3, organ specificity, and relation to aging and longevity. *Journal of bioenergetics and biomembranes* 31, 347-66 (1999).

Barth, P. G., R. J. Wanders and P. Vreken (1999). "X-linked cardioskeletal myopathy and neutropenia (Barth syndrome)-MIM 302060." J Pediatr 135(3): 273-276.

Barth, K. H., S. W. Brusilow, et al. (1981). "Percutaneous transluminal angioplasty of homograft renal artery stenosis in a 10-year-old girl." Pediatrics 67(5): 675-677.

Barth, P.G., R.J. Wanders, and P. Vreken. 1999a. X-linked cardioskeletal myopathy and neutropenia (Barth syndrome)-MIM 302060. J Pediatr. 135:273-276.

Barth, P.G., R.J. Wanders, P. Vreken, E.A. Janssen, J. Lam, and F. Baas. 1999b. X-linked cardioskeletal myopathy and neutropenia (Barth syndrome) (MIM 302060). J Inherit Metab Dis. 22:555-567.

Barth PG, Scholte HR, Berden JA, Van dK-VMJM, Luyt-Houwen IE, Van tV-KET, Van dHJJ, Sobotka-Plojhar MA. 1983. An X-linked mitochondrial disease affecting cardiac muscle, skeletal muscle andneutrophil leucocytes. Journal of the Neurological Sciences 62:327-355.

Bartlett, K. & Eaton, S. Mitochondrial beta-oxidation. *European journal of biochemistry / FEBS* 271, 462-9 (2004).

Battelli, D., Bellei, M., Arrigoni-Martelli, E., Muscatello, U. & Bobyleva, V. Interaction of carnitine with mitochondrial cardiolipin. *Biochimica et biophysica acta* 1117, 33-6 (1992).

Bazan, S., Mileykovskaya, E., Mallampalli, V.K., Heacock, P., Sparagna, G.C. & (, W. Cardiolipin-dependent reconstitution of respiratory supercomplexes from purified Saccharomyces cerevisiae complexes III and IV. *The Journal of biological chemistry* 288, 401-11 (2013).

Bennett, B. D., E. H. Kimball, M. Gao, R. Osterhout, S. J. Van Dien and J. D. Rabinowitz (2009). "Absolute metabolite concentrations and implied enzyme active site occupancy in Escherichia coli." Nat Chem Biol 5(8): 593-599.

Beranek, A., Rechberger, G., Knauer, H., Wolinski, H., Kohlwein, S.D. & Leber, R. Identification of a cardiolipin-specific phospholipase encoded by the gene CLD1 (YGR110W) in yeast. *The Journal of biological chemistry* 284, 11572-8 (2009).

Beyer, K. & Klingenberg, M. ADP/ATP carrier protein from beef heart mitochondria has high amounts of tightly bound cardiolipin, as revealed by 31P nuclear magnetic resonance. *Biochemistry* 24, 3821-6 (1985).

Beyer, K. & Nuscher, B. Specific cardiolipin binding interferes with labeling of sulfhydryl residues in the adenosine diphosphate/adenosine triphosphate carrier protein from beef heart mitochondria. *Biochemistry* 35, 15784-90 (1996).

Bione, S., P. D'Adamo, E. Maestrini, A. K. Gedeon, P. A. Bolhuis and D. Toniolo (1996). "A novel X-linked gene, G4.5. is responsible for Barth syndrome." Nat Genet 12(4): 385-389.

Birner, R., R. Nebauer, et al. (2003). "Synthetic lethal interaction of the mitochondrial phosphatidylethanolamine biosynthetic machinery with the prohibitin complex of Saccharomyces cerevisiae." Mol Biol Cell 14(2): 370-383.

Bisaccia, F. & Palmieri, F. Specific elution from hydroxylapatite of the mitochondrial phosphate carrier by cardiolipin. *Biochimica et biophysica acta* 766, 386-94 (1984).

Bleyl, S. B., B. R. Mumford, M. C. Brown-Harrison, L. T. Pagotto, J. C. Carey, T. J. Pysher, K. Ward and T. K. Chin (1997). "Xq28-linked noncompaction of the left ventricular myocardium: prenatal diagnosis and pathologic analysis of affected individuals." Am J Med Genet 72(3): 257-265.

Bolhuis, P. A., G. W. Hensels, et al. (1991). "Mapping of the locus for X-linked cardioskeletal myopathy with neutropenia and abnormal mitochondria (Barth syndrome) to Xq28." Am J Hum Genet 48(3): 481-485.

Bonnet, D., Martin, D., Pascale, D.L., Villain, E., Jouvet, P., Rabier, D., Brivet, M. & Saudubray, J.M. Arrhythmias and conduction defects as presenting symptoms of fatty acid oxidation disorders in children. *Circulation* 100, 2248-53 (1999).

Boubekeur, S., O. Bunoust, N. Camougrand, M. Castroviejo, M. Rigoulet and B. Guerin (1999). "A mitochondrial pyruvate dehydrogenase bypass in the yeast Saccharomyces cerevisiae." J Biol Chem 274(30): 21044-21048.

Bremer, J. Carnitine--metabolism and functions. *Physiological reviews* 63, 1420-80 (1983).

Bricker, D.K., Taylor, E.B., Schell, J.C., Orsak, T., Boutron, A., Chen, Y.C., Cox, J.E., Cardon, C.M., Van Vranken, J.G., Dephoure, N., Redin, C., Boudina, S., Gygi, S.P., Brivet, M., Thummel, C.S. & Rutter, J. A mitochondrial pyruvate carrier required for pyruvate uptake in yeast, Drosophila, and humans. *Science* 337, 96-100 (2012).

Briquet, M. (1977). "Transport of pyruvate and lactate in yeast mitochondria." Biochim Biophys Acta 459(2): 290-299.

Byrne, K. P. and K. H. Wolfe (2005). "The Yeast Gene Order Browser: combining curated homology and syntenic context reveals gene fate in polyploid species." Genome Res **15**(10): 1456-1461.

Campuzano, V., L. Montermini, Y. Lutz, L. Cova, C. Hindelang, S. Jiralerspong, Y. Trottier, S. J. Kish, B. Faucheux, P. Trouillas, F. J. Authier, A. Durr, J. L. Mandel, A. Vescovi, M. Pandolfo and M. Koenig (1997). "Frataxin is reduced in Friedreich ataxia

patients and is associated with mitochondrial membranes." Hum Mol Genet **6**(11): 1771-1780.

Cao, J., Shen, W., Chang, Z. & Shi, Y. ALCAT1 is a polyglycerophospholipid acyltransferase potently regulated by adenine nucleotide and thyroid status. *American journal of physiology. Endocrinology and metabolism* 296, E647-53 (2009).

Cardonick, E. H., K. Kuhlman, et al. (1997). "Prenatal clinical expression of 3-methylglutaconic aciduria: Barth syndrome." Prenat Diagn 17(10): 983-988.

Care, A., K. A. Vousden, et al. (2004). "A synthetic lethal screen identifies a role for the cortical actin patch/endocytosis complex in the response to nutrient deprivation in Saccharomyces cerevisiae." Genetics 166(2): 707-719.

Chang, S.C., Heacock, P.N., Clancey, C.J. & Dowhan, W. The PEL1 gene (renamed PGS1) encodes the phosphatidylglycero-phosphate synthase of Saccharomyces cerevisiae. *The Journal of biological chemistry* 273, 9829-36 (1998).

Chen, S., He, Q. & Greenberg, M.L. Loss of tafazzin in yeast leads to increased oxidative stress during respiratory growth. *Molecular microbiology* 68, 1061-72 (2008a).

Chen, S., Tarsio, M., Kane, P.M. & Greenberg, M.L. Cardiolipin mediates cross-talk between mitochondria and the vacuole. *Molecular biology of the cell* 19, 5047-58 (2008b).

Chen, Y., Y. Zhang, V. Siewers and J. Nielsen (2015). "Ach1 is involved in shuttling mitochondrial acetyl units for cytosolic C2 provision in Saccharomyces cerevisiae lacking pyruvate decarboxylase." FEMS Yeast Res 15(3).

Chen, Y., V. Siewers and J. Nielsen (2012). "Profiling of cytosolic and peroxisomal acetyl-CoA metabolism in Saccharomyces cerevisiae." PLoS One **7**(8): e42475.

Ciriacy, M. (1975). "Genetics of alcohol dehydrogenase in Saccharomyces cerevisiae. II. Two loci controlling synthesis of the glucose-repressible ADH II." Mol Gen Genet 138(2): 157-164.

Clarke, S.L.N., Bowron, A., Gonzalez, I.L., Groves, S.J., Newbury-Ecob, R., Clayton, N., Martin, R.P., Tsa-Goodman, B., Garratt, V., Ashworth, M., Bowen, V.M., McCurdy, K.R., Damin, M.K., Spencer, C.T., Toth, M.J., Kelley, R.I. & Steward, C.G. Barth syndrome. *Orphanet journal of rare diseases* 8, 23 (2013).

Claypool, S.M. Cardiolipin, a critical determinant of mitochondrial carrier protein assembly and function. *Biochimica et biophysica acta* 1788, 2059-68 (2009).

Claypool, S.M., Oktay, Y., Boontheung, P., Loo, J.A. & Koehler, C.M. Cardiolipin defines the interactome of the major ADP/ATP carrier protein of the mitochondrial inner membrane. *The Journal of cell biology* 182, 937-50 (2008).

Collister, M., M. P. Didmon, F. MacIsaac, M. J. Stark, N. Q. MacDonald and S. M. Keyse (2002). "YIL113w encodes a functional dual-specificity protein phosphatase which specifically interacts with and inactivates the Slt2/Mpk1p MAP kinase in S. cerevisiae." FEBS Lett **527**(1-3): 186-192.

Cowles, C. R., W. B. Snyder, C. G. Burd and S. D. Emr (1997). "Novel Golgi to vacuole delivery pathway in yeast: identification of a sorting determinant and required transport component." EMBO J **16**(10): 2769-2782.

Crabeel, M., F. Messenguy, F. Lacroute and N. Glansdorff (1981). "Cloning arg3, the gene for ornithine carbamoyltransferase from Saccharomyces cerevisiae: expression in Escherichia coli requires secondary mutations; production of plasmid beta-lactamase in yeast." Proc Natl Acad Sci U S A **78**(8): 5026-5030.

Cruciat, C.M., S. Brunner, F. Baumann, W. Neupert, and R.A. Stuart. 2000. The cytochrome bc1 and cytochrome c oxidase complexes associate to form a single supracomplex in yeast mitochondria. The Journal of biological chemistry. 275:18093-18098.

Daum, G. Lipids of mitochondria. *Biochimica et biophysica acta* 822, 1-42 (1985).

Davey, K.M., Parboosingh, J.S., McLeod, D.R., Chan, A., Casey, R., Ferreira, P., Snyder, F.F., Bridge, P.J. & Bernier, F.P. Mutation of DNAJC19, a human homologue of yeast inner mitochondrial membrane co-chaperones, causes DCMA syndrome, a novel autosomal recessive Barth syndrome-like condition. *Journal of medical genetics* 43, 385-93 (2006).

de Andrade Rosa, I., Einicker-Lamas, M., Roney Bernardo, R., Previatto, L.M., Mohana-Borges, R., Morgado-Diaz, J.A. & Benchimol, M. Cardiolipin in hydrogenosomes: evidence of symbiotic origin. *Eukaryotic cell* 5, 784-7 (2006).

De Virgilio, C., N. Burckert, G. Barth, J. M. Neuhaus, T. Boller and A. Wiemken (1992). "Cloning and disruption of a gene required for growth on acetate but not on ethanol: the acetyl-coenzyme A synthetase gene of Saccharomyces cerevisiae." Yeast 8(12): 1043-1051.

Dickinson, F. M. (1996). "The purification and some properties of the Mg(2+)-activated cytosolic aldehyde dehydrogenase of Saccharomyces cerevisiae." Biochem J 315 (Pt 2): 393-399.

Dowhan, W. Molecular basis for membrane phospholipid diversity: why are there so many lipids? *Annual review of biochemistry* 66, 199-232 (1997).

Dudek, J., Cheng, I.F., Balleininger, M., Vaz, F.M., Streckfuss-Bomeke, K., Hubscher, D., Vukotic, M., Wanders, R.J., Rehling, P. & Guan, K. Cardiolipin deficiency affects respiratory chain function and organization in an induced pluripotent stem cell model of Barth syndrome. *Stem cell research* 11, 806-19 (2013).

Dzugasova, V., Obernauerova, M., Horvathova, K., Vachova, M., Zakova, M. & Subik, J. Phosphatidylglycerolphosphate synthase encoded by the PEL1/PGS1 gene in Saccharomyces cerevisiae is localized in mitochondria and its expression is regulated by phospholipid precursors. *Current genetics* 34, 297-302 (1998).

Ellis, J. M., S. M. Mentock, M. A. Depetrillo, T. R. Koves, S. Sen, S. M. Watkins, D. M. Muoio, G. W. Cline, H. Taegtmeyer, G. I. Shulman, M. S. Willis and R. A. Coleman (2011). "Mouse cardiac acyl coenzyme a synthetase 1 deficiency impairs Fatty Acid oxidation and induces cardiac hypertrophy." Mol Cell Biol 31(6): 1252-1262.

Fiermonte, G., Dolce, V. & Palmieri, F. Expression in Escherichia coli, functional characterization, and tissue distribution of isoforms A and B of the phosphate carrier from bovine mitochondria. *The Journal of biological chemistry* 273, 22782-7 (1998).

Fiol, C.J. & Bieber, L.L. Sigmoid kinetics of purified beef heart mitochondrial carnitine palmitoyltransferase. Effect of pH and malonyl-CoA. *The Journal of biological chemistry* 259, 13084-8 (1984).

Flint, D.H., Tuminello, J.F. & Emptage, M.H. The inactivation of Fe-S cluster containing hydro-lyases by superoxide. *The Journal of biological chemistry* 268, 22369-76 (1993).

Franken, J. & Bauer, F.F. Carnitine supplementation has protective and detrimental effects in Saccharomyces cerevisiae that are genetically mediated. *FEMS yeast research* 10, 270-81 (2010).

Franken, J., Kroppenstedt, S., Swiegers, J.H. & Bauer, F.F. Carnitine and carnitine acetyltransferases in the yeast Saccharomyces cerevisiae: a role for carnitine in stress protection. *Current genetics* 53, 347-60 (2008).

Frye, Richard E., and Paul J. Benke. "Pyruvate Dehydrogenase Complex Deficiency." EMedicine. 11Dec. 2007. WebMD. 14 Dec. 2008.

Fujino, T., J. Kondo, M. Ishikawa, K. Morikawa and T. T. Yamamoto (2001). "Acetyl-CoA synthetase 2, a mitochondrial matrix enzyme involved in the oxidation of acetate." J Biol Chem 276(14): 11420-11426.

Fujiwara, T., K. Tanaka, et al. (1999). "Bni1p regulates microtubule-dependent nuclear migration through the actin cytoskeleton in Saccharomyces cerevisiae." Mol Cell Biol 19(12): 8016-8027.

Gallas, M.R., Dienhart, M.K., Stuart, R.A. & Long, R.M. Characterization of Mmp37p, a Saccharomyces cerevisiae mitochondrial matrix protein with a role in mitochondrial protein import. *Molecular biology of the cell* 17, 4051-62 (2006).

Gallet, P. F., J. M. Petit, A. Maftah, A. Zachowski and R. Julien (1997). "Asymmetrical distribution of cardiolipin in yeast inner mitochondrial membrane triggered by carbon catabolite repression." Biochem J 324 (Pt 2): 627-634.

Gardner, P.R. Superoxide-driven aconitase FE-S center cycling. *Bioscience reports* 17, 33-42 (1997).

Gaspard, G. J. and C. R. McMaster (2015). "The mitochondrial quality control protein Yme1 is necessary to prevent defective mitophagy in a yeast model of Barth syndrome." J Biol Chem **290**(14): 9284-9298.

Gebert, N., Gebert, M., Oeljieklaus, S., von der Malsburg, K., Stroud, D.A., Kulawiak, B., Wirth, C., Zahedi, R.P., Dolezal, P., Wiese, S., Simon, o., Schulze-Specking, A., Truscott, K.N., Sickmann, A., Rehling, P., Guiard, B., Hunte, C., Warscheid, B., van der Laan, M., Pfanner, N. & Wiedemann, N. Dual function of Sdh3 in the respiratory chain and TIM22 protein translocase of the mitochondrial inner membrane. *Molecular cell* 44, 811-8 (2011).

Gebert, N., Joshi, A.S., Kutik, S., Becker, T., McKenzie, M., Guan, X.L., Mooga, V.P., Stroud, D.A., Kulkarni, G., Wenk, M.R., Rehling, P., Meisinger, C., Ryan, M.T., Wiedemann, N., Greenberg, M.L. & Pfanner, N. Mitochondrial cardiolipin involved in outer-membrane protein biogenesis: implications for Barth syndrome. *Current biology : CB* 19, 2133-9 (2009).

Gerber, J., Neumann, K., Prohl, C., Muhlenhoff, U. & Lill, R. The yeast scaffold proteins Isu1p and Isu2p are required inside mitochondria for maturation of cytosolic Fe/S proteins. *Molecular and cellular biology* 24, 4848-57 (2004).

Gimeno, R.E. Fatty acid transport proteins. *Current opinion in lipidology* 18, 271-6 (2007).

Gohil, V.M., Hayes, P., Matsuyama, S., Schagger, H., Schlame, M. & Greenberg, M.L. Cardiolipin biosynthesis and mitochondrial respiratory chain function are interdependent. *The Journal of biological chemistry* 279, 42612-8 (2004).

Gohil, V. M., M. N. Thompson and M. L. Greenberg (2005). "Synthetic lethal interaction of the mitochondrial phosphatidylethanolamine and cardiolipin biosynthetic pathways in Saccharomyces cerevisiae." J Biol Chem 280(42): 35410-35416.

Green, R., G. Lesage, et al. (2003). "A synthetic analysis of the Saccharomyces cerevisiae stress sensor Mid2p, and identification of a Mid2p-interacting protein, Zeo1p, that modulates the PKC1-MPK1 cell integrity pathway." Microbiology 149(Pt 9): 2487-2499.

Grivennikova, V.G. & Vinogradov, A.D. Generation of superoxide by the mitochondrial Complex I. *Biochimica et biophysica acta* 1757, 553-61 (2006).

Grossi, S., A. Puglisi, et al. (2004). "Pol12, the B subunit of DNA polymerase alpha, functions in both telomere capping and length regulation." Genes Dev 18(9): 992-1006.

Gu, Z., F. Valianpour, et al. (2004). "Aberrant cardiolipin metabolism in the yeast taz1 mutant: a model for Barth syndrome." Mol Microbiol 51(1): 149-158.

Guest, J. R., S. J. Angier and G. C. Russell (1989). "Structure, expression, and protein engineering of the pyruvate dehydrogenase complex of Escherichia coli." Ann N Y Acad Sci 573: 76-99.

Hagen, T.M., Wehr, C.M. & Ames, B.N. Mitochondrial decay in aging. Reversal through supplementation of acetyl-L-carnitine and N-tert-butyl-alpha-phenyl-nitrone. *Annals of the New York Academy of Sciences* 854, 214-23 (1998).

Hahn, J. S. and D. J. Thiele (2002). "Regulation of the Saccharomyces cerevisiae Slt2 kinase pathway by the stress-inducible Sdp1 dual specificity phosphatase." J Biol Chem **277**(24): 21278-21284.

Hall, R.E., Henriksson, K.G., Lewis, S.F., Haller, R.G. & Kennaway, N.G. Mitochondrial myopathy with succinate dehydrogenase and aconitase deficiency. Abnormalities of several iron-sulfur proteins. *The Journal of clinical investigation* 92, 2660-6 (1993).

Haller, R.G., Henriksson, K.G., Jorfeldt, L., Hultman, E., Wiborn, R., Sahlin, K., Areskog, N.H., Gunder, M., Ayyad, K. & Blomqvist, C.G. Deficiency of skeletal muscle succinate dehydrogenase and aconitase. Pathophysiology of exercise in a novel human muscle oxidative defect. *The Journal of clinical investigation* 88, 1197-206 (1991).

Hartman, J. L. t., B. Garvik, et al. (2001). "Principles for the buffering of genetic variation." Science 291(5506): 1001-1004.

Hausmann, A., Samans, B., Lill, R. & Muhlenhoff, U. Cellular and mitochondrial remodeling upon defects in iron-sulfur protein biogenesis. *The Journal of biological chemistry* 283, 8318-30 (2008).

Heikoop, J. C., C. W. van Roermund, W. W. Just, R. Ofman, R. B. Schutgens, H. S.
Heymans, R. J. Wanders and J. M. Tager (1990). "Rhizomelic
chondrodysplasia punctata. Deficiency of 3-oxoacyl-coenzyme A thiolase in
peroxisomes and impaired processing of the enzyme." J Clin Invest **86**(1): 126-130.

Hettema, E. H. and H. F. Tabak (2000). "Transport of fatty acids and metabolites
across the peroxisomal membrane." Biochim Biophys Acta **1486**(1): 18-27.

Hishida, T., T. Ohno, et al. (2002). "Saccharomyces cerevisiae MGS1 is essential in
strains deficient in the RAD6-dependent DNA damage tolerance pathway." EMBO J
21(8): 2019-2029.

Hoch, F.L. Cardiolipins and biomembrane function. *Biochimica et biophysica acta* 1113,
71-133 (1992).

Hoffmann, B., Stockl, A., Schlame, M., Beyer, K. & Klingenberg, M. The reconstituted
ADP/ATP carrier activity has an absolute requirement for cardiolipin as shown in
cysteine mutants. *The Journal of biological chemistry* 269, 1940-4 (1994).

Hong, M.Y., Chapkin, R.S., Barhoumi, R., Burghardt, R.C., Turner, N.D., Henderson,
C.E., Sanders, L.M., Fan, Y.Y., Davidson, L.A., Murphy, M.E., Spinka, C.M., Carroll,
R.J. & Lupton, J.R. Fish oil increases mitochondrial phospholipid unsaturation,
upregulating reactive oxygen species and apoptosis in rat colonocytes.
Carcinogenesis 23, 1919-25 (2002).

Houten, S.M. & Wanders, R.J. A general introduction to the biochemistry of mitochondrial
fatty acid beta-oxidation. *Journal of inherited metabolic disease* 33, 469-77 (2010).

Hunte, C. Specific protein-lipid interactions in membrane proteins. *Biochemical Society transactions* 33, 938-42 (2005).

Hynes, M. J., S. L. Murray, A. Andrianopoulos and M. A. Davis (2011). "Role of carnitine acetyltransferases in acetyl coenzyme A metabolism in Aspergillus nidulans." Eukaryot Cell **10**(4): 547-555.

Ingwall, J. S. (2009). "Energy metabolism in heart failure and remodelling." Cardiovasc Res **81**(3): 412-419.

Jakovcic, S., G. S. Getz, M. Rabinowitz, H. Jakob and H. Swift (1971). "Cardiolipin content of wild type and mutant yeasts in relation to mitochondrial function and development." J Cell Biol 48(3): 490-502.

Jia, Z., Pei, Z., Maiguel, D., Toomer, C.J. & Watkins, P.A. The fatty acid transport protein (FATP) family: very long chain acyl-CoA synthetases or solute carriers? *Journal of molecular neuroscience : MN* 33, 25-31 (2007).

Jiang, F., Rizavi, H.S. & Greenberg, M.L. Cardiolipin is not essential for the growth of Saccharomyces cerevisiae on fermentable or non-fermentable carbon sources. *Molecular microbiology* 26, 481-91 (1997).

Jiang, F., Ryan, M.T., Schlame, M., Zhao, M., Gu, Z., Klingenberg, M., Pfanner, N. & Greenberg, M.L. Absence of cardiolipin in the crd1 null mutant results in decreased mitochondrial membrane potential and reduced mitochondrial function. *The Journal of biological chemistry* 275, 22387-94 (2000).

Jogl, G. & Tong, L. Crystal structure of carnitine acetyltransferase and implications for the catalytic mechanism and fatty acid transport. *Cell* 112, 113-22 (2003).

Johnson, D.C., Dean, D.R., Smith, A.D. & Johnson, M.K. Structure, function, and formation of biological iron-sulfur clusters. *Annual review of biochemistry* 74, 247-81 (2005).

Johnston, J., Kelley, R.I., Feigenbaum, A., Cox, G.F., Iyer, G.S., Funanage, V.L. & Proujansky, R. Mutation characterization and genotype-phenotype correlation in Barth syndrome. *American journal of human genetics* 61, 1053-8 (1997).

Johnston, M. (1999). "Feasting, fasting and fermenting. Glucose sensing in yeast and other cells." Trends Genet 15(1): 29-33.

Joshi, A.S., Thompson, M.N., Fei, N., Huttemann, M. & Greenberg, M.L. Cardiolipin and mitochondrial phosphatidylethanolamine have overlapping functions in mitochondrial fusion in Saccharomyces cerevisiae. *The Journal of biological chemistry* 287, 17589-97 (2012).

Joshi, A.S., Zhou, J., Gohil, V.M., Chen, S. & Greenberg, M.L. Cellular functions of cardiolipin in yeast. *Biochimica et biophysica acta* 1793, 212-8 (2009).

Joshi, A. S., N. Fei and M. L. Greenberg (2016). "Get1p and Get2p are required for maintenance of mitochondrial morphology and normal cardiolipin levels." FEMS Yeast Res 16(3).

Kadenbach, B., Mende, P., Kolbe, H.V., Stipani, I. & Palmieri, F. The mitochondrial phosphate carrier has an essential requirement for cardiolipin. *FEBS letters* 139, 109-12 (1982).

Kessler, D. & Papenbrock, J. Iron-sulfur cluster biosynthesis in photosynthetic organisms. *Photosynthesis research* 86, 391-407 (2005).

Kiebish, M.A., Yang, K., Liu, X., Mancuso, D.J., Guan, S., Zhao, Z., Sims, H.F., Cerqua, R., Cade, W.T., Han, X. & Gross, R.W. Dysfunctional cardiac mitochondrial bioenergetic, lipidomic, and signaling in a murine model of Barth syndrome. *Journal of lipid research* 54, 1312-25 (2013).

Klingenberg, M. Mechanism and evolution of the uncoupling protein of brown adipose tissue. *Trends in biochemical sciences* 15, 108-12 (1990).

Kodde, I. F., J. van der Stok, R. T. Smolenski and J. W. de Jong (2007). "Metabolic and genetic regulation of cardiac energy substrate preference." Comp Biochem Physiol A Mol Integr Physiol **146**(1): 26-39.

Kollberg, G., Tulinius, M., Melberg, A., Darin, N., Anderson, O., Holmgren, D., Oldfors, A. & Holme, E. Clinical manifestation and a new ISCU mutation in iron-sulphur cluster deficiency myopathy. *Brain : a journal of neurology* 132, 2170-9 (2009).

Koshkin, V. & Greenberg, M.L. Cardiolipin prevents rate-dependent uncoupling and provides osmotic stability in yeast mitochondria. *The Biochemical journal* 364, 317-22 (2002).

Koshkin, V. & Greenberg, M.L. Oxidative phosphorylation in cardiolipin-lacking yeast mitochondria. *The Biochemical journal* 347 Pt 3, 687-91 (2000).

Kozak, B. U., H. M. van Rossum, M. A. Luttik, M. Akeroyd, K. R. Benjamin, L. Wu, S. de Vries, J. M. Daran, J. T. Pronk and A. J. van Maris (2014). "Engineering acetyl coenzyme A supply: functional expression of a bacterial pyruvate dehydrogenase complex in the cytosol of Saccharomyces cerevisiae." MBio **5**(5): e01696-01614.

Krivoruchko, A., Y. Zhang, V. Siewers, Y. Chen and J. Nielsen (2015). "Microbial acetyl-CoA metabolism and metabolic engineering." Metab Eng **28**: 28-42.

Kuan, J. & Saier, M.H., Jr. Expansion of the mitochondrial carrier family. *Research in microbiology* 144, 671-2 (1993).

Kunau, W. H., V. Dommes and H. Schulz (1995). "beta-oxidation of fatty acids in mitochondria, peroxisomes, and bacteria: a century of continued progress." Prog Lipid Res **34**(4): 267-342.

Kunze, M., I. Pracharoenwattana, S. M. Smith and A. Hartig (2006). "A central role for the peroxisomal membrane in glyoxylate cycle function." Biochim Biophys Acta **1763**(12): 1441-1452.

Kunze, M. and A. Hartig (2013). "Permeability of the peroxisomal membrane: lessons from the glyoxylate cycle." Front Physiol **4**: 204.

Kuravi, V.K., Kurischko, C., Puri, M. & Luca, F.C. Cbk1 kinase and Bck2 control MAP kinase activation and inactivation during heat shock. Molecular biology of the cell 22, 4892-907 (2011).

Kushnareva, Y., Murphy, A.N. & Andreyev, A. Complex I-mediated reactive oxygen species generation: modulation by cytochrome c and NAD(P)+ oxidation-reduction state. *The Biochemical journal* 368, 545-53 (2002).

Kutik, S., Rissler, M., Guan, X.L., Guiard, B., Shui, G., Gebert, N., Heacock, P.N., Rehling, P., Dowhan, W., Wenk, M.R., Pfanner, N. & Wiedemann, N. The translocator maintenance protein Tam41 is required for mitochondrial cardiolipin biosynthesis. *The Journal of cell biology* 183, 1213-21 (2008).

Lange, C., Nett, J.H., Trumpower, B.L. & Hunte, C. Specific roles of protein-phospholipid interactions in the yeast cytochrome bc1 complex structure. *The EMBO journal* 20, 6591-600 (2001).

Lawson, J. E., R. H. Behal and L. J. Reed (1991). "Disruption and mutagenesis of the Saccharomyces cerevisiae PDX1 gene encoding the protein X component of the pyruvate dehydrogenase complex." Biochemistry 30(11): 2834-2839.

Lee, H.J., Mayette, J., Rapoport, S.I. & Bazinet, R.P. Selective remodeling of cardiolipin fatty acids in the aged rat heart. *Lipids in health and disease* 5, 2 (2006).

Lee, M. S. and F. A. Spencer (2004). "Bipolar orientation of chromosomes in Saccharomyces cerevisiae is monitored by Mad1 and Mad2, but not by Mad3." Proc Natl Acad Sci U S A 101(29):10655-10660.

Lee, Y. J., J. W. Jang, K. J. Kim and P. J. Maeng (2011). "TCA cycle-independent acetate metabolism via the glyoxylate cycle in Saccharomyces cerevisiae." Yeast **28**(2): 153-166.

Lenaz, G., Bovina, C., Castelluccio, C., Fato, R., Formiggini, G., Genova, M.L., Marchetti, M., Pich, M.M., Pallotti, F., Parenti Castelli, G. & Biagini, G. Mitochondrial complex I defects in aging. *Molecular and cellular biochemistry* 174, 329-33 (1997).

Lewin, M.B. & Timiras, P.S. Lipid changes with aging in cardiac mitochondrial membranes. *Mechanisms of ageing and development* 24, 343-51 (1984).

Li, J., Kogan, M., Knight, S.A., Pain, D. & Dancis, A. Yeast mitochondrial protein, Nfs1p, coordinately regulates iron-sulfur cluster proteins, cellular iron uptake, and iron distribution. *The Journal of biological chemistry* 274, 33025-34 (1999).

Li, J., Liu, X., Wang, H., Zhang, W., Chan, D.C. & Shi, Y. Lysocardiolipin acyltransferase 1 (ALCAT1) controls mitochondrial DNA fidelity and biogenesis through modulation of MFN2 expression. *Proceedings of the National Academy of Sciences of the United States of America* 109, 6975-80 (2012).

Li, J., Romestaing, C., Han, X., Li, Y., Hao, X., Wu, Y., Sun, C., Liu, X., Jefferson, L.S., Xiong, J., Lanoue, K.F., Chang, Z., Lynch, C.J., Wang, H. & Shi, Y. Cardiolipin remodeling by ALCAT1 links oxidative stress and mitochondrial dysfunction to obesity. *Cell metabolism* 12, 154-65 (2010).

Lill, R. & Muhlenhoff, U. Maturation of iron-sulfur proteins in eukaryotes: mechanisms, connected processes, and diseases. *Annual review of biochemistry* 77, 669-700 (2008).

Liu, X., Ye, B., Miller, S., Yuan, H., Zhang, H., Tian, L., Nie, J., Imae, R., Arai, H., Li, Y., Cheng, Z. & Shi, Y. Ablation of ALCAT1 mitigates hypertrophic cardiomyopathy through effects on oxidative stress and mitophagy. *Molecular and cellular biology* 32, 4493-504 (2012).

Longo, N., Amat di San Filippo, C. & Pasquali, M. Disorders of carnitine transport and the carnitine cycle. *American journal of medical genetics. Part C, Seminars in medical genetics* 142C, 77-85 (2006).

Ma, L., F. M. Vaz, Z. Gu, R. J. Wanders and M. L. Greenberg (2004). "The human TAZ gene complements mitochondrial dysfunction in the yeast taz1Delta mutant. Implications for Barth syndrome." J Biol Chem 279(43): 44394-44399.

Maftah, A., Ratinaud, M.H., Dumas, M., Bonte, F., Meybeck, A. & Julien, R. Human epidermal cells progressively lose their cardiolipins during ageing without change in mitochondrial transmembrane potential. *Mechanisms of ageing and development* 77, 83-96 (1994).

Malhotra, A., Xu, Y., Ren, M. & Schlame, M. Formation of molecular species of mitochondrial cardiolipin. 1. A novel transacylation mechanism to shuttle fatty acids between sn-1 and sn-2 positions of multiple phospholipid species. *Biochimica et biophysica acta* 1791, 314-20 (2009).

Maranzana, E., Barbero, G., Falasca, A.I., Lenaz, G. & Genova, M.L. Mitochondrial Respiratory Supercomplex Association Limits Production of Reactive Oxygen Species from Complex I. *Antioxidants & redox signaling* (2013).

Mazzocco, M.M., A.E. Henry, and R.I. Kelly. (2007). "Barth syndrome is associated with a cognitive phenotype." J Dev Behav Pediatr 28:22-30.

McGarry, J. D. and N. F. Brown (1997). "The mitochondrial carnitine palmitoyl-transferase system. From concept to molecular analysis." Eur J Biochem **244**(1): 1-14.

McKenzie, M., Lazarou, M., Thorburn, D.R. & Ryan, M.T. Mitochondrial respiratory chain supercomplexes are destabilized in Barth Syndrome patients. *Journal of molecular biology* 361, 462-9 (2006).

Meaden, P. G., F. M. Dickinson, A. Mifsud, W. Tessier, J. Westwater, H. Bussey and M. Midgley (1997). "The ALD6 gene of Saccharomyces cerevisiae encodes a cytosolic, Mg(2+)-activated acetaldehyde dehydrogenase." Yeast 13(14): 1319-1327.

Merkel, O., M. Fido, J. A. Mayr, H. Pruger, F. Raab, G. Zandonella, S. D. Kohlwein and F. Paltauf (1999). "Characterization and function in vivo of two novel phospholipases B/lysophospholipases from Saccharomyces cerevisiae." J Biol Chem **274**(40): 28121-28127.

Merkel, O., O. V. Oskolkova, F. Raab, R. El-Toukhy and F. Paltauf (2005). "Regulation of activity in vitro and in vivo of three phospholipases B from Saccharomyces cerevisiae." Biochem J **387**(Pt 2): 489-496.

Miran, S. G., J. E. Lawson and L. J. Reed (1993). "Characterization of PDH beta 1, the structural gene for the pyruvate dehydrogenase beta subunit from Saccharomyces cerevisiae." Proc Natl Acad Sci U S A 90(4): 1252-1256.

Mitchell, R.W. & Hatch, G.M. Regulation of cardiolipin biosynthesis by fatty acid transport protein-1 IN HEK 293 cells. *Biochimica et biophysica acta* 1788, 2015-21 (2009).

Mochel, F., Knight, M.A., Tong, W.H., Hernandez, D., Ayyad, K., Taivassalo, T., Andersen, P.M., Singleton, A., Rouault, T.A., Fischbeck, K.H. & Haller, R.G. Splice mutation in the iron-sulfur cluster scaffold protein ISCU causes myopathy with exercise intolerance. *American journal of human genetics* 82, 652-60 (2008).

Murthy, M.S. & Pande, S.V. Mechanism of carnitine acylcarnitine translocase-catalyzed import of acylcarnitines into mitochondria. *The Journal of biological chemistry* 259, 9082-9 (1984).

Nalecz, K.A., Bolli, R., Wojtczak, L. & Azzi, A. The monocarboxylate carrier from bovine heart mitochondria: partial purification and its substrate-transporting properties in a reconstituted system. *Biochimica et biophysica acta* 851, 29-37 (1986).

Nalecz, M. J., K. A. Nalecz and A. Azzi (1991). "Purification and functional characterisation of the pyruvate (monocarboxylate) carrier from baker's yeast mitochondria (Saccharomyces cerevisiae)." Biochim Biophys Acta 1079(1): 87-95.

Nelson, D.R., Lawson, J.E., Klingenberg, M. & Douglas, M.G. Site-directed mutagenesis of the yeast mitochondrial ADP/ATP translocator. Six arginines and one lysine are essential. *Journal of molecular biology* 230, 1159-70 (1993).

Neubauer, S. (2007). "The failing heart--an engine out of fuel." N Engl J Med **356**(11): 1140-1151.

Neuspiel, M., Schauss, A.C., Braschi, E., Zunino, R., Rippstein, P., Rachubinski, R.A., Andrade-Navarro, M.A. & McBride, H.M. Cargo-selected transport from the mitochondria to peroxisomes is mediated by vesicular carriers. *Current biology : CB* 18, 102-8 (2008).

Nielsen, J., M. Fussenegger, J. Keasling, S. Y. Lee, J. C. Liao, K. Prather and B. Palsson (2014). "Engineering synergy in biotechnology." Nat Chem Biol **10**(5): 319-322.

Niu, X. D., K. S. Browning, R. H. Behal and L. J. Reed (1988). "Cloning and nucleotide sequence of the gene for dihydrolipoamide acetyltransferase from Saccharomyces cerevisiae." Proc Natl Acad Sci U S A 85(20): 7546-7550.

Noel, H. & Pande, S.V. An essential requirement of cardiolipin for mitochondrial carnitine acylcarnitine translocase activity. Lipid requirement of carnitine acylcarnitine translocase. *European journal of biochemistry / FEBS* 155, 99-102 (1986).

Nury, H., Dahout-Gonzalez, C., Trezeguet, V., Lauquin, G.J., Brandolin, G. & Pebay-Peyroula, E. Relations between structure and function of the mitochondrial ADP/ATP carrier. *Annual review of biochemistry* 75, 713-41 (2006).

Odorizzi, G., M. Babst and S. D. Emr (1998). "Fab1p PtdIns(3)P 5-kinase function essential for protein sorting in the multivesicular body." Cell **95**(6): 847-858.

Orngreen, M.C., Ejstrup, R. & Vissing, J. Effect of diet on exercise tolerance in carnitine palmitoyltransferase II deficiency. *Neurology* 61, 559-61 (2003).

Osman, C., Haag, M., Wieland, F.T., Brugger, B. & Langer, T. A mitochondrial phosphatase required for cardiolipin biosynthesis: the PGP phosphatase Gep4. *The EMBO journal* 29, 1976-87 (2010).

Palmieri, F. Mitochondrial carrier proteins. *FEBS letters* 346, 48-54 (1994).

Palmieri, L., F. M. Lasorsa, A. De Palma, F. Palmieri, M. J. Runswick and J. E. Walker (1997). "Identification of the yeast ACR1 gene product as a succinate-fumarate transporter essential for growth on ethanol or acetate." FEBS Letters **417**(1): 114-118.

Palmieri, L., A. Vozza, A. Honlinger, K. Dietmeier, A. Palmisano, V. Zara and F. Palmieri (1999). "The mitochondrial dicarboxylate carrier is essential for the growth of Saccharomyces cerevisiae on ethanol or acetate as the sole carbon source." Mol Microbiol **31**(2): 569-577.

Pande, S.V., Murthy, M.S. & Noel, H. Differential effects of phosphatidylcholine and cardiolipin on carnitine palmitoyltransferase activity. *Biochimica et biophysica acta* 877, 223-30 (1986).

Pangborn, M. C. (1947). "The composition of cardiolipin." J Biol Chem 168(1): 351-361.

Pangborn M. Isolation and purification of a serologically active phospholipid from beef heart. *Journal of biological chemistry* 143, 247-256 (1942)

Paquin, C. E. and V. M. Williamson (1986). "Ty insertions at two loci account for most of the spontaneous antimycin A resistance mutations during growth at 15 degrees C of Saccharomyces cerevisiae strains lacking ADH1." Mol Cell Biol 6(1): 70-79.

Paradies, G. & Ruggiero, F.M. Age-related changes in the activity of the pyruvate carrier and in the lipid composition in rat-heart mitochondria. *Biochimica et biophysica acta* 1016, 207-12 (1990).

Paradies, G., Petrosillo, G., Paradies, V. & Ruggiero, F.M. Oxidative stress, mitochondrial bioenergetics, and cardiolipin in aging. *Free radical biology & medicine* 48, 1286-95 (2010).

Paradies, G., Petrosillo, G., Pistolese, M. & Ruggiero, F.M. Reactive oxygen species generated by the mitochondrial respiratory chain affect the complex III activity via cardiolipin peroxidation in beef-heart submitochondrial particles. *Mitochondrion* 1, 151-9 (2001).

Paradies, G., Petrosillo, G., Pistolese, M. & Ruggiero, F.M. The effect of reactive oxygen species generated from the mitochondrial electron transport chain on the cytochrome c oxidase activity and on the cardiolipin content in bovine heart submitochondrial particles. *FEBS letters* 466, 323-6 (2000).

Paradies, G., Ruggiero, F.M., Petrosillo, G. & Quagliariello, E. Age-dependent decrease in the cytochrome c oxidase activity and changes in phospholipids in rat-heart mitochondria. *Archives of gerontology and geriatrics* 16, 263-72 (1993).

Paradies, G., Ruggiero, F.M., Petrosillo, G. & Quagliariello, E. Age-dependent decline in the cytochrome c oxidase activity in rat heart mitochondria: role of cardiolipin. *FEBS letters* 406, 136-8 (1997).

Paradies, G., Ruggiero, F.M., Petrosillo, G. & Quagliariello, E. Peroxidative damage to cardiac mitochondria: cytochrome oxidase and cardiolipin alterations. *FEBS letters* 424, 155-8 (1998).

Patil, V.A. & Greenberg, M.L. Cardiolipin-mediated cellular signaling. *Advances in experimental medicine and biology* 991, 195-213 (2013).

Patil, V.A., Fox, J.L., Gohil, V.M., Winge, D.R. & Greenberg, M.L. Loss of cardiolipin leads to perturbation of mitochondrial and cellular iron homeostasis. *The Journal of biological chemistry* 288, 1696-705 (2013).

Petrosillo, G., Portincasa, P., Grattagliano, I., Casanova, G., Matera, M., Ruggiero, F.M., Ferri, D. & Paradies, G. Mitochondrial dysfunction in rat with nonalcoholic fatty liver Involvement of complex I, reactive oxygen species and cardiolipin. *Biochimica et biophysica acta* 1767, 1260-7 (2007).

Pfeiffer, K., Gohil, V., Stuart, R.A., Hunte, C., Brandt, U., Greenberg, M.L. & Schagger, H. Cardiolipin stabilizes respiratory chain supercomplexes. *The Journal of biological chemistry* 278, 52873-80 (2003).

Piper, P. W., C. Ortiz-Calderon, C. Holyoak, P. Coote and M. Cole (1997). "Hsp30, the integral plasma membrane heat shock protein of Saccharomyces cerevisiae, is a stress-inducible regulator of plasma membrane H(+)-ATPase." Cell Stress Chaperones **2**(1): 12-24.

Platta, H.W., Magraoui, F.E., Schlee, D., Grunau, S., Girzalsky, W. & Erdmann, R. Ubiquitination of the peroxisomal import receptor Pex5p is required for its recycling. *The Journal of cell biology* 177, 197-204 (2007).

Pronk, J. T., H. Yde Steensma and J. P. Van Dijken (1996). "Pyruvate metabolism in Saccharomyces cerevisiae." Yeast 12(16): 1607-1633.

Remize, F., E. Andrieu and S. Dequin (2000). "Engineering of the pyruvate dehydrogenase bypass in Saccharomyces cerevisiae: role of the cytosolic Mg(2+) and mitochondrial K(+) acetaldehyde dehydrogenases Ald6p and Ald4p in acetate formation during alcoholic fermentation." Appl Environ Microbiol 66(8): 3151-3159.

Reuter, S.E. & Evans, A.M. Carnitine and acylcarnitines: pharmacokinetic, pharmacological and clinical aspects. *Clinical pharmacokinetics* 51, 553-72 (2012).

Rinaldo, P., Matern, D. & Bennett, M.J. Fatty acid oxidation disorders. *Annual review of physiology* 64, 477-502 (2002).

Ristow, M., Pfister, M.F., Yee, A.J., Schubert, M., Michael, L., Zhang, C.Y., Ueki, K., Michael, M.D., Lowell, B.B. & Kahn, C.R. Frataxin activates mitochondrial energy conversion and oxidative phosphorylation. *Proceedings of the National Academy of Sciences of the United States of America* 97, 12239-43 (2000).

Roemer, T. and H. Bussey (1991). "Yeast beta-glucan synthesis: KRE6 encodes a predicted type II membrane protein required for glucan synthesis in vivo and for glucan synthase activity in vitro." Proc Natl Acad Sci U S A 88(24): 11295-11299.

Rouault, T.A. & Tong, W.H. Iron-sulfur cluster biogenesis and human disease. *Trends in genetics : TIG* 24, 398-407 (2008).

Rouault, T.A. Biogenesis of iron-sulfur clusters in mammalian cells: new insights and relevance to human disease. *Disease models & mechanisms* 5, 155-64 (2012).

Runko, A.P., Griswold, A.J. & Min, K.T. Overexpression of frataxin in the mitochondria increases resistance to oxidative stress and extends lifespan in Drosophila. *FEBS letters* 582, 715-9 (2008).

Rutherford, J.C., Ojeda, L., Balk, J., Muhlenhoff, U., Lill, R. & Winge, D.R. Activation of the iron regulon by the yeast Aft1/Aft2 transcription factors depends on mitochondrial but not cytosolic iron-sulfur protein biogenesis. *The Journal of biological chemistry* 280, 10135-40 (2005).

Saffi, J., L. Sonego, Q. D. Varela and M. Salvador (2006). "Antioxidant activity of L-ascorbic acid in wild-type and superoxide dismutase deficient strains of Saccharomyces cerevisiae." Redox Rep 11(4): 179-184.

Saito, K. (2014). "Reminiscence of phospholipase B in Penicillium notatum." Proc Jpn Acad Ser B Phys Biol Sci **90**(9): 333-346.

Saudubray, J.M., Martin, D., de Lonlay, P., Touati, G., Poggi-Travert, F., Bonnet, D., Jouvet, P., Boutron, M., Slama, A., Vianey-Saban, C., Bonnefont, J.P., Rabier, D., Kamoun, P. & Brivet, M. Recognition and management of fatty acid oxidation defects: a series of 107 patients. *Journal of inherited metabolic disease* 22, 488-502 (1999).

Schagger, H. & Pfeiffer, K. Supercomplexes in the respiratory chains of yeast and mammalian mitochondria. *The EMBO journal* 19, 1777-83 (2000).

Schagger, H. Respiratory chain supercomplexes of mitochondria and bacteria. *Biochimica et biophysica acta* 1555, 154-9 (2002).

Schlame, M. & Ren, M. Barth syndrome, a human disorder of cardiolipin metabolism. *FEBS letters* 580, 5450-5 (2006).

Schlame, M., Rua, D. & Greenberg, M.L. The biosynthesis and functional role of cardiolipin. *Progress in lipid research* 39, 257-88 (2000).

Schlame, M. and M. L. Greenberg (1997). "Cardiolipin synthase from yeast." Biochim Biophys Acta 1348(1-2): 201-206.

Schlame, M. and M. Ren (2009). "The role of cardiolipin in the structural organization of mitochondrial membranes." Biochim Biophys Acta 1788(10): 2080-2083.

Schlame, M., D. Rua and M. L. Greenberg (2000). "The biosynthesis and functional role of cardiolipin." Prog Lipid Res 39(3): 257-288.

Schlame, M., J. A. Towbin, P. M. Heerdt, R. Jehle, S. DiMauro and T. J. Blanck (2002). "Deficiency of tetralinoleoyl-cardiolipin in Barth syndrome." Ann Neurol 51(5): 634-637.

Schlame, M., M. Ren, Y. Xu, M. L. Greenberg and I. Haller (2005). "Molecular symmetry in mitochondrial cardiolipins." Chem Phys Lipids 138(1-2): 38-49.

Schlame, M., R. I. Kelley, A. Feigenbaum, J. A. Towbin, P. M. Heerdt, T. Schieble, R. J. Wanders, S. DiMauro and T. J. Blanck (2003). "Phospholipid abnormalities in children with Barth syndrome." J Am Coll Cardiol 42(11): 1994-1999.

Schulz, T.J., Westermann, D., Isken, F., Voigt, A., Laube, B., Thierbach, R., Kuhlow, D., Zarse, K., Schomburg, L., Pfeiffer, A.F., Tschope, C. & Ristow, M. Activation of mitochondrial energy metabolism protects against cardiac failure. *Aging* 2, 843-53 (2010).

Schumann, U. & Subramani, S. Special delivery from mitochondria to peroxisomes. *Trends in cell biology* 18, 253-6 (2008).

Sedlak, E. & Robinson, N.C. Phospholipase A(2) digestion of cardiolipin bound to bovine cytochrome c oxidase alters both activity and quaternary structure. *Biochemistry* 38, 14966-72 (1999).

Sen, T., Sen, N., Jana, S., Khan, F.H., Chatterjee, U. & Chakrabarti, S. Depolarization and cardiolipin depletion in aged rat brain mitochondria: relationship with oxidative stress and electron transport chain activity. *Neurochemistry international* 50, 719-25 (2007).

Sen, T., Sen, N., Tripathi, G., Chatterjee, U. & Chakrabarti, S. Lipid peroxidation associated cardiolipin loss and membrane depolarization in rat brain mitochondria. *Neurochemistry international* 49, 20-7 (2006).

Shiba, Y., E. M. Paradise, J. Kirby, D. K. Ro and J. D. Keasling (2007). "Engineering of the pyruvate dehydrogenase bypass in Saccharomyces cerevisiae for high-level production of isoprenoids." Metab Eng **9**(2): 160-168.

Sparagna, G.C. & Lesnefsky, E.J. Cardiolipin remodeling in the heart. *Journal of cardiovascular pharmacology* 53, 290-301 (2009).

Spencer, C.T., Byrne, B.J., Bryant, R.M., Margossian, R., Maisenbacher, M., Breitenger, P., Benni, P.B., Redfearn, S., Marcus, E. & Cade, W.T. Impaired cardiac reserve and severely diminished skeletal muscle O(2) utilization mediate exercise intolerance in Barth syndrome. *American journal of physiology. Heart and circulatory physiology* 301, H2122-9 (2011).

Stanley, W. C., F. A. Recchia and G. D. Lopaschuk (2005). "Myocardial substrate metabolism in the normal and failing heart." Physiol Rev **85**(3): 1093-1129.

Steensma, H. Y., L. Holterman, I. Dekker, C. A. van Sluis and T. J. Wenzel (1990). "Molecular cloning of the gene for the E1 alpha subunit of the pyruvate dehydrogenase complex from Saccharomyces cerevisiae." Eur J Biochem 191(3): 769-774.

Stepp, J. D., K. Huang and S. K. Lemmon (1997). "The yeast adaptor protein complex, AP-3, is essential for the efficient delivery of alkaline phosphatase by the alternate pathway to the vacuole." J Cell Biol **139**(7): 1761-1774.

Suter, B., A. Tong, et al. (2004). "The origin recognition complex links replication, sister chromatid cohesion and transcriptional silencing in Saccharomyces cerevisiae." Genetics 167(2): 579-591.

Tamura, Y., Harada, Y., Nishikawa, S., Yamano, K., Kamiya, M., Shiota, T., Kuroda, T., Kuge, O., Sesaki, H., Imai, K., Tomil, K. & Endo, T. Tam41 is a CDP-diacylglycerol synthase required for cardiolipin biosynthesis in mitochondria. *Cell metabolism* 17, 709-18 (2013).

Tamura, Y., Harada, Y., Yamano, K., Watanabe, K., Ishikawa, D., Ohshima, C., Nishikawa, S., Yamamoto, H. & Endo, T. Identification of Tam41 maintaining integrity of the TIM23 protein translocator complex in mitochondria. *The Journal of cell biology* 174, 631-7 (2006).

Tong, A. H., M. Evangelista, A. B. Parsons, H. Xu, G. D. Bader, N. Page, M. Robinson, S. Raghibizadeh, C. W. Hogue, H. Bussey, B. Andrews, M. Tyers and C. Boone (2001). "Systematic genetic analysis with ordered arrays of yeast deletion mutants." Science 294(5550): 2364-2368.

Trotter, P. J. (2001). "The genetics of fatty acid metabolism in Saccharomyces cerevisiae." Annu Rev Nutr 21: 97-119.

Tsai, C. L. and D. P. Barondeau (2010). "Human frataxin is an allosteric switch that activates the Fe-S cluster biosynthetic complex." Biochemistry **49**(43): 9132-9139.

Tuller, G., Hrastnik, C., Achleitner, G., Schiefthaler, U., Klein, F. & Duam, G. YDL142c encodes cardiolipin synthase (Cls1p) and is non-essential for aerobic growth of Saccharomyces cerevisiae. *FEBS letters* 421, 15-8 (1998).

Turrens, J.F., Alexandre, A. & Lehninger, A.L. Ubisemiquinone is the electron donor for superoxide formation by complex III of heart mitochondria. *Archives of biochemistry and biophysics* 237, 408-14 (1985).

Uhlinger, D. J., C. Y. Yang and L. J. Reed (1986). "Phosphorylation-dephosphorylation of pyruvate dehydrogenase from bakers' yeast." Biochemistry 25(19): 5673-5677.

Valianpour, F., V. Mitsakos, D. Schlemmer, J.A. Towbin, J.M. Taylor, P.G. Ekert, D.R. Thorburn, A. Munnich, R.J. Wanders, P.G. Barth, and F.M. Vaz. 2005.

Monolysocardiolipins accumulate in Barth syndrome but do not lead to enhanced apoptosis. J Lipid Res. 46:1182-1195.

van den Berg, M. A. and H. Y. Steensma (1995). "ACS2, a Saccharomyces cerevisiae gene encoding acetyl-coenzyme A synthetase, essential for growth on glucose." Eur J Biochem 231(3): 704-713.

van den Berg, M. A., P. de Jong-Gubbels, C. J. Kortland, J. P. van Dijken, J. T. Pronk and H. Y. Steensma (1996). "The two acetyl-coenzyme A synthetases of Saccharomyces cerevisiae differ with respect to kinetic properties and transcriptional regulation." J Biol Chem 271(46): 28953-28959.

van den Bosch, H., Schutgens, R.B., Wanders, R.J. & Tager, J.M. Biochemistry of peroxisomes. *Annual review of biochemistry* 61, 157-97 (1992).

van der Klei, I.J. & Veenhuis, M. Yeast peroxisomes: function and biogenesis of a versatile cell organelle. *Trends in microbiology* 5, 502-9 (1997).

van der Leij, F.R., Huijkman, N.C., Boomsma, C., Kuipers, J.R. & Bartelds, B. Genomics of the human carnitine acyltransferase genes. *Molecular genetics and metabolism* 71, 139-53 (2000).

van der Vusse, G.J., van Bilsen, M. & Glatz, J.F. Cardiac fatty acid uptake and transport in health and disease. *Cardiovascular research* 45, 279-93 (2000).

van Loon, A. P., B. Pesold-Hurt and G. Schatz (1986). "A yeast mutant lacking mitochondrial manganese-superoxide dismutase is hypersensitive to oxygen." Proc Natl Acad Sci U S A 83(11): 3820-3824.

van Roermund, C.W., Elgersma, Y., Singh, N., Wanders, R.J. & Tabak, H.F. The membrane of peroxisomes in Saccharomyces cerevisiae is impermeable to NAD(H) and acetyl-CoA under in vivo conditions. *The EMBO journal* 14, 3480-6 (1995).

van Roermund, C. W., E. H. Hettema, M. van den Berg, H. F. Tabak and R. J. Wanders (1999). "Molecular characterization of carnitine-dependent transport of acetyl-CoA from peroxisomes to mitochondria in Saccharomyces cerevisiae and identification of a plasma membrane carnitine transporter, Agp2p." EMBO J **18**(21): 5843-5852.

Vaz, F. M., R. H. Houtkooper, et al. (2003). "Only one splice variant of the human TAZ gene encodes a functional protein with a role in cardiolipin metabolism." J Biol Chem 278(44): 43089-43094.

Veenhuis, M. & Harder, W. Microbodies in yeasts: structure, function and biogenesis. *Microbiological sciences* 5, 347-51 (1988).

Verleur, N., E. H. Hettema, C. W. van Roermund, H. F. Tabak and R. J. Wanders (1997). "Transport of activated fatty acids by the peroxisomal ATP-binding-cassette transporter Pxa2 in a semi-intact yeast cell system." Eur J Biochem **249**(3): 657-661.

Vorapreeda, T., C. Thammarongtham, S. Cheevadhanarak and K. Laoteng (2012). "Alternative routes of acetyl-CoA synthesis identified by comparative genomic analysis: involvement in the lipid production of oleaginous yeast and fungi." Microbiology 158(Pt 1): 217-228.

Vreken, P., A. E. van Lint, A. H. Bootsma, H. Overmars, R. J. Wanders and A. H. van Gennip (1999). "Quantitative plasma acylcarnitine analysis using electrospray tandem mass spectrometry for the diagnosis of organic acidaemias and fatty acid

oxidation defects." J Inherit Metab Dis **22**(3): 302-306.

Walker, J.E. The mitochondrial transporter family. *Current opinion in structural Biology.* 2 (4): 519-526 (1992).

Wanders, R.J., Jansen, G.A. & Lloyd, M.D. Phytanic acid alpha-oxidation, new insights into an old problem: a review. *Biochimica et biophysica acta* 1631, 119-35 (2003).

Wanders, R.J., Ruiter, J.P., L, I.J., Waterham, H.R. & Houten, S.M. The enzymology of mitochondrial fatty acid beta-oxidation and its application to follow-up analysis of positive neonatal screening results. *Journal of inherited metabolic disease* 33, 479-94 (2010).

Watkins, S.M., Carter, L.C. & German, J.B. Docosahexaenoic acid accumulates in cardiolipin and enhances HT-29 cell oxidant production. *Journal of lipid research* 39, 1583-8 (1998).

Wei, Y., M. Lin, D. J. Oliver and P. S. Schnable (2009). "The roles of aldehyde dehydrogenases (ALDHs) in the PDH bypass of Arabidopsis." BMC Biochem **10**: 7.

Witt, W., M. E. Schweingruber and A. Mertsching (1984). "Phospholipase B from the plasma membrane of Saccharomyces cerevisiae. Separation of two forms with different carbohydrate content." Biochim Biophys Acta **795**(1): 108-116.

Wriessnegger, T., Gubitz, G., Leitner, E., Ingolic, E., Cregg, J., de la Cruz, B.J. & Daum, G. Lipid composition of peroxisomes from the yeast Pichia pastoris grown on different carbon sources. *Biochimica et biophysica acta* 1771, 455-61 (2007).

Xu, Y., Kelley, R.I., Blanck, T.J. & Schlame, M. Remodeling of cardiolipin by phospholipid transacylation. *The Journal of biological chemistry* 278, 51380-5 (2003).

Xu, Y., A. Malhotra, M. Ren and M. Schlame (2006). "The enzymatic function of tafazzin." J Biol Chem 281(51): 39217-39224.

Xu, Y., R. I. Kelley, T. J. Blanck and M. Schlame (2003). "Remodeling of cardiolipin by phospholipid transacylation." J Biol Chem 278(51): 51380-51385.

Ye, H., Pilon, M. & Pilon-Smits, E.A. CpNifS-dependent iron-sulfur cluster biogenesis in chloroplasts. *The New phytologist* 171, 285-92 (2006).

Yeung, B. G., H. L. Phan and G. S. Payne (1999). "Adaptor complex-independent clathrin function in yeast." Mol Biol Cell **10**(11): 3643-3659.

Zhang, M., Mileykovskaya, E. & Dowhan, W. Cardiolipin is essential for organization of complexes III and IV into a supercomplex in intact yeast mitochondria. *The Journal of biological chemistry* 280, 29403-8 (2005).

Zhang, M., E. Mileykovskaya, and W. Dowhan. 2002b. Gluing the respiratory chain together. Cardiolipin is required for supercomplex formation in the inner mitochondrial membrane. The Journal of biological chemistry. 277:43553-43556.

Zhong, Q., Gvozdenovic-Jeremic, J., Webster, P., Zhou, J. & Greenberg, M.L. Loss of function of KRE5 suppresses temperature sensitivity of mutants lacking mitochondrial anionic lipids. *Molecular biology of the cell* 16, 665-75 (2005).

Zhong, Q., Li, G., Gvozdenovic-Jeremic, J. & Greenberg, M.L. Up-regulation of the cell integrity pathway in saccharomyces cerevisiae suppresses temperature sensitivity of the pgs1Delta mutant. *The Journal of biological chemistry* 282, 15946-53 (2007).

Zhou, J., Zhong, Q., Li, G. & Greenberg, M.L. Loss of cardiolipin leads to longevity defects that are alleviated by alterations in stress response signaling. *The Journal of biological chemistry* 284, 18106-14 (2009).

Zinser, E., Sperka-Gottlieb, C.D., Fasch, E.V., Kohlwein, S.D., Paltauf, F. & Daum, G. Phospholipid   synthesis and lipid composition of subcellular membranes in the unicellular eukaryote Saccharomyces cerevisiae. *Journal of bacteriology* 173, 2026-34 (1991).

ABSTRACT

CARDIOLIPIN IS REQUIRED FOR OPTIMAL ACETYL-COA METABOLISM

by

VAISHNAVI RAJA

December 2016

Advisor: Dr. Miriam L. Greenberg

Major: Biological Sciences

Degree: Doctor of Philosophy

The phospholipid cardiolipin (CL) is crucial for many cellular functions and signaling pathways, both inside and outside of mitochondria. My thesis focuses on the role of CL in energy metabolism. Many reactions of electron transport and oxidative phosphorylation, the transport of metabolites needed for these processes, and the stabilization of electron transport chain supercomplexes, require CL. Recent studies indicate that CL is required for the synthesis of iron-sulfur (Fe-S) co-factors, which are essential for numerous metabolic pathways. Activation of carnitine-acetylcarnitine translocase, which transports acetyl-CoA into the mitochondria, is CL dependent. The presence of substantial amounts of CL in the peroxisomal membrane suggests that CL may be important for peroxisomal functions. Understanding the role of CL in energy metabolism may identify physiological modifiers that exacerbate the loss of CL and underlie the variation in symptoms observed in Barth syndrome, a genetic disorder of CL metabolism.

In order to identify biochemical pathways exacerbated by the loss of CL, I carried out a Synthetic Genetic Array (SGA) screen of the yeast CL mutant *crd1Δ*. The results

indicated that *crd1Δ* is synthetically lethal with mutants in pyruvate dehydrogenase (PDH), which catalyzes the conversion of pyruvate to acetyl-CoA. Previous studies have shown that synthesis of acetyl-CoA depends primarily on pyruvate conversion in the mitochondria and the cytosol. The *crd1Δ* mutant exhibited decreased acetyl-CoA levels and decreased growth on acetate as a sole carbon source. Gene expression and protein levels of PDH were increased, but PDH specific activity remained unaltered. These findings suggest that defective ability to convert acetate to acetyl-CoA and possibly decreased enzymatic activity of PDH may account for perturbed acetyl-CoA synthesis in CL-deficient cells.

Consistent with a requirement for CL in acetyl-CoA synthesis, perturbation of CL synthesis leads to decreased activity of carnitine-acetylcarnitine translocase, a transporter found in the mitochondrial membrane specific for import of acetylcarnitine into the mitochondria. Growth of *crd1Δ* at elevated temperature and on acetate medium is restored by supplementation of carnitine, acetylcarnitine, or oleate. Interestingly, synthetic lethality was observed between *crd1Δ* and mutants in the glyoxylate cycle, suggesting that this cycle is essential to replenish TCA cycle intermediates in CL-deficient cells. The studies described in this thesis are the first to demonstrate that CL is required for synthesis and transport of acetyl-CoA.

To obtain an understanding of tafazzin function, an SGA screen was carried out to identify mutants that synthetically interact with *taz1Δ*. Interesting interactions were observed with phospholipase B, ornithine carbamoyltransferase, and genes required for mitochondrial iron homeostasis and vacuolar protein sorting. These findings suggest that tafazzin may be involved in cellular processes other than CL remodeling.

AUTOBIOGRAPHICAL STATEMENT

EDUCATION

2010-2016   Ph.D in Biology, Wayne State University, Detroit, USA

2007-2010   M.S in Molecular Biotechnology & Biology,
               Wayne State University, Detroit, USA (did not complete)

2002-2006   B.Tech in Industrial Biotechnology, Anna University, India

AWARDS AND FELLOWSHIPS

2015   Third Prize at Graduate Exhibition 2015 (Poster presentation), WSU

2015   WSU Graduate Student Professional Travel Award

2014-2015   Thomas C. Rumble University Graduate Fellowship

2013-2014   Outstanding Graduate Research Assistant Award

2014   Third Prize at Lipids @ Wayne symposium (Poster presentation), WSU

2014   Barth Syndrome Foundation Conference Travel Award

2012-2013   Outstanding Graduate Teaching Assistant Award

2012 - 2013   Enhancement Award for Doctoral Student Travel Award

2012   Barth Syndrome Foundation Conference Travel Award

PUBLICATIONS

Raja V and Greenberg ML. 2014. The functions of cardiolipin in cellular metabolism – potential modifiers of the Barth syndrome phenotype. *Chemistry and Physics of Lipids,* **179:**49-56.

Raja V, Joshi AS, Li G, Maddipati KR, and Greenberg ML. Loss of cardiolipin leads to perturbation of acetyl-CoA synthesis. *(In preparation)*

Raja V, Joshi AS, van Roermund CWT, Maddipati KR, Hüttemann M, and Greenberg ML. Loss of cardiolipin leads to defects in the TCA cycle due to perturbation of acetyl-CoA transport. *(In preparation)*